



ADDIS ABABA UNIVERSITY
ADDIS ABABA INSTITUTE OF TECHNOLOGY
SCHOOL OF ELECTRICAL AND COMPUTER ENGINEERING

**Energy Management of Three Wheeler Hybrid Electric Vehicle
by Using Model Predictive Controller**

A thesis submitted to School of Graduate Studies, Addis Ababa Institute of Technology, Addis Ababa University in partial fulfillment of the requirement for the Degree of Master of Science in Electrical Engineering (Control Engineering)

by:- **Dereje Abera**

Advisor:- **Dereje Shiferaw (Ph.D)**

August 2024 G.C

Addis Ababa, Ethiopia



ADDIS ABABA UNIVERSITY

ADDIS ABABA INSTITUTE OF TECHNOLOGY

SCHOOL OF ELECTRICAL AND COMPUTER ENGINEERING

**Energy Management of Three Wheeler Hybrid
Electric Vehicle by Using Model Predictive
Controller**

APPROVED BY BOARD OF EXAMINERS

Name	Date	Signature
_____	_____	_____
(Dean, School of Graduate Committee)		
_____	_____	_____
(Advisor)		
_____	_____	_____
(Internal Examiner)		
_____	_____	_____
(External Examiner)		

Acknowledgment

I am immensely grateful to God for granting me the strength and wisdom to complete this thesis. I extend my heartfelt appreciation to my advisor, Dr. Dereje Shiferaw, for his continuous guidance, encouragement, and support throughout this journey. I am also deeply thankful to my loving family for their unwavering belief in me and their endless support. Their encouragement has been my rock. Without their love and support, this achievement would not have been possible.

Abstract

In response to environmental issues and declining global crude oil reserves researchers and automobile manufacturers are exploring novel vehicle technologies. Hybrid Electric Vehicles (HEVs) reduce fuel usage and greenhouse gas emissions. The transportation sector consumes around 66% of global oil consumption, with small passenger cars and trucks accounting for 50%.

For meeting future energy demands and reducing pollution a power-split hybrid electric car is a possible solution . It combines features of both conventional and electric vehicles. Energy can be managed optimally because it comes from two subsystems: the engine and the battery. This thesis presents a model predictive control approach with constraint handling that outperforms previous strategies for efficient energy management of hybrid electric vehicles. A comprehensive mathematical model of a three wheeler Auto Rickshaw power split hybrid electric car is created, including the engine, planetary gear, motor/generator, and battery.

The presented model utilizes an interior-point optimizer-based nonlinear predictive control approach with operational limitations and a cost function. The goal is to reduce fuel usage and keep the battery's charge within predefined limitations. The generated model was simulated in MATLAB, including motor, generator, engine speed, and battery SoC. The proposed MPC results for the HWFET(modified) and EUDC(modified) cycles show specific fuel consumption of 0.5162 and 0.5817 liters/100 km, respectively. The ADVISOR 2003 rule-based method yields 1.00 and 1.1 liters/100 km for the HWFET(modified) and EUDC(modified) cycles, respectively, supporting these findings. The suggested MPC improves specific fuel consumption by 48.39% and 47.12% in HWFET(modified) and EUDC(modified) drive cycles, respectively. So MPC based three wheeler power split HEVs would play a significant role to significantly lower fuel consumption and environmental pollution and foreign currency to import fuel.

Contents

Declaration

Acknowledgment I

Abstract II

1 Introduction 1

1.1	Objective	3
1.1.1	General objectives	3
1.1.2	Specific objectives	3
1.2	Statement of the Problem	3
1.3	Significance of the study	4
1.4	Structure of the thesis	5

2 Literature Review 6

2.1	Energy management strategies	6
2.2	HEV classification	8
2.3	Literature review on HEV	9
2.4	Literature review on MPC	10
2.5	Literature review on other types of controller	11
2.6	Summary	13

3 Mathematical Modelling of Hybrid Electric Vehicle 14

3.1	Hybrid electric vehicle architecture	14
3.1.1	Parallel HEV	14
3.1.2	Series HEV	14
3.1.3	Parallel-series HEV	15
3.2	Planetary gear-sets	15
3.3	Configuration of power split HEVs	20
3.4	Simulation techniques	21
3.4.1	Forward-facing simulation	21
3.4.2	Backward-facing Simulation	23

3.5	Gear forces	24
3.6	Mathematical modelling of three wheeler power split HEV	26
3.7	Model verification	37
4	Energy Management Strategy	42
4.1	Rule-based control strategies	44
4.1.1	Deterministic rule-based EMSs	44
4.1.2	Fuzzy logic-based EMSs	46
4.2	Model Predictive Control	47
4.2.1	Operating Principle of MPC	49
4.2.2	Design parameters of MPC	52
4.2.3	Mathematical formulation of NMPC	55
4.2.4	MPC mathematical formulation for three wheeler HEV	58
4.3	Algorithm for the proposed MPC strategy	65
5	Simulation Result	67
5.1	The simulation procedure	67
5.1.1	CasADi	67
5.1.2	ADVISOR	67
5.2	Simulation Result	70
6	Conclusion and Future Work	85
7	Appendices	93
7.1	Fuel consumption	93

List of Acronyms

MPC : model predictive control

NMPC : Non-linear model predictive control

HEVs : Hybrid Electric Vehicles

EM : Electric Motor

EVs : Electric Vehicles

EV : Electric Vehicle

HEV : Hybrid Electric Vehicle

GHG : Green house gas

PHEVs : Plug-in hybrid electric vehicles

ICE : internal combustion engine

EMS : energy management systems

EMSs : energy management strategies

DP : Dynamic programming

PMP : pontryagin's minimum principle

LP : linear programming

GA : Genetic algorithm

ECMS : Energy Control Management Strategy

SISO : Single-input single-output

MIMO : Multiple-input multiple-output

CVT : continuously variable transmission

A-ECMS : adaptive equivalent consumption minimisation strategy

OOL : optimal operation line

TLBO : teaching learning based optimization

PSO : particle swarm optimization

ADMM : alternate direction method of multipliers

FLC : fuzzy logic controller

HWFET : Highway Fuel Economy Test Cycle

EUDC : Extra-Urban Driving Cycle

SOC : state of charge

OCP : optimal control problem

NLP : nonlinear programming problem

ADVISOR : Advanced Vehicle Simulator

NREL : National Renewable Energy Laboratory

GUIs : Graphic user interfaces

EPL : Eclipse Public License

m : Mass of Vehicle

A_f : Frontal area of Vehicle

C_d : Drag Coefficient

r_w : Radius of Wheel

g : gravity

I_e : Engine Inertia

I_m : Motor Inertia

I_g : Generator Inertia

I_w : Wheel Inertia

W_g : Speed of Generator

W_e : Speed of Engine

W_m : Speed of Motor

V_{oc} : Open Circuit Voltage

R_b : Internal Resistance

Q_b : Battery Capacity

S_{oc} : State of Chargez

C_f : Fuel flow Rate constant

R : Number of Teeth of Ring gear of Planetary Gear System

S : Number of Teeth of Sun gear of Planetary Gear System

T_g : Torque of Generator

T_m : Torque of Motor

T_e : Torque of Engine

g_f : Final Drive Ratio

T_{ndc} : Total no of data points in the driving cycle.

C_i : i^{th} data point in the driving cycle

List of Figures

3.1	Electric Vehicle using Hybrid Technology in Parallel	14
3.2	Series Hybrid Electric Vehicle	15
3.3	Parallel Series Hybrid Electric Vehicle	15
3.4	Planetary gear	16
3.5	A Power-Split HEV Configuration	19
3.6	Schematic diagram of power-split configured hybrid electric vehicle.	20
3.7	Forward-facing block diagram	21
3.8	The forward simulator diagram	23
3.9	Backward Simulator model	24
3.10	Gear force	25
3.11	Power train configuration of the Toyota Hybrid System	27
3.12	Free body diagram of the mechanical path.	28
3.13	Model Verification	37
3.14	The states plot for the reference input value	38
3.15	Vehicle speed plot for the reference value	38
3.16	The states plot for $T_m=40$	39
3.17	Vehicle speed plot for $T_m=40$	39
3.18	The states plot for $T_e=40$	39
3.19	Vehicle speed plot for $T_e=40$	40
3.20	The states plot for $W_g=40$	40
3.21	Vehicle speed plot for $W_g=40$	41
3.22	The states plot for $T_g=10$	41
3.23	Vehicle speed plot for $T_g=10$	41
4.1	The principle of the model predictive control	48
4.2	The basic structure of model predictive control.	48
4.3	u and x in the past	50
4.4	Predicted optimum Control action	51
4.5	Predicted State	51
4.6	Actual State	52
4.7	Next Step Prediction	53

4.8	Control Horizon with constant value after M steps	54
4.9	Control moves to be computed by the optimizer	55
4.10	Algorithm of the proposed MPC strategy	66
5.1	ADVISOR first page	68
5.2	ADVISOR second page	69
5.3	ADVISOR third page	70
5.4	ADVISOR 4th page	72
5.5	HWFET(modified) drive cycle	73
5.6	EUDC(modified) drive cycle	73
5.7	Battery SoC using ADVISOR2003 in EUDC(modified) drive cycle	74
5.8	Battery SoC using ADVISOR2003 in HWFET(modified) drive cycle	74
5.9	Battery SoC using the proposed MPC over EUDC(modified)	74
5.10	Battery SoC using the proposed MPC over HWFET(modified)	75
5.11	Motor speed in HWFET(modified) cycle	75
5.12	Generator speed in HWFET(modified) cycle	76
5.13	Engine speed in HWFET(modified) cycle	76
5.14	Generator torque in HWFET(modified) cycle	77
5.15	Engine torque in HWFET(modified) cycle	78
5.16	Motor torque in HWFET(modified) cycle	78
5.17	Motor Speed in EUDC(modified) cycle	80
5.18	Generator Speed in EUDC(modified) cycle	80
5.19	Engine Speed in EUDC(modified) cycle	81
5.20	Motor torque in EUDC(modified) cycle	81
5.21	Generator torque in EUDC(modified) cycle	82
5.22	Engine torque in EUDC(modified) cycle	82
5.23	Fuel flow rate under HWFET(modified) drive cycle in ADVISOR	83
5.24	Fuel flow rate under EUDC(modified) drive cycle in ADVISOR	83
5.25	Fuel flow rate by MPC under HWFET(modified) drive cycle	84
5.26	Fuel flow rate by MPC under EUDC(modified) drive cycle	84
7.1	Approximation of BSFC as a function of T_e and N_e , together with map data from GT-Suite	94

List of Tables

- 3.1 Possible planetary gear-set inputs and outputs 17
- 3.2 Different parameters used for model Verification 37
- 5.1 Different parameters utilized in the modeling process for the three-wheeler HEV. . . 71
- 5.2 Drive cycle characteristics 71
- 5.3 Fuel economy comparison. 79

1 Introduction

Recently, there has been a greater focus on hybrid electric vehicles(HEVs) due to growing concerns about emissions and fuel economy. It is becoming a critical concern due to global environmental change.The geopolitical issues surrounding oil providers and the steadily declining natural supplies of oil are prompting people to think about other forms of transportation. Although not completely eliminating it, hybrid electric vehicles (HEVs) greatly reduce the usage of fossil fuels.

The way that gasoline and energy are used in a vehicle must be considered in order to understand the use of hybrid electric vehicles from an efficiency standpoint. First, consider a traditional car, where chemical energy is transformed into mechanical energy to provide all the energy needed for a trip. The drive line components, the auxiliary devices (air conditioning, power steering), and the vehicle's propulsion all use the mechanical energy produced by the engine.The driving pattern (speed, accelerator, grade) and pedal position (acceleration and brake commands) are used to calculate the engine's mechanical power. In a hybrid electric vehicle(HEV), the engine's power is combined with electric power (super capacitor, batteries) to produce all of the necessary power. The proportion of the two energy sources is a degree of freedom that allows the engine's operating conditions to be changed in relation to its counterpart (a traditional vehicle), potentially increasing the engine's average efficiency.

One benefit of hybrid electric cars is that its reversible electric motor can recover kinetic energy through regenerative braking. This feature makes the vehicle extremely useful. producing electricity in this manner to charge the batteries. Energy that is often lost as heat in mechanical brakes can be recovered by regenerative braking. Since only a small portion of kinetic energy can really be recovered, the overall efficiency of the vehicle is greatly increased. Any type of storage device is possible, including hydraulic (pressure accumulators), mechanical (flywheels, springs), and electrical (batteries, capacitors). Other advantages of HEV include the ability to turn the engine ON or OFF when not in use (at very low speeds or stops), as well as improved fuel efficiency due to the engine's reduction.

Because of green house gas(GHG) emissions and global warming, there is a growing awareness of the need to save energy and safeguard the environment.In industrialized nations, laws have been established to safeguard the environment, and as new concerns arise, these laws are becoming more stringent every day. The primary source of pollution in the environment is the transportation sector

and related sectors. Several nations have ratified the Kyoto Protocol, an international pact that calls for a 5.2 % reduction in pollutant gas emissions by 2012. It was determined that a traditional vehicle's energy conversion efficiency is only 20%.

Plug-in HEV, whose batteries are charged via the grid, offer a mediocre level of fuel economy. plugin-hybrid electric vehicles(PHEVs) are replacing liquid fuels by storing electrical energy in their batteries and using the less expensive grid electricity. When it comes to batteries, PHEVs use bigger ones than HEVs. Batteries are the main energy source while internal combustion engine(ICE) is the secondary energy source, in contrast to HEVs. These cars can be equipped with infrastructure for recharging both at home in garages and at other locations. Better batteries would eliminate the need for hybrid vehicles entirely.

Energy management techniques are essential for increasing HEV fuel efficiency and lowering greenhouse gas emissions. A parallel hybrid rickshaw(Three wheeler Vehicle) that uses less gasoline has been proposed, since battery-operated rickshaws have already been adopted. There were issues with the short range of distance. The suggestion was made to replace the batteries at a different fueling station, however that facility was not accessible in rural regions, thus a hybrid electric rickshaw was put forth as a preferable option. An HEV conversion makes sense for two technical reasons for a rickshaw. Its low speed is the first, and frequent braking is the second. Since traffic is of a high stop/kilometer and has a lengthy idle period at moderate speeds. Thus, these elements aid in obtaining superior fuel efficiency. Regenerative braking, which is possible when braking often, allows for the recovery of inertial power.

The benefit of HEV is that the engine and motor share the overall torque requirement, but this presents certain control-related issues. This thesis discusses minimizing fuel use of three wheler HEV by dividing power between the two energy sources optimally.

EMS has typically been utilized for other types of vehicles, but rarely for Three Wheeler vehicle(Bajaj). There are two reasons for ignoring this vehicle: its presence in undeveloped countries and its tiny size. The compact size limits the available room for hybridization. This thesis advise utilizing the space under the rear seats.

1.1 Objective

1.1.1 General objectives

Design a model predictive control system for a three-wheeled hybrid electric vehicle for an energy management strategy .

1.1.2 Specific objectives

- To define the nonlinear dynamics of a three wheeler HEV using a comprehensible modelling technique.
- Obtain the parameters of the three-wheeler HEV from the ADVISOR 2003 software.
- Design Energy management controller using MPC for minimizing fuel consumption using CasADi in MATLAB.
- Analyze the rule-based EMS result of the ADVISOR platform for the three wheeler HEV.
- Comparing the result obtained from the ADVISOR 2003 software and the MPC controller of the three wheeler HEV.

1.2 Statement of the Problem

Due to global environmental change ,regularly depleting natural resources of oil and geopolitical problems associated with oil providers the concerns about emissions and fuel economy has grown Recently and People are starting to consider alternative modes of transportation.from those alternatives the one is The all electric vehicle(EV) which is environmentally favorable because it emits no pollutants. But its limits are driving the globe to seek out some intermediate solutions, such as the use of HEV.Even though they don't completely eliminate it, HEVs drastically lower the usage of fossil fuels. All of the power required in a hybrid electric vehicle (HEV) is produced by combining the power of the engine with electric power (super capacitor, batteries). To provide appropriate power sharing between the electric motor and internal combustion engine(ICE) and to effectively handle the various driving modes energy management strategy(EMS) is needed. The primary goal of the energy management strategy is to lower fuel consumption in HEVs by controlling the power demand across

various energy sources. so in this thesis Model predictive controller(MPC) is selected to analyze Energy management strategy.

1.3 Significance of the study

Presently in Ethiopia and the remaining world, there is scarcity of fuel. This is mainly due to the fact that fuel is found in a limited amount and only found in specific countries in the world. According to the Reporter Ethiopia, Ethiopian News, Ethiopia has more than 250,000 three Wheelers(Bajaj), which currently run on fuel and produce carbon emissions. This quantity of users of three-wheelers One strategy to lower the unemployment rate in Ethiopia is the significant increase in transportation that has occurred in recent years. However, the owner must spend a large sum of money because the three-wheeler vehicle uses gasoline. The fuel causes global warming by polluting the air. In order to solve the above issues manufacturing of HEV(i.e intermediate solution between Electric vehicle and ICE vehicle) are growing. The main target in manufacturing HEV is managing the power distribution between the fuel and the motor.

The reason for focusing on three wheeler HEV are:

1. It is common in poor countries. Developing countries' transportation systems differ from those of wealthy countries. Major cities in developing countries face a variety of transportation issues, one of which is traffic congestion, which increases travel time. Restricting personal car use and promoting compact vehicles could be one option to alleviate traffic congestion and lower transportation expenses in emerging cities.
2. It is the most common mode of transportation. Hybridization of three wheeler vehicle maximizes vehicle efficiency and cost-effectiveness. Three wheeler vehicle(Bajaj) provide a feeder service for the bus rapid transit (BRT) system.

Using Energy Management Techniques to save fuel can benefit car owners who are struggling financially and minimize the amount of fuel to be imported by foreign currency. This thesis mainly focus on Model predictive control (MPC) energy management strategy of three wheeler Hybrid Electric vehicle and this will help the vehicle manufacturing industry sector. Furthermore, this work will lay the foundation for future researchers and students to gain experience and broaden their knowledge on HEV energy management strategy so that they will be motivated for further finding.

1.4 Structure of the thesis

- Chapter 2 provides key literature reviews.
- Chapter 3 comprises of the mathematical modeling of the hybrid electric vehicle and verification of the model.
- Chapter 4 emphasizes on the rule-based and MPC Energy Management Techniques for HEVs.
- Chapter 5 describes the Comparative Analysis of the rule-based result of ADVISOR 2003 and EMS for the three wheeler HEV using MPC.
- Chapter 6 outlines the conclusion and the future research direction.

2 Literature Review

Researchers and the car industry are looking for energy-efficient propulsion systems due to rising energy demands, finite fuel supplies, and emission laws. In today's world, owning an automobile has become necessary. The advancement of internal combustion engines has had a significant impact on the automotive industry. However, the greenhouse gases that cause pollution and endanger the ozone layer are carbon dioxide (CO₂), carbon monoxide (CO), hydrocarbons (HC), and oxides of nitrogen (NO_x). Batteries and electric motors have been employed as alternative energy sources alongside internal combustion engines (ICEs). Hybridization may drastically reduce fuel use and greenhouse gas emissions. This idea has led to the development of new vehicle types in the transportation industry, including fuel-efficient electric vehicles (EVs), hybrid electric vehicles (HEVs), and plugin-hybrid electric vehicles (PHEVs), which also aid in the reduction of harmful emissions. Hybrid electric vehicles undoubtedly offer certain advantages over traditional automobiles, even though they require more expensive and additional components.

2.1 Energy management strategies

Numerous energy management techniques have been developed for HEVs to provide appropriate power sharing between the electric motor and internal combustion engine (ICE) and to effectively handle the various driving modes. The major purpose of the energy management approach is to reduce fuel consumption in HEVs by regulating power demand across several energy sources. Energy management controllers for hybrid electric vehicles perform a series of control actions, such as instantaneous power splitting between various energy sources. The overall impact of these controllers can be measured in terms of fuel consumption during a given driving cycle, total pollution emissions, or any other criterion, the optimization goal of which is to minimize them.

Over the last decade, there has been a surge of interest in energy management research. The energy management strategies (optimal/non-optimal) have been developed using a variety of computational techniques, such as Rule Based Control, Fuzzy Logic Based Control, Adaptive Control, Dynamic Programming, Quadratic Programming, and Model Predictive Control. Each of these methods has benefits and drawbacks.

Model Predictive Control has been used on all vehicle kinds up to this point, but it has not been studied for three-wheeler auto-rickshaws. This vehicle is disregarded for two reasons: first, it is found in poor nations; second, it is little. Its tiny size means that less room is accessible for hybridization.

To satisfy future human demands, it is critical to prioritize environmental protection, fossil fuel sustainability, and economic resource availability. Fossil fuels are depleting, as the world's population grows, leading fuel costs to climb. The residuals of burned fossil fuels pollute the environment. Pollution control is a major global challenge. To curb the pace of pollution, some countries are adopting rigorous laws. The transportation sector is a major source of pollution. Buses and cars powered by internal combustion engines have a direct impact on city pollution. To address these difficulties, researchers and scientists are developing new modes of vehicles or structural innovation.

The electric vehicle is an environmentally favorable alternative because it emits no pollutants. However, its limits are driving the globe to seek out some intermediate solutions, such as the use of hybrid electric vehicles (HEVs). In the current situation, a viable option is hybrid electric transportation, which combines the benefits of both sides, namely the qualities of pure internal combustion engine-based vehicles and pure electrified vehicles. Vehicles powered by internal combustion engines may be able to refill with gasoline or diesel in a matter of minutes and with a high energy density; they may also include a lightweight fuel container that may be used to transport additional fuel to remote locations but is prone to pollution. The best feature of electric vehicles is that they emit no pollution. Another advantage is that the engine may be run within an efficient zone at certain rpm and power levels. Because a HEV is powered by two sources: a smaller internal combustion engine and a battery. As a result, power can be collected from any of the two methods, giving the user the option of selecting a power source. This position allows the engine to function in its most efficient zone regardless of driving conditions. This fact leads to HEV energy management solutions.

Over the last decade, various energy management strategy (EMS) for HEVs have been tested. EMS strategies are classified as rule-based or optimization-based. Rule-based methods (thermostats and power followers) are guided by a system of rules created based on intuition, human expertise, or mathematical models and, in most cases, without prior knowledge of driving information. Of-

Offline optimization (global) and online optimization (instantaneous) strategies are the two types of optimization-based tactics. Dynamic programming(DP), linear programming(LP), Pontryagin's minimum principle(PMP) algorithm, and genetic algorithm(GA) are examples of offline optimization methodologies. They require prior information of the driving cycle and hence find a globally optimal solution. Moreover, DP is a good benchmark for other optimization strategies. MPC, robust and intelligent control strategies are examples of online optimization strategies. The energy control management strategy(ECMS) method is built around a co-state / equivalent factor that is extremely sensitive to the driving cycle and road conditions. MPC offers excellent constraint management capabilities. With contemporary research, learning-based solutions are also evolving. MPC has a few advantages over other management approaches. One of its best characteristics is the way it handles restrictions. Input and output can both be constrained. MPC is suitable for both single input, single-input single-output(SISO) and multiple-input multiple-output(MIMO) control systems. In MPC, the receding horizon compensates for any disturbance and can also be applied online[1, 2, 3] .

2.2 HEV classification

HEVs are classified into three types: parallel hybrid electric vehicles, series hybrid electric vehicles, and power-split/series-parallel hybrid electric vehicles.

A parallel hybrid electric vehicle is one in which power is supplied to the wheels by both the engine and the battery in parallel due to the mechanical and electrical nature of their respective power flow paths. Put another way, the battery and engine may work together or separately in this configuration. Parallel HEVs include the Chevrolet Malibu and Greenline series, the Honda Insight and Civic models, and the Chevrolet Malibu.

In hybrid electric vehicle models, the engine's function is to provide battery charging. The engine and generator are connected as a consequence. Two well-known hybrid electric car series variants are the Opel Flextronic and the Fisher Karma.

As the name implies, a power split / series-parallel HEV arrangement can operate in either a series or parallel method. It is made up of a miniaturized ICE, a battery, motor/generator set 1 (which

largely functions as a generator), motor/generator set 2 (which primarily functions as a motor), and a planetary gear set. The motor is also responsible for capturing regenerative energy. Planetary gear functions as a continuously variable transmission(CVT), allowing the engine speed to be independent of road load. As a result, the engine can function in its most efficient zone of operation. A planetary gear set is made up of several separate gears, including a central sun gear, planet gears that circle around and mesh with the central sun gear, and an outer gear called ring gear. Three or four planet gears mesh with the sun gear on one side. Planet gears on the other side mesh with the outer ring gear. A common carrier is rigidly attached to three or four planet gears. Sun gear is connected to motor/generator set 1. A sturdy carrier connects the internal combustion engine(ICE). The outer ring gear is linked to the motor/generator set 2. This ring gear is also connected to the vehicle wheels via a differential gear with the necessary gear ratio. Toyota Prius, Chevrolet Volt, Toyota Camry, Lexus RX400h, Lexus NX300h, and Toyota Ford Fusion are examples of power split hybrid electric automobiles.

In 1881, Gustave Trouve constructed the first electric vehicle [4]. This electric car had a 0.1 horsepower D.C. motor installed that was run on lead-acid batteries. Because of their restricted operating range, electric vehicles have not received much attention.HEVs use batteries to help with propulsion, which reduces the demand for fossil fuels and hazardous pollutants. Ferdinand Porsche created the Lohner-Porsche Mixte Hybrid in 1901 [5], which was the first hybrid electric vehicle fueled by gasoline. In hybrid electric cars, batteries are charged using regenerative braking or internal combustion engine power. But because fossil fuel is readily available and engine technologies are developing at a decent rate, HEVs have been overlooked. These days, the situation is always shifting due to the quickly decreasing fuel and the laws governing emissions control.

Numerous studies on the EMS of various types of HEV designs have been completed, and the sections below summarize prior studies and research.

2.3 Literature review on HEV

The advantages of a fuel-efficient and environmentally friendly hybrid electric three-wheeler in mitigating the negative consequences of an expanding motorized three-wheeler fleet are well understood.The design of hybrid electric three-wheelers has been thoroughly studied in the literature using

various hybrid combinations. Vezzini et al. [6] created a prototype for a series hybrid electric three-wheeler. Amjad et al. studied plug-in series hybrid technology for three-wheelers in [7]. A common hybrid setup for three-wheelers is the parallel powertrain configuration. Hofman et al. [8] analyzed parallel micro-hybrid architecture for three-wheelers. Roy and Indulal [9] investigated parallel hybrid technology for three-wheelers, concentrating on a design that connects motor and engine power via the road. Padmanaban et al. [10] studied the application of plug-in technology in parallel hybrid electric three-wheelers. Maddumage et al. The study on [11] has conducted a comparative investigation of hybrid three-wheeler setups. The study compares fuel and pollution effects of hybrid powertrain designs for three-wheeled electric vehicles, including conventional, parallel, series, and complicated configurations. Studies show that hybrid technology for three-wheelers may drastically cut fuel usage and emissions. The authors of [12] conducted a research to evaluate the performance of several HEV configurations, including series, parallel, and power-split HEVs. They determined that the power-split arrangement surpassed the others in terms of fuel efficiency.

2.4 Literature review on MPC

The study on [12] uses a stochastic model predictive control to manage and report energy for a parallel hybrid car. In this study, the author proposes a control strategy based on a predicted stochastic model of driving behavior for reducing not just fuel consumption but also emissions. The authors of [13] suggested using model predictive control to improve the gear ratio and torque split of a parallel HEV with a CVT. In [14], researchers used Pontryagin's Maximum Principle to optimize the energy split between the IC engine and electric motor of a parallel hybrid electric automobile. A research was done in [15] on the adaptation of Stochastic MPC utilizing ECMS for a parallel hybrid electric bus to reduce fuel consumption. The study on [16] compares rule-based and dynamic programming over model predictive control on series hybrid electric tracked bulldozers to enhance fuel economy. The study on [17] proposes energy management of series plug-in HEVs for various energy storage systems using MPC. A parallel plug-in HEV setup was studied to compare the interior-point based-MPC technique to the alternative direction method of multipliers (ADMM) algorithm [18].

2.5 Literature review on other types of controller

Wang and Lukic [19] employed DP to calculate the proper engine/motor split in a series-parallel powertrain. Lin et al. [20] found that optimum control rules may be extracted from DP findings and used to develop a near-optimal rule-based control technique for a parallel hybrid. The near-optimal rule-based method led to a 28% increase in fuel efficiency compared to standard automobiles. Lin et al. [21] investigated a simple approach for producing empirical control strategy rules using DP data, utilizing the power request ratio between engine and motor and transmission speed. The study on [22] investigates optimal energy regulation in series HEVs using dynamic programming. The authors of the study [23] developed an improved dynamic programming approach that was implemented across the series configuration of hybrid electric vehicles by including the brake recovering rule. Asghar et al. [4] developed a sub-optimal rule-based power management technique for a parallel hybrid electric three-wheeler based on DP findings. The report's approach for extracting rules from DP data is substantial, but it falls short of covering transmission gear strategy, numerical difficulties, exhaust emissions, and powertrain component sizing procedures for developing a hybrid electric three-wheeler control system.

In [24], a fuzzy-logic controller(FLC) for parallel hybrid electric vehicles is developed. The study on [25] describes a multi-input fuzzy logic controller for a power-split hybrid car and compares it to rule-based EMSs in terms of fuel economy and pollution. The FLC system distributes power based on the intended driver torque, vehicle speed, and battery state of charge. This technique outperforms conventional rule-based EMSs in terms of fuel economy and adaptability. Lee et al. [26] proposed a fuzzy logic-based energy management technique to reduce NOx emissions and meet driver power demands. The suggested fuzzy logic controller's control inputs are an electrical motor speed and an acceleration pedal stroke. The proposed fuzzy logic controller is estimated to cut NOx emissions by 20percent compared to conventional vehicles. However, the biggest disadvantage of this strategy is that it does not ensure the battery's SOC charge sustainability. To solve this issue, Lee et al. [27] developed a more advanced fuzzy logic controller that comprises a power balance controller and a driver intention predictor for energy management. Baumann et al. [28] developed an inclusive fuzzy logic controller using road load estimate to account for the difference between engine torque and required torque. Tian et al. [29] introduced an EMS for a plug-in hybrid electric bus based on adaptive fuzzy logic, with an ideal SOC reference created by a neural network and followed by a fuzzy logic

controller.

The authors [30] investigated energy optimization on parallel HEVs and determined that Pontryagin's minimum principle (PMP) method outperforms rule-based strategies. However, as previously stated, the PMP algorithm can only be utilized for offline optimization. In order to study the instantaneous optimal control of a power-split HEV with planetary gear set, adaptive equivalent consumption minimization strategy (A-ECMS) was implemented. Its superiority over engine optimal operation line (OOL) strategy, a type of rule-based strategy, was shown [31]. However, ECMS is sensitive to driving cycle and cannot deal with constraints. In [32], a series plug-in HEV setup is utilized to investigate the superiority of the teaching learning based optimization (TLBO) algorithm against an ADVISOR software rule-based strategy. The study on [33] compares and demonstrates the superior performance of the particle swarm optimization (PSO) algorithm and two of its variations over the rule-based strategy using a simple HEV with engine and motor, yet the PSO algorithm may have a low convergence rate.

2.6 Summary

The interior-point approach was discovered to be more convergent than the ADMM methodology, despite the fact that both algorithms are computationally significantly faster than standard optimisation convex algorithms. Based on the research articles mentioned above, power-split HEV setups have not yet been used with the interior-point based-MPC approach, a quick convergence algorithm. As a result, the goals of this study are to optimize energy sources and reduce fuel consumption for three wheeler power-split HEV configurations, as well as to compare the results of MPC strategy with the results of rule-based strategy over standard cycles such as the HWFET(modified) cycle and Extra-Urban Driving Cycle(EUDC)(modified).

3 Mathematical Modelling of Hybrid Electric Vehicle

3.1 Hybrid electric vehicle architecture

The following are the primary types of HEVs:

- 1) parallel HEV
- 2) series HEV
- 3) parallel-series HEV

3.1.1 Parallel HEV

Electric motors and internal combustion engines (ICEs) can be separately powered or share propulsion power due to their mechanical coupling (Figure 3.1). Parallel setup is more complicated and costly, but it provides greater efficiency and performance.

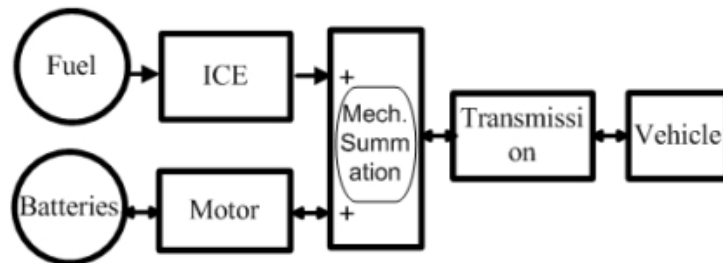


Figure 3.1: Electric Vehicle using Hybrid Technology in Parallel

3.1.2 Series HEV

There is no mechanical link between an electric motor and an internal combustion engine (ICE) (Figure 3.2). They are electrically connected, and the wheels are driven by a motor. All unique actions in series hybrid electric vehicles require two distinct energy conversion operations. Fuel to electricity conversion and electric to mechanical operation (motor) for wheel driving are examples of energy conversion activities.

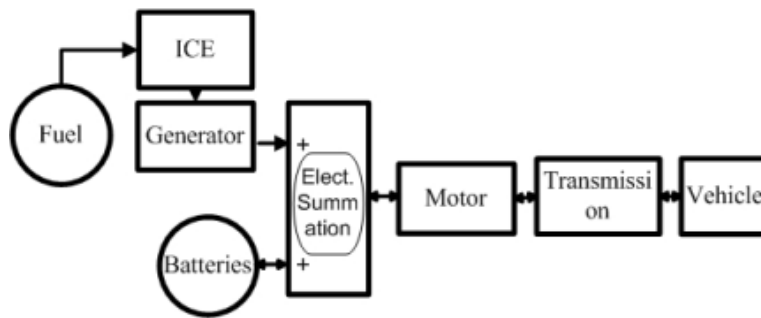


Figure 3.2: Series Hybrid Electric Vehicle

3.1.3 Parallel-series HEV

It (Figure 3.3) is a framework that combines parallel and series configurations. In general, it increases the all-electric range of a hybrid electric vehicle.

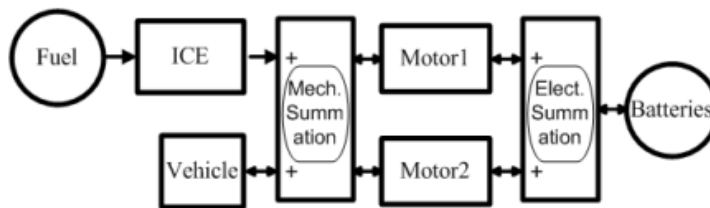


Figure 3.3: Parallel Series Hybrid Electric Vehicle .

All HEV arrangements can be utilized in PHEVs. There are two forms of battery consumption.

1. *Charge sustaining mode* is used in hybrid electric vehicles(HEVs) when the state of charge(SOC) at the start and conclusion of the journey remains constant.
2. *Charge draining mode*In plugin-hybrid electric vehicles (PHEVs), the batteries are charged using grid electricity, so they deplete to an acceptable minimal level at the conclusion of the journey.

3.2 Planetary gear-sets

Most typical geartrains have only one input and output, and consequently a single overall ratio. A planetary gearset is significantly more versatile than a simple gearbox since it has two inputs and

one output. Planetary gearsets are substantially more difficult to build and analyze than standard gearsets. Their application is made more challenging (but fascinating!) by their frequent display of very contradictory behavior. To determine a planetary gearset's performance and efficiency, a few straightforward standards may be employed, much as with conventional gearsets.

Shown in the figure 3.4 below is the most typical sort of planetary gear-set. One or more planets, a ring gear, a carrier (commonly referred to as the arm or the spider), and the sun make up its four main parts. The planets 'orbit' the sun, meaning that their shafts are not fixed in space, which is the main distinction between planetary gearsets and regular gearsets. The reason for this interesting phenomenon is the epicyclic motion.

Like other planetary gear-sets, the gear-set in figure 3.4 has two inputs and one output. The table 3.1 below shows that we are in total control of which shafts function as inputs and which as outputs. A single gear ratio for the set is often the result of one of the inputs being fixed. Certain situations, like a hybrid engine, have neither input fixed; instead, the speed of both inputs determines the output.

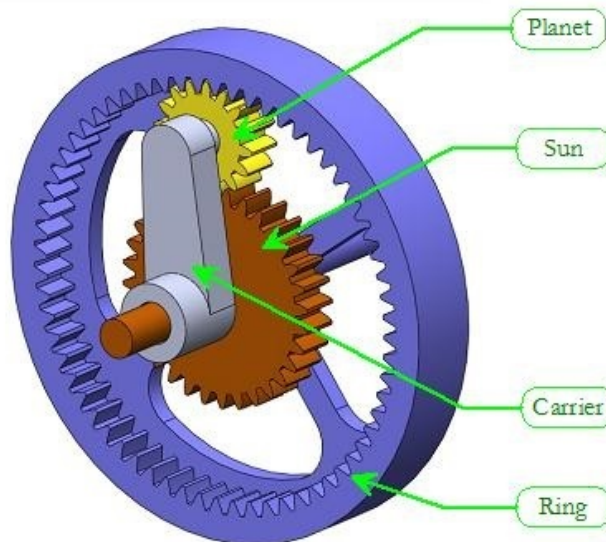


Figure 3.4: Planetary gear

The powertrain system of a hybrid electric vehicle (HEV) consists of an internal combustion engine (ICE) and a high-voltage battery. They utilize less gasoline than conventional cars because of

Option	Inputs	Output
1	sun and carrier	ring
2	ring and sun	carrier
3	ring and carrier	sun

Table 3.1: Possible planetary gear-set inputs and outputs

energy recovery from regenerative braking and improved power train efficiency with battery backup. Several automakers produce power-split (parallel-series) hybrid electric power train combinations, which offer both series and parallel functioning. The Ford Fusion Hybrid, Ford Escape Hybrid, and Toyota Prius are a few hybrid electric vehicles(HEVs) with a power-split drive-train. In this study, this particular kind of hybrid three wheeler car is chosen .

A hybrid electric vehicle (HEV) typically consists of an electric motor with a battery pack and an internal combustion engine (ICE). A hybrid electric vehicle (HEV) can utilize a minimum of five strategies to enhance fuel efficiency and minimize harmful emissions, dependent upon the design of the vehicle and level of hybridization.

IDLE-OFF CAPABILITY:The engine can be shut off while the car is stationary (idling). Pollution and fuel consumption may both be decreased by eliminating idle speed operation. If the vehicle comes to a stop at a traffic light, for example, the engine may be turned off and the HEV's all-electric propulsion can be used to power the auxiliary load.

REGENERATIVE BRAKING:When a vehicle brakes, the inertial forces it acquired during acceleration are released as heat. The electric motor has the ability to regenerate and store these inertial forces in the batteries. This might happen when an electric machine is being used to charge batteries. As a result, regenerative braking is used in all types of HEVs

POWER ASSIST:An electric motor may help the driver's power needs in addition to the ICE, depending on the HEV architecture.

ENGINE DOWNSIZING:Engine capacity design is also advantageous for fuel economy. The addition of an electric machine and a storage battery in a HEV increases the overall power delivered to the vehicle significantly. The engine is designed with a small power output in mind, allowing it to operate at peak efficiency while the motor provides the extra power.

ELECTRIC-ONLY DRIVE CAPABILITY:Depending on the HEV design and level of hybridization, the engine can be shut down and the vehicle operated entirely on electric power. Later on, the engine can be run at maximum efficiency, and the surplus power can be used to recharge the batteries.

This figure 3.5 illustrates the main components of a power-split HEV. In this configuration, the engine and generator are linked to the planet carrier and sun gear of a planetary gear set, respectively. Through the use of a torque coupler, the torque output from a planetary gear set ring and the output of a second motor/generator are combined to power the vehicle drive line. A battery offers an additional

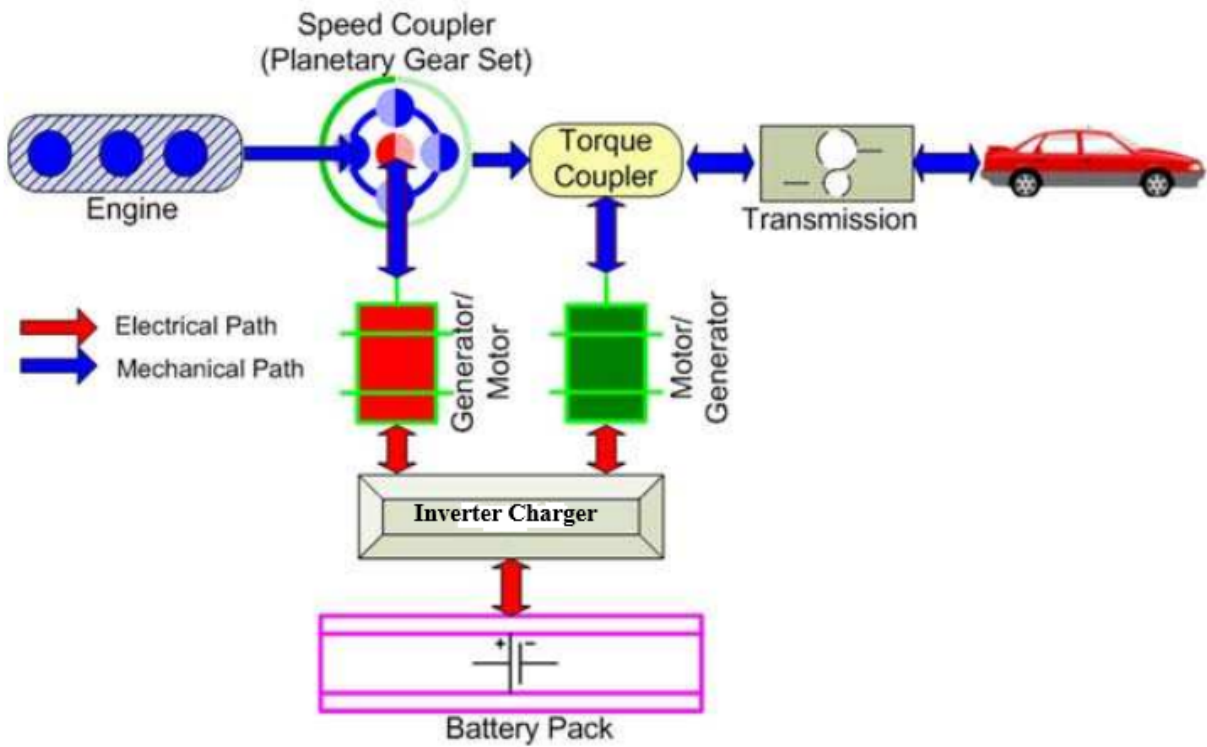


Figure 3.5: A Power-Split HEV Configuration

level of flexibility in terms of delivering or storing energy. Consequently, these hybrid electric vehicles(HEVs)’ power management has two degrees of freedom. A power-split hybrid electric vehicle’s two degrees of freedom and varied operating modes allow it to run more efficiently, lowering fuel consumption.

A power-management model for a power-split hybrid electric vehicle is derived in this section. Based on model predictive control, this model will be utilized to develop model-based power management techniques.

A power-split HEV component’s schematic diagram is displayed in Figure 3.6. The figure illustrates these electrical, engine, transmission, and chassis subsystems make up the HEV powertrain. An internal combustion engine converts the chemical power of fuel into mechanical energy, which is what largely drives HEVs. A planetary gear package combines engine and generator power in the transaxle. The planetary gear set’s ring gear and the motor’s power are combined via a torque coupler. The powertrain’s output speed is additionally decreased by a final drive. Three components make up

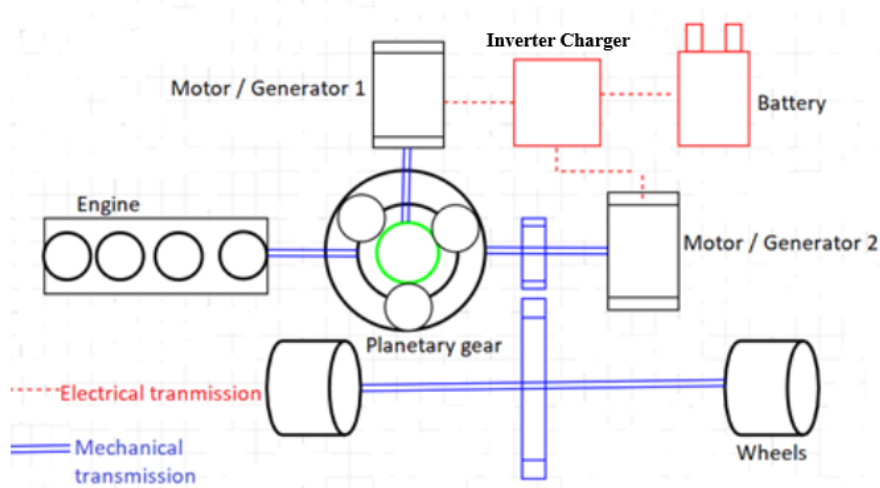


Figure 3.6: Schematic diagram of power-split configured hybrid electric vehicle.

the electrical system: a high voltage battery package, two electrical devices known as the motor and generator. Both driving and storing energy are possible with the battery.

3.3 Configuration of power split HEVs

A hybrid electric vehicle with a power split arrangement is seen in Figure 3.6. The following essential components make up this kind of hybrid electric vehicle: a battery, planetary gear set, generator motor set 1 (generator), generator motor set 2 (motor), which operates as a traction motor, and a smaller, more efficient internal combustion engine.

The key component is a planetary gear mechanism, which is made up of a ring gear, three or four planet gears linked to a common carrier, and a sun gear. The ring gear is connected to generator motor set 2 and the wheels of the vehicle by a gear ratio, while the sun gear is connected to generator motor set 1. The engine is connected to a common carrier. In order to keep things simple, generator motor set 1 will be remembered as a generator and generator motor set 2 as a motor. The carrier, ring, and sun gears are intended to be integrated with the engine, generator, and motor masses and shafts.

3.4 Simulation techniques

The simulation methodologies are divided into two groups based on the direction of power flow: forward-facing and backward-facing simulation.

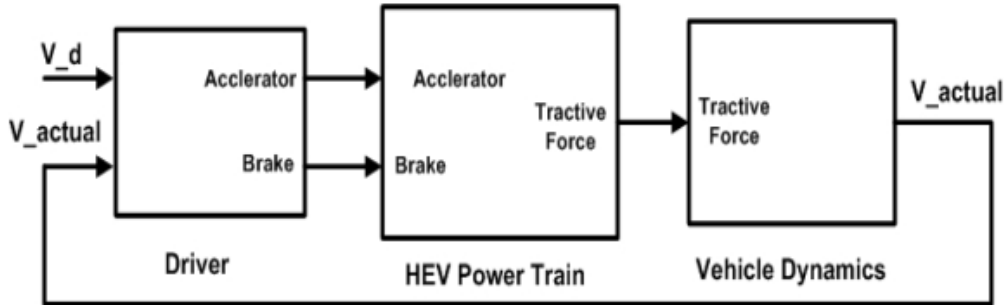


Figure 3.7: Forward-facing block diagram

3.4.1 Forward-facing simulation

The forward-facing simulation approach calculates power flow in the same direction as tractive energy flow. Figure 3.7 depicts the main Simulink block diagram. There are three main blocks: the driver, the HEV power train, and the vehicle dynamics blocks, and the consequence of this main block is the vehicle's actual velocity. Figure 3.8 depicts the information flow in a generic forward vehicle simulator. This approach is similar to a real-world driving scenario in which the vehicle is driven based on the driver's pedal position and brake inputs. The acceleration and braking orders are programmed by the driver to achieve the desired speed and braking. The throttle instruction is converted into real power/torque demand depending on the intended and actual speeds.

The energy management controller (HEV controller)'s primary function is to distribute torque between the ICE and the motor. Vehicle speed is achieved using tractive torques in conjunction with gearbox and vehicle dynamics. The fundamental advantage of the forward-facing approach is that quantities such as torques and command signals may be measured at each stage of a physical drivetrain. Energy management principles can thus be immediately applied to hardware.

The variables utilized in the Forward simulator are described in detail below.

V_d : Vehicle's velocity (desired) [m/s]

V_{actual} : Vehicle's velocity (actual)[m/s]

T_{req} : Engine Torque request [Nm]

T_{mreq} : Motor Torque request [Nm]

Brake req : Brake request [Nm]

P_{batt} : Battery Power [W]

T_e : Engine Torque outcome [Nm]

T_m : Motor Torque outcome [Nm]

P_{gb} : Power before gear box [W]

T_{tot} : Total Torque [Nm]

T_{racF} : Traction Force [N]

The following tasks can be carried out with this simulator:

1. Vehicle system behavior during defined driving cycles.

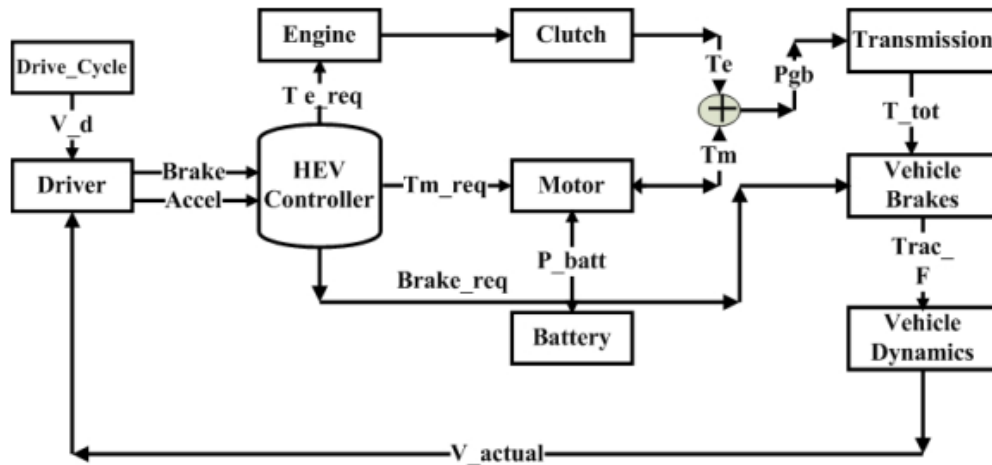


Figure 3.8: The forward simulator diagram

2. Calculate the battery's state of charge(SOC) and immediate and cumulative fuel usage.

This simulation technique's main disadvantage is its modest simulation speed. Along with the associated input and output signals, a detailed description of the fundamental parts of a forward vehicle simulator is provided.

3.4.2 Backward-facing Simulation

The power flow is calculated backward for the backward-facing simulation technique. As a result, this simulation technique is diametrically opposed to what happens in a real-world driving circumstance. It is predicated on the idea that every part ought to function as intended if the car adheres to the driving cycle. As a result, a driver model is not necessary for this type of simulation approach. This technique converts the anticipated or calculated quantities at the wheels to the quantities at the power sources' outputs. The controller's job is to divide the power/torque request among the energy sources, such as an internal combustion engine(ICE) and an electric motor(EM). So the backward simulation technique is ineffective for controller design and validation. This method's simplicity and computation speed are its main advantages. As a result, this technique is commonly utilized in HEV simulations. Figure 3.9 depicts the information flow in the reverse simulator. The following tasks can be carried out with this simulator. Evaluation of instantaneous and cumulative fuel consumption and determination of SOC of the battery;

Figure 3.9 depicts various components of a backward vehicle simulator, together with the relevant input and output signals. The variables utilized in the backward simulator are described further below. The battery's state of charge (SOC) pattern and the total fuel consumption are produced by this simulator.

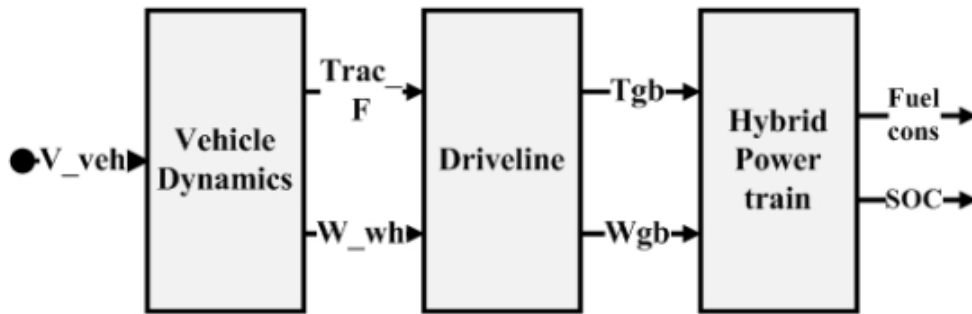


Figure 3.9: Backward Simulator model

The variables utilized in the Backward simulator are described in detail below.

V_{veh} : Vehicle velocity [m/s]

SOC : State of charge

W_{wh} : Speed at wheel [rad/s]

T_{gb} : Torque before gear box [Nm]

W_{gb} : Speed before gear box [rad/s]

$T_{rac}\ F$: Traction Force [N]

3.5 Gear forces

Since the gear's contact force in figure 3.10 is tangent to both gears, the torque it generates is equal to the force multiplied by the radius.

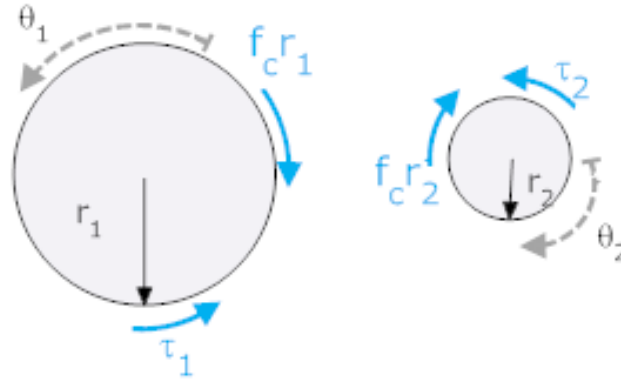


Figure 3.10: Gear force

We can do a torque balance on each of the two gears

Gear 1

$$\tau_1 = f_c r_1 \quad \text{so } f_c = \frac{\tau_1}{r_1}$$

Gear 2

$$\tau_2 = f_c r_2 \quad \text{so } f_c = \frac{\tau_2}{r_2}$$

We are not usually interested in f_c , so we remove from the equations and we get

$$\frac{\tau_1}{r_1} = \frac{\tau_2}{r_2}$$

$$\tau_1 r_2 = \tau_2 r_1$$

As a result, the force acting on the planetary gear's Sun and Ring gear teeth is equal, and for the sake of this research, that force is represented by F.

It is simple to demonstrate that the same connection applies even when the contact pressures are defined in the opposite direction (up on gear 1 and down on gear 2).

3.6 Mathematical modelling of three wheeler power split HEV

Dynamics of three wheeler power split HEV

Figure 3.11 depicts the power-split HEV power train configuration. The planetary gear has three nodes: the sun gear, the carrier gear, and the ring gear, which are connected to the generator (MG1), engine, and vehicle, respectively. An extra electric motor (MG2) is connected to the ring gear enabling direct motor propulsion and efficient regenerative braking. The engine delivers power to the vehicle via two paths: mechanical and electrical. The mechanical path transmits power from the carrier gear to the ring gear, which is subsequently connected to the vehicle's final drive. The planetary gear transfers some of the engine's power. The generator transforms power to electricity. The electricity is then transmitted to either the battery or an electric motor. The electrical path for engine power is less efficient than the mechanical path in terms of instantaneous efficiency. However, storing energy in the battery allows for more efficient use later, improving overall vehicle fuel economy.

An electric motor and internal combustion engine are both used to charge the battery in a hybrid electric vehicle (HEV) equipped with a planetary gear system. This is a general rundown of how it functions:

1. **Regenerative Braking:** The vehicle's kinetic energy is converted into electrical energy by the electric motor, which functions as a generator when the automobile slows down. After that, the battery is recharged using this energy.
2. **Engine-Generated Power:** When the internal combustion engine is running and creating more power than is required for propulsion, the excess power can be diverted to the electric motor, which then serves as a generator, charging the battery.

The planetary gear set divided the engine's power between driving the wheels and powering the generator that charged the batteries. This technology optimizes the engine's output, decreases fuel consumption, and keeps the battery charged, all of which contribute to the HEV's overall efficiency. For specific details on how this system operates in a particular vehicle model, it's best to consult the manufacturer's technical documentation.

The mechanical connection through gear teeth meshing ensures that the rotational speed of the ring gear ω_r , sun gear ω_s , and carrier gear ω_c always follows the following relationship:

$$R\dot{\omega}_s + S\dot{\omega}_r = \dot{\omega}_c(S + R) \quad (3.1)$$

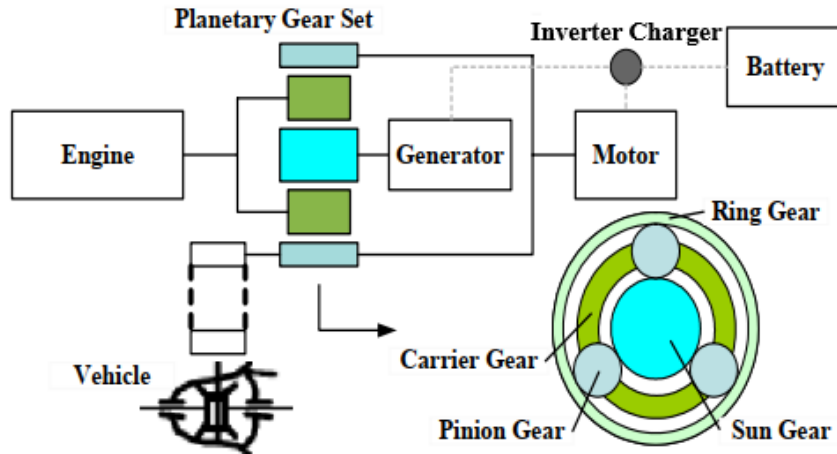


Figure 3.11: Power train configuration of the Toyota Hybrid System

The planetary gear has three "nodes" but only two degrees of freedom due to the speed constraint (equation 3.1). The planetary gear connects three power devices, allowing for separate input torques from the engine, motor, and generator. The rotational speeds are calculated using the Euler equation.

Figure 3.12 depicts the free body diagram, which includes rotational degrees of freedom for translational motions. The dash-line box highlights the planetary gear system and its internal forces. The pinion gears are assumed to be lightweight and act as an efficient force transmission system. Applying Euler's law, we have

$$\dot{\omega}_r I_r = FR - T_r \quad (3.2)$$

$$\dot{\omega}_c I_c = T_c - FR - FS \quad (3.3)$$

$$\dot{\omega}_s I_s = FS - T_s \quad (3.4)$$

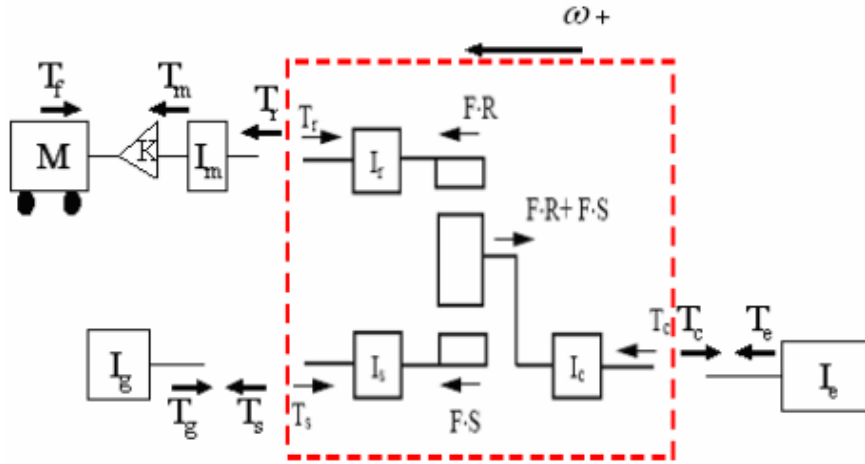


Figure 3.12: Free body diagram of the mechanical path.

In this equation, T_r , T_s , and T_c represent the torques on the ring gear shaft, sun gear shaft, and carrier shaft, whereas I_r , I_s , and I_c represent the inertia. F represents the internal force on the pinion gear. To simplify the equations, we assume no viscous or Coulomb friction. The three power sources outside the planetary gear affect the total system's motion by exerting torque on their respective inertia. Moving to the left indicates positive motion for all inertias. Positive engine and motor torque lead to vehicle acceleration. The generator torque was defined as positive to resist vehicle motion. Positive generator torque slows the vehicle and extracts power from the system. For the generator inertia, the governing equation is

$$\dot{\omega}_g I_g = T_s - T_g \quad (3.5)$$

T_g represents the generator's input torque, whereas g and I_g represent its rotary speed and inertia. Based on 3.4 and 3.5, we have:

$$\dot{\omega}_g (I_g + I_s) = FS - T_g \quad (3.6)$$

On the carrier gear shaft, the engine speed is determined by the equation.

$$\dot{\omega}_e I_e = T_e - T_c \quad (3.7)$$

T_e represents the engine torque, whereas e and I_e represent the engine's rotational speed and inertia. From 3.3 and 3.7.

$$\dot{\omega}_e (I_e + I_c) = T_e - FR - FS \quad (3.8)$$

Figure 3.11 depicts a schematic of a power-split HEV arrangement. The split of engine power by a speed coupler (planetary gear set) allows both series and parallel power flow modes, which distinguishes this arrangement from the series and parallel variants. Because the thesis is focused on a model-based optimization technique, this section includes the development of a system model. For further details, please refer to the literature [34, 35].

The following assumptions have been made:

- The dynamics of an engine, motor, and generator are faster than those of a powertrain and vehicle.
- The motor is directly connected to the speed coupler's ring gear.
- When compared to other causes of power losses, power loss in the final transmission may be neglected.
- All of the components connecting the motor to the wheel are rigid.

As a result, the dynamics of a backward-facing power split HEV may be reduced to those of the vehicle and battery.[36, 37, 38, 39]

Assuming minimal pinion gear inertia and neglecting vehicle dynamics except along the longitudinal direction, backward-facing vehicle dynamics may be represented as follows [36, 37].

First the power-train dynamics are as follows:

$$I_g \frac{d\omega_g}{dt} = -T_g + F \times S \quad (3.9)$$

$$I_e \frac{d\omega_e}{dt} = T_e - F \times (S + R) \quad (3.10)$$

$$\left(I_m + \frac{I_w}{g_f^2} + \frac{mr_w^2}{g_f^2} \right) \frac{d\omega_m}{dt} = T_m - \frac{T_d}{g_f} + F \times R \quad (3.11)$$

$$m \frac{dv}{dt} = \frac{T_d}{r_w} - \frac{1}{2} \rho A_f C_d v^2 - mg \sin(\theta) - \mu mg \cos(\theta) \quad (3.12)$$

Where as:

- S—The number of teethes of sun gear
- R—The number of teethes of ring gear
- F—Contact force acting on each teeth of planetary gear components
- I_g —generator inertia
- I_e —engine inertia
- I_m —Motor inertia and
- I_w —represent Wheel Inertia

And:

- $\frac{T_d}{r_w}$ —Traction Force
- $\rho A_f C_d v^2$ —Aerodynamic drag resistance
- $m_g \sin(\theta)$ —Grading Resistance

- $\mu mg \cos(\theta)$ —Rolling resistance

The symbols for the torques are:

- T_e —Torques of an ICE engine
- T_g —Torques of generator
- T_m —Torques of motor and
- T_d — Required driver torque based on the driving cycle.

The speed are denoted by:

- ω_e —Speed of engine
- ω_g —Speed of generator and
- ω_m —Speed of motor

The hybrid electric Vehicle's parameters are as follows:

- v is vehicle's speed
- m is Vehicle's mass
- A_f is Vehicle's frontal area
- r_w is Vehicle's wheel radius

The following constant represent:

- μ —Rolling resistance
- C_d —Drag Coefficient
- ρ —Air Density and

- g_f —Final drive ratio
- g —gravitational acceleration
- θ — road slope which is zero in this case

The following formula limits the planetary gear speeds [36, 37].

$$R\omega_m + S\omega_g = (S + R)\omega_e \quad (3.13)$$

The driving cycle's data points can be used to determine the motor's rotational speed, which is represented by the following equation [37].

$$\omega_m = \frac{g_f V}{r_w} \quad (3.14)$$

Where V represents the vehicle's speed.

The battery dynamics may be summarized in the form of state of charge as shown below [36, 37].

$$\frac{dS_{oc}}{dt} = - \frac{V_{oc} - \sqrt{V_{oc}^2 - 4R_b P_b}}{2R_b Q_b} \quad (3.15)$$

$$P_b = T_m \omega_m \eta_m + \frac{T_g W_g}{\eta_g} \quad (3.16)$$

where the battery's charging state, open-circuit voltage, internal resistance, power, and capacity are denoted by the variables S_{oc} , V_{oc} , R_b , P_b , and Q_b , respectively. Additionally, it is assumed that the generator and motor have respective efficiencies of 84% and 94%. The behavior of an engine in relation to the mass flow rate of fuel can be roughly described for the control-oriented vehicle model

as [37].

$$\dot{m}_f \approx C_f (P_{req} - P_b) \quad (3.17)$$

The mass flow rate of fuel is denoted by \dot{m}_f , the battery power at a particular time is denoted by P_b , a constant is C_f , and the needed power at the wheels at a given instant is denoted by P_{req} , which is calculated based on the required torque and steering angle at the wheels.

Taking time derivative of equation 3.13

$$R \frac{d\omega_m}{dt} + S \frac{d\omega_g}{dt} = (S + R) \frac{d\omega_e}{dt} \quad (3.18)$$

By arranging the above equation,

$$\frac{d\omega_g}{dt} = \frac{1}{S} [(S + R) \frac{d\omega_e}{dt} - R \frac{d\omega_m}{dt}] \quad (3.19)$$

Substitute equation 3.19 into equation equation 3.9 gives

$$\frac{I_g}{S} [(S + R) \frac{d\omega_e}{dt} - R \frac{d\omega_m}{dt}] = -T_g + F \times S \quad (3.20)$$

Setting up the equation above and designating F as its owner results in

$$F = \frac{I_g}{S^2} [(S + R) \frac{d\omega_e}{dt} - R \frac{d\omega_m}{dt}] + \frac{T_g}{S} \quad (3.21)$$

Substituting equation 3.21 into 3.10 yields

$$I_e \frac{d\omega_e}{dt} = T_e - \left[\frac{I_g}{S^2} [(S + R) \frac{d\omega_e}{dt} - R \frac{d\omega_m}{dt}] + \frac{T_g}{S} \right] (S + R) \quad (3.22)$$

Rearranging the above equation gives

$$\left[I_e + I_g \left(\frac{S+R}{S} \right)^2 \right] \frac{d\omega_e}{dt} - \left[\frac{R(S+R)}{S^2} I_g \right] \frac{d\omega_m}{dt} = T_e - \frac{(S+R)}{S} T_g \quad (3.23)$$

Substituting equation 3.21 into 3.11 gives

$$\left(I_m + \frac{I_w}{g_f^2} + \frac{mr_w^2}{g_f^2} \right) \frac{d\omega_m}{dt} = T_m - \frac{T_d}{G_f} + \left[\frac{I_g}{S^2} \left((S+R) \frac{d\omega_e}{dt} - R \frac{d\omega_m}{dt} \right) + \frac{T_g}{S} \right] R \quad (3.24)$$

Rearranging the above equation yields

$$\left[I_m + \frac{I_w}{g_f^2} + \frac{mr_w^2}{g_f^2} + \left(\frac{R}{S} \right)^2 I_g \right] \frac{d\omega_m}{dt} - \left[\frac{R(S+R)}{S^2} I_g \right] \frac{d\omega_e}{dt} = T_m + \frac{R}{S} T_g - \frac{T_d}{G_f} \quad (3.25)$$

Combining Equation 3.23 and (3.25 gives a matrix

$$\begin{bmatrix} I_e + \left(\frac{S+R}{S} \right)^2 I_g & -\frac{R(S+R)}{S^2} I_g \\ -\frac{R(S+R)}{S^2} I_g & I_m + \frac{I_w}{g_f^2} + \frac{mr_w^2}{g_f^2} + \left(\frac{R}{S} \right)^2 I_g \end{bmatrix} \begin{bmatrix} \frac{d\omega_e}{dt} \\ \frac{d\omega_m}{dt} \end{bmatrix} = \begin{bmatrix} T_e - \left(\frac{S+R}{S} \right) T_g \\ T_m + \left(\frac{R}{S} \right) T_g - \frac{T_d}{G_f} \end{bmatrix} \quad (3.26)$$

so

$$\begin{bmatrix} \frac{d\omega_e}{dt} \\ \frac{d\omega_m}{dt} \end{bmatrix} = \begin{bmatrix} I_e + \left(\frac{S+R}{S} \right)^2 I_g & -\frac{R(S+R)}{S^2} I_g \\ -\frac{R(S+R)}{S^2} I_g & I_m + \frac{I_w}{g_f^2} + \frac{R}{S} I_g + m \frac{r_w^2}{G_f^2} \end{bmatrix}^{-1} \begin{bmatrix} T_e - \left(\frac{S+R}{S} \right) T_g \\ T_m + \left(\frac{R}{S} \right) T_g - \frac{T_d}{G_f} \end{bmatrix} \quad (3.27)$$

Let

$$T = \begin{bmatrix} I_e + \left(\frac{S+R}{S} \right)^2 I_g & -\frac{R(S+R)}{S^2} I_g \\ -\frac{R(S+R)}{S^2} I_g & I_m + \frac{I_w}{g_f^2} + \frac{R}{S} I_g + m \frac{r_w^2}{G_f^2} \end{bmatrix} \quad (3.28)$$

so

$$\begin{bmatrix} \frac{d\omega_e}{dt} \\ \frac{d\omega_m}{dt} \end{bmatrix} = T^{-1} \begin{bmatrix} T_e - \left(\frac{S+R}{S} \right) T_g \\ T_m + \left(\frac{R}{S} \right) T_g - \frac{T_d}{G_f} \end{bmatrix} \quad (3.29)$$

Again let

$$T^{-1} = \begin{bmatrix} A_1 & A_1 \\ A_3 & A_4 \end{bmatrix} \quad (3.30)$$

Then

$$\frac{d\omega_e}{dt} = A_1 T_e + A_2 T_m + \left(A_2 \frac{R}{S} - A_1 \frac{S+R}{S} \right) T_g - A_2 \frac{T_d}{G_f} \quad (3.31)$$

The aforementioned dynamics of the power-split HEV may be simplified to the following nonlinear model where the speed is known from the driving cycle, such as the Extra-Urban Driving Cycle (EUDC): [36, 37].

$$\dot{x} = f(x, u) \quad (3.32)$$

$$x^T = [m_f, soc, \omega_e] \quad (3.33)$$

$$u^T = [T_e, T_g, T_m, \omega_g] \quad (3.34)$$

$$f(x, u) = \begin{bmatrix} c_f (P_{req} - P_b) \\ -\frac{V_{oc} - \sqrt{V_{oc}^2 - 4R_b P_b}}{2R_b Q_b} \\ A_1 T_e + A_2 T_m + \left(A_1 \frac{S+R}{S} - A_2 \frac{R}{S} \right) T_g - \frac{A_2}{g_f} T_d \end{bmatrix} \quad (3.35)$$

subject to the following constraints:

$$\dot{m}_{f \min} \leq \dot{m}_f \leq \dot{m}_{f \max}$$

$$soc_{\min} \leq SOc \leq soc_{\max}$$

$$\omega_{e \min} \leq \omega_e \leq \omega_{e \max}$$

$$T_{e \min} \leq T_e \leq T_{e \max}$$

(3.36)

$$T_{g \min} \leq T_g \leq T_{g \max}$$

$$T_{m \min} \leq T_m \leq T_{m \max}$$

$$\omega_{g \min} \leq \omega_g \leq \omega_{g \max}$$

3.7 Model verification

In three-wheeler hybrid electric vehicle(HEV) dynamics, four control inputs (Tm-U1, Te-U2, Tg-U3, and Wg-U4) are used to evaluate the model. Different input values are used to observe how they affect the states and speed compared to the reference input.

Symbols	Value	Symbols	Value
m	610kg	V_{oc}	174V
A_f	$1.86m^2$	R_b	1.12
C_d	0.44	Q_b	6Ah
ρ	$1.2kg/m^3$	SOC_{max}	0.75
μ	0.015	G_f	4.24
g	$9.81m/s^2$	C_f	0.0874
I_E	$0.18kgm^2$	R	78
I_m	$0.0226kgm^2$	S	30
I_g	$0.0226kgm^2$	I_w	$3.3807kgm^2$
η_m	0.94	η_g	0.84
R_w	0.2m		

Table 3.2: Different parameters used for model Verification

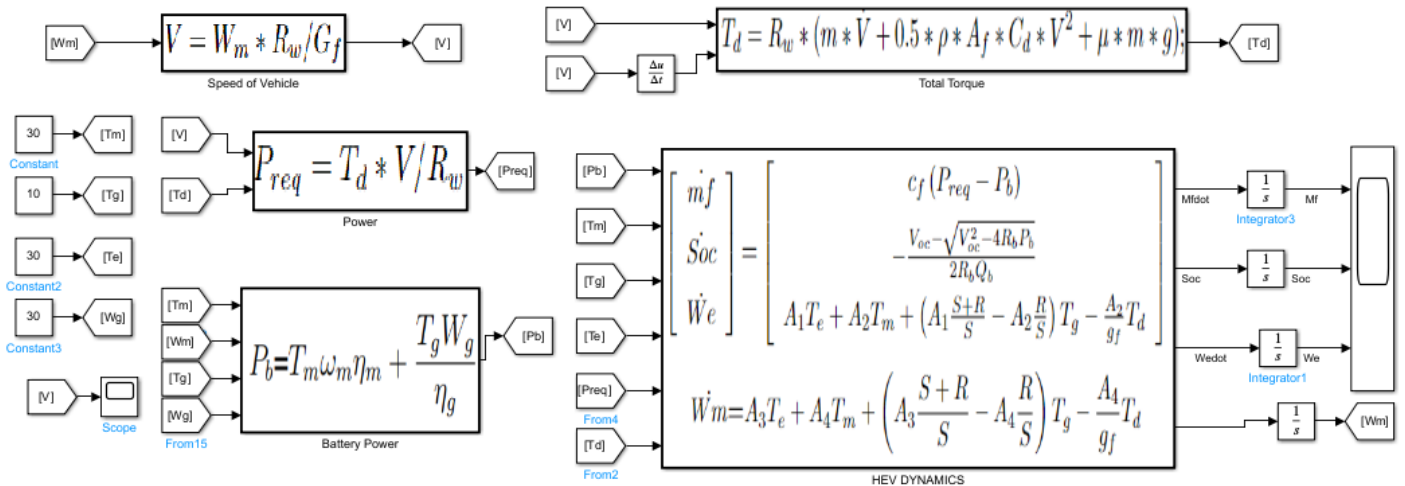


Figure 3.13: Model Verification

figure 3.14 and figure 3.15 show the the plot of the states and speed when the inputs are equal to the reference values (Tm=30,Tg=10,Te=30 and Wg=30) . This model verification part compares

these outputs to outputs with varied input values.

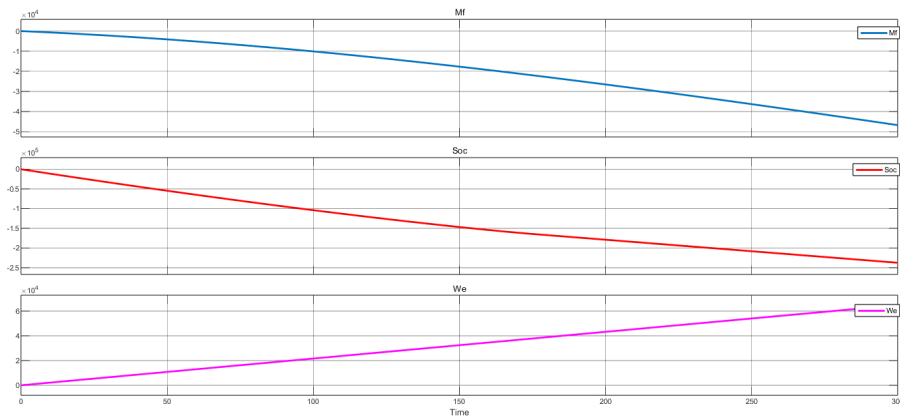


Figure 3.14: The states plot for the reference input value

1. figure 3.16 and figure 3.17 show the the plot of the states and speed when the reference value of input T_m changed to $T_m=40$. The figures show

- The decreasing of mf
- The Soc decreases
- The same or unaffected We
- The Increasing of V

2. figure 3.16 and figure 3.19 show the states and speed when the reference value of input T_e changed to $T_e=40$. The figures show

- The increasing of mf

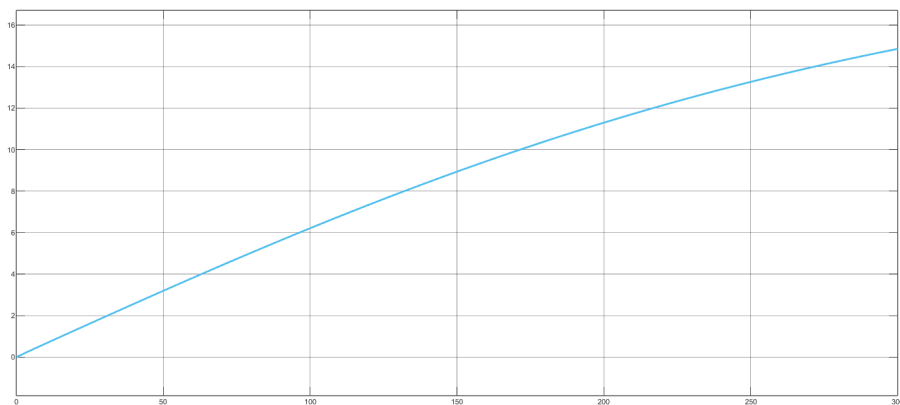


Figure 3.15: Vehicle speed plot for the reference value

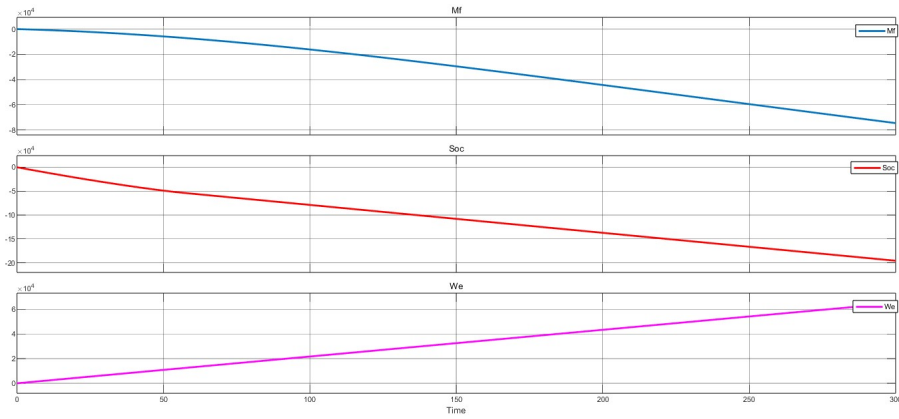


Figure 3.16: The states plot for $T_m=40$

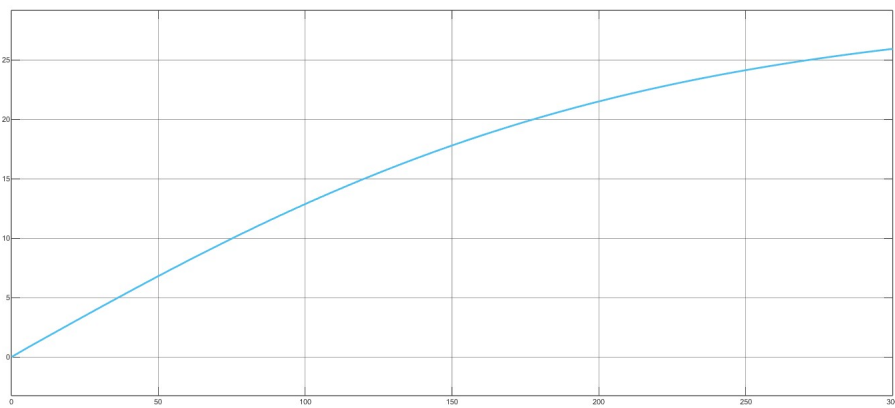


Figure 3.17: Vehicle speed plot for $T_m=40$

- The increasing of Soc
- The same or unaffected We
- The Increasing of V

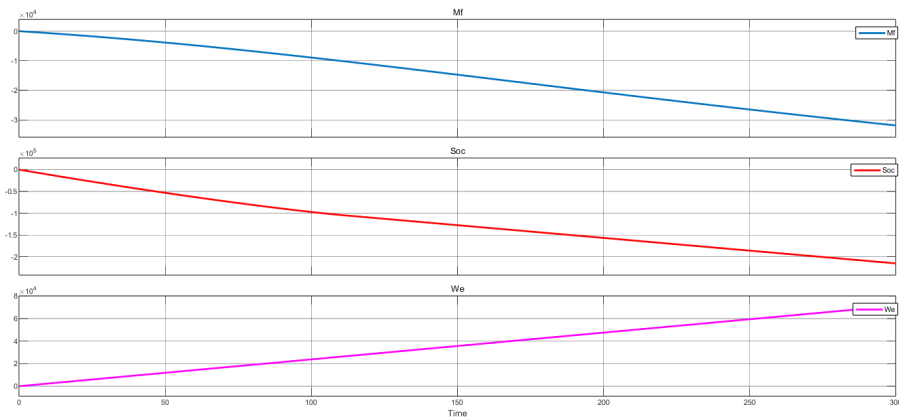


Figure 3.18: The states plot for $T_e=40$

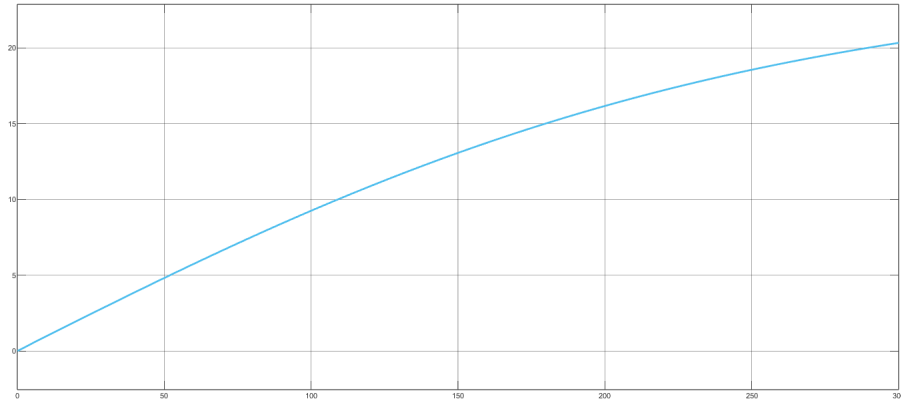


Figure 3.19: Vehicle speed plot for $T_e=40$

3. figure 3.20 and figure 3.21 show the states and speed when the reference value of input W_g changed to $W_g=40$. The figures show

- The decreasing of mf
- The increasing Soc
- The same We or unaffected We
- The same or unaffected V

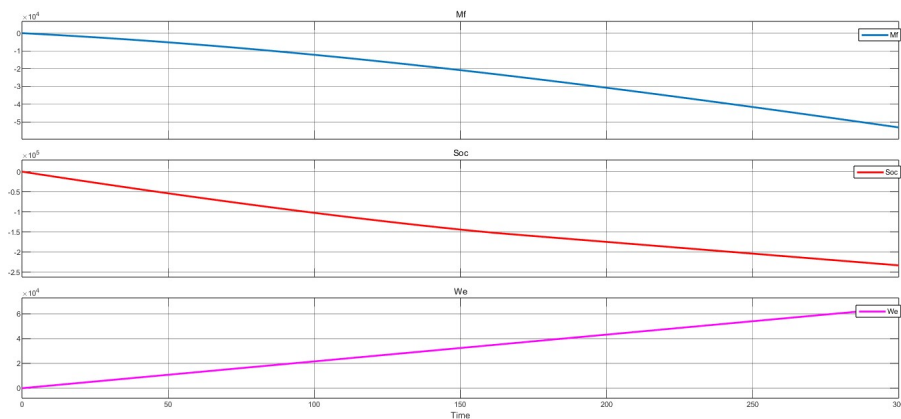


Figure 3.20: The states plot for $W_g=40$

4. figure 3.22 and figure 3.23 show the plot of the states and speed when the reference value of input T_g changed to $T_g=10$. The figures show

- The increasing of mf
- The increasing of Soc

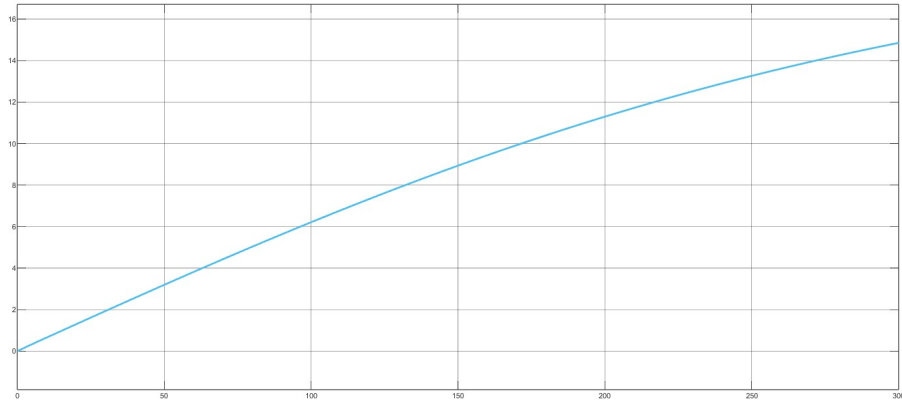


Figure 3.21: Vehicle speed plot for $Wg=40$

- The same or unaffected We
- The Increasing of V

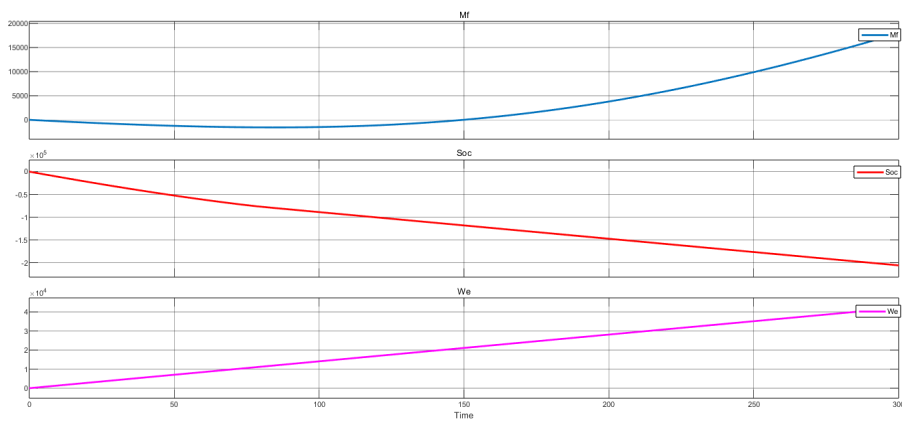


Figure 3.22: The states plot for $Tg=10$

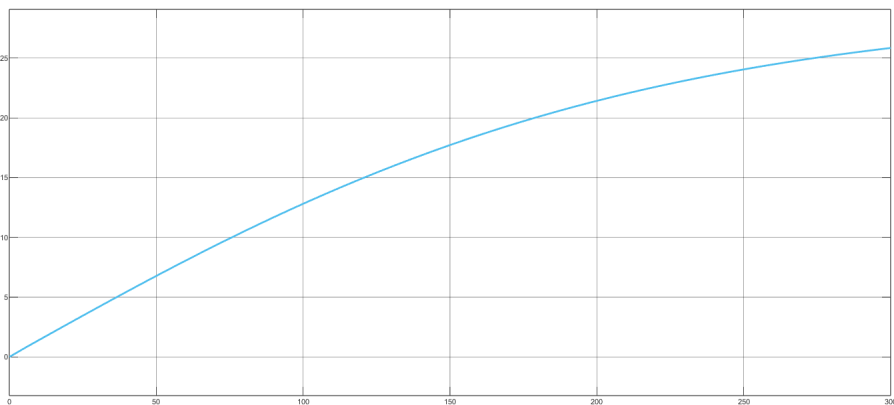


Figure 3.23: Vehicle speed plot for $Tg=10$

4 Energy Management Strategy

The EMS control approach is to meet the driver's power request while minimizing fuel consumption, reducing greenhouse gas emissions, and ensuring vehicle performance and driveability. Fuel efficiency and emission reduction are incompatible goals. So, in a control plan, a trade-off exists between two objectives.

The literature describes several types of energy management techniques, each with its own set of characteristics and implementation options. Guzzella and Sciarreta [40] proposed the following subdivisions:

1. Numerical optimization solutions involve analyzing the entire drive cycle and searching for global optimizations. This category includes dynamic programming, stochastic dynamic programming, predictive modeling, and numerical search approaches.

2. Analytical optimization methodologies consider the entire drive cycle by formulating a problem and searching for solutions in analytical form, resulting in faster numerical solutions. This category includes Pontryagin's minimum principle and the Hamilton-Jacobi-Bellman equation.

3. Equivalent consumption minimization techniques aim to minimize a well-defined instantaneous cost function at each step of the optimization process, thereby lowering the global cost function.

Multiple criteria are used to categorize HEV energy management methods. The literature classifies optimization methods into three categories based on the amount of information used. Optimization strategies include global and local approaches, as well as heuristic methods.

1. Global optimization strategies, whether numerical or analytical, require knowledge of past, present, and future driving conditions. This category includes dynamic programming and Pontryagin's Minimum Principle.

2. Local optimization solutions convert the global optimal problem into a series of local optimal problems. Stochastic dynamic programming, energy control management strategy (ECMS), and

model predictive control fall under this group.

3. Heuristic strategies, depending on the manner of operation, Rule-based control strategies are fundamental control methods. Rules are created using mathematical models, human intellect, and heuristics, without prior knowledge of the drive cycle. Static behavior is present in these controllers.

We compare techniques based on their solution type (Global or Local), computation time, structural complexity, and prior knowledge of driving patterns. Structural complexity includes complexity classes, the relationships between them, and the internal structure of those classes. Computation time refers to how long it takes to complete a process. Robustness refers to a controller's ability to perform well under specific assumptions for a given set of parameters. In the presence of uncertainty, robust controllers are constructed with specific parameters or disturbance sets. An optimization problem having a local optimal point (either maximal or minimal) results in a solution inside a neighboring set of solutions. Unlike local solutions, a global optimal solution encompasses all possible options.

Hybrid Electric Vehicles are made up of many types of energy sources and power converters, and they often combine an internal combustion engine(ICE) with an electric motor. HEVs appear to be the most economically viable answer so far, and likely for the future decades. The overall goal of developing HEVs is to reduce fuel consumption and emissions while meeting drivers' power demands by studying effective energy control management strategy(ECMS). Energy management seeks to achieve an ideal power split under complex driving conditions while minimizing fuel consumption and pollutants. It is well known that gains in hybrid electric vehicle(HEV) fuel efficiency, and consequently emissions reductions, are heavily reliant on energy control management strategy(ECMS) [41]. The complex configuration and behavior of multi-source hybrid energy systems limit EMS performance. The EMS aims to rapidly adjust power flows from energy converters to achieve control objectives, regardless of the powertrain topology [42]. The optimal control algorithms utilized during a particular driving cycle provide a sample research outline in the subject of energy management strategies.

This thesis compares a rule-based control technique with a model predictive control (MPC) strategy for managing energy in a three-wheeler hybrid electric vehicle.

4.1 Rule-based control strategies

In general, rule-based EMSs may be developed by creating logical rules based on the HEV system's properties and operating mode. The rules are derived using a "if-then" structure that considers the battery's level of charge, driver power demand, and vehicle velocity. Given these principles, the power split may be used to fulfill the driver's power requirements while maintaining the SOC within a certain range. Rather than previous knowledge of the driving cycle, this technique is based on logical principles and local constraints. The control parameters cannot be altered owing to a lack of future knowledge about the driving cycle, making it less adaptable to changing driving circumstances. Rule-based control strategies typically take two approaches: deterministic rule-based control and fuzzy rule-based control.

4.1.1 Deterministic rule-based EMSs

In this approach, a series of logical rules are created based on the engine map and motor efficiency map to divide power between the engine and motor, taking into consideration both the motor's efficiency and the engine and battery's state of charge. Because of their simplicity, control rules can be easily implemented online using a look-up table. Thus, it is commonly used in commercial vehicle controller applications. The standards are frequently developed based on certain driving cycles (for example, EUDC). However, the shifting traffic conditions limit its adaptability to varied driving cycles. Peng et al. [35] demonstrate a rule-based EMS for a parallel hybrid electric vehicle.

As a result, traditional rule-based power management is inefficient for real-world driving cycles because there is no unique technique to designing logical rules. In most cases, this is determined by the engineer's driving history and cycles. The next subsections go into greater information about rule-based techniques, such as on/off and power follower energy management strategy(EMS).

I. on/off EMSs This technique ensures that a battery SOC remains between its predetermined minimum and maximum criteria when the engine is turned on or off. The essential control rules are as follows.

A. When the battery's state of charge(SOC) falls below the minimal threshold, the engine operates

in the maximum efficiency or sub-optimal emissions region, providing constant power. A portion of the engine power is delivered to the motor to meet its power requirements, while the remainder is used to charge the battery.

B. When the battery SOC reaches the pre-set maximum threshold, the engine is turned off, leaving just the battery to power the vehicle.

In some situations, this energy management strategy(EMS) may provide a surge of instantaneous power from the battery, shortening the battery charge and discharge period and increasing the frequency with which the engine starts and stops. The main benefit is that the engine's average efficiency increases and the battery charging and discharging duration shortens, but it also has certain drawbacks, such as increased power loss owing to frequent engine start-stop, lower total energy efficiency, and shorter battery life [43]. Although this method is simpler than the ideal energy management strategy(EMS), it cannot meet the vehicle's power needs under all operating scenarios.

II. The power follower energy management strategy(EMS) To meet the driver's power need, the output engine power and the time to start or shut down the engine are determined based on the battery SOC and vehicle load, respectively. The control rules are as follows.

A. If the power demand is less than the engine's maximum power at its operating speed, the operation point is set to work at the lowest output power line.

B. If the battery state of charge(SOC) is higher than the preset minimum value and lower than the maximum value, and the driver power demand is less than the battery capacity but greater than the maximum engine power at the operating speed, the engine operates at the maximum output power line, with the battery supplying the remainder of the power demand.

C. If only the battery state of charge(SOC) exceeds the preset maximum value and can meet the power demand, the engine should be turned off. The key advantage of this method is that it reduces the frequency of battery charging and discharging while also lowering system energy loss, hence extending battery life. This technology improves the adaptability of engine output power to power demand, but the engine operation zone expands, lowering overall efficiency.

Rule-based energy management strategies (EMS) are straightforward to implement online; nevertheless, they are not ideal and cannot provide optimal performance for a wide range of driving cycles. It is also unable to adjust the control parameters to get the optimum fuel efficiency due to the complexity of the driving circumstances.

4.1.2 Fuzzy logic-based EMSs

Fuzzy logic control theory is a hybrid of fuzzy set theory and fuzzy logic. The first extends TRUE and FALSE (1 and 0) set theory, whereas the second extends ordinary logic in output selection [44]. Fuzzy relations rely largely on data set similarity, and fuzzy reasoning is articulated using the IF-THEN format, giving birth to several notable reasoning techniques, such as the Mamdani method [45] and the Takagi-Sugeno method [46].

Fuzzy logic-based EMSs aim to distribute electricity using fuzzy principles. Fuzzy logic rules are often developed using the driver's power demand and state of charge (SOC). A fuzzy logic controller consists of a set of linguistic rules, each with one antecedent and two outcomes. Looking at a hybrid system as a nonlinear and time-varying plant, fuzzy logic controllers may be implemented in real-time with suboptimal control utilizing a set of fuzzy logic rules. Furthermore, establishing a membership function is crucial for optimizing the power distribution. In the reference [47], the membership function is improved using GA.

4.2 Model Predictive Control

In a control problem, the controller's goal is to compute the input to the plant so that the output matches the intended reference. This input is computed using a MPC technique, which predicts the plant's future output. MPC employs a plant model to anticipate future plant behavior. The optimizer ensures that the expected future plant output matches the desired reference.

Model predictive control improves a system's output by calculating its input trajectory [48]. The key idea behind MPC is that future control output is projected via online optimization based on historical data as well as future input and output. Figure 4.1 shows a simple schematic of an MPC. In the case that the reference and expected outputs disagree, the control sequence can be calculated by combining the historical input, historical output, and predictive input.

Model predictive control (MPC) has become more popular in energy management strategies. MPC-based energy management strategies (EMSs) optimize power splits across a prediction horizon and update control inputs by translating global optimization into local optimization for the whole driving state. Compared to prior energy management systems (EMSs), MPC employs a rolling horizon optimization technique based on system prediction data. An MPC has the benefit of explicitly controlling constraints like state variables, input, and output. To anticipate system dynamics, constraints might be treated as quadratic or nonlinear programming problems (Huang, 2017). Traditional optimization techniques are inadequate in addressing the implications of unexpected future operating circumstances on vehicle performance. MPC efficiently addresses this problem by local optimization, rolling optimization, and feedback correction.

Since the late 1970s, MPC has seen significant development. MPC is not a specific control technique, but rather a collection of methods that employ a model to minimize a cost function and generate appropriate control inputs. The process involves predicting future output using a model, calculating control inputs based on a cost function, moving the prediction horizon, and repeating the process. Figure 4.2 illustrates the basic notion of MPC.

A prediction model is used to forecast future outputs based on current and past input and output

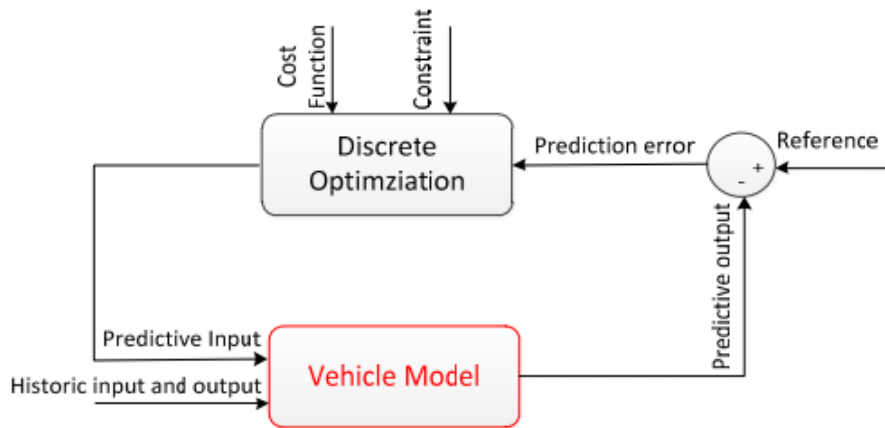


Figure 4.1: The principle of the model predictive control

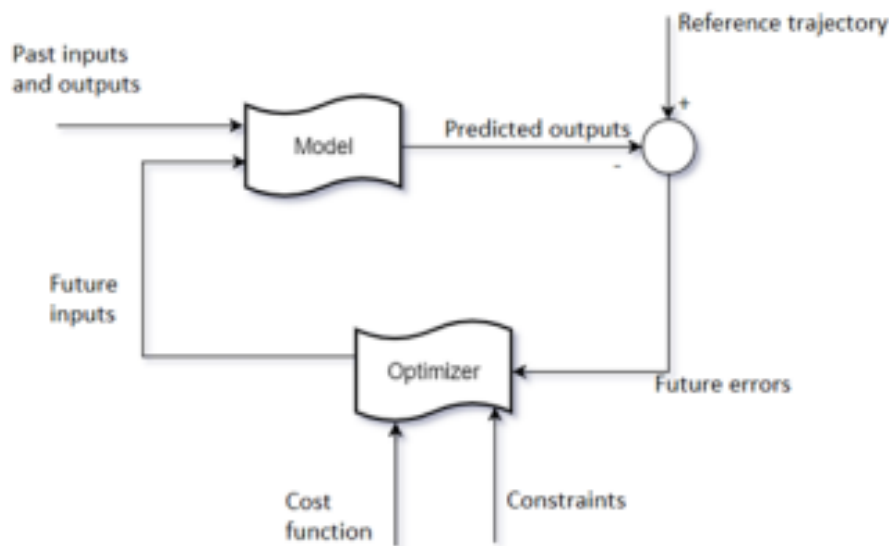


Figure 4.2: The basic structure of model predictive control.

values, as well as a suggested control input sequence. The optimizer calculates future control inputs based on a cost function and constraints. The cost function takes into account possible future tracking failures. Linear MPC is commonly used for plants that may be modeled as linear models. It produces reasonable results when the plant is operating at or near steady-state. However, there are many instances where dynamic behavior must be considered, such as when a plant is in continuous change. Such applications require nonlinear MPC. As a result, the primary advantage of nonlinear MPC is its ability to handle a system's nonlinear dynamics [49].

Model predictive control (MPC) is capable of handling multiple-input multiple-output (MIMO) systems with potential input-output interactions [50]. The advantage of MPC is that it is a multivari-

able controller that controls output while considering all system variables' interactions. The controller has the ability to handle both states and control restrictions, which are crucial in control systems to avoid unintended consequences. MPC's preview feature incorporates future reference information into control problems, improving controller performance. MPC is roughly optimum control, requiring online optimization at each time step. As a result, it requires a powerful, fast processor and a vast memory.

4.2.1 Operating Principle of MPC

Considering a single-input single-output(SISO) system ($X(k + 1) = f(X(k); U(k))$), the working principle of MPC is presented using two graphs: The State (X) and the Control Action (U). In Figure 4.3, U represents the control action, and X represents the evolved state prior to k. The MPC evaluates future N time steps to determine the optimal sequence of control actions (figure 4.4) that can be applied to the system to reach the desired state reference (figure 4.5). Finally, the decision variables (after k) optimization problem will be addressed to determine the optimal sequence of control actions for predicting states that lead to the reference state.

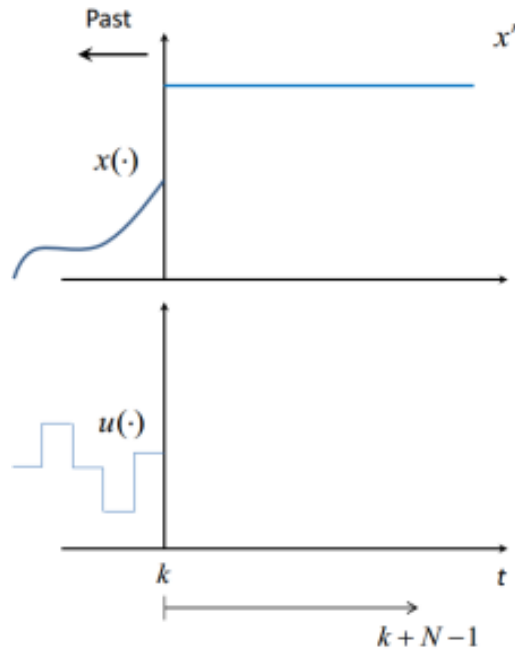


Figure 4.3: u and x in the past

Figure 4.3, figure 4.4 and figure 4.5 illustrate MPC Prediction Procedure.

MPC applies only the first step of the control sequence to the system, disregarding the rest (fig 4.6). The plant's output will alter depending on the input control supplied to it. The plant's actual output may differ from what the MPC predicted previously. This could be due to a variety of factors, including unmeasured disturbance, which is why, after applying the first control action, another MPC step (fig 4.7) is performed, and a new control sequence is calculated, and the first step control action is applied again. The MPC performs repetitive tasks to approach the reference in a systematic manner, which is where the optimizer comes in. Taking new measurements at each time step helps to adjust for unmeasured disturbances and model imperfections that cause the system output to deviate from the model's forecast.

MPC accomplishes three primary tasks (MPC Strategy Summary):

- Predict the state's behavior or evolution.
- Optimize online by minimizing the difference between prediction and reference state by adjusting control actions accordingly.
- Receding horizon implementation occurs at each sample period or time step.

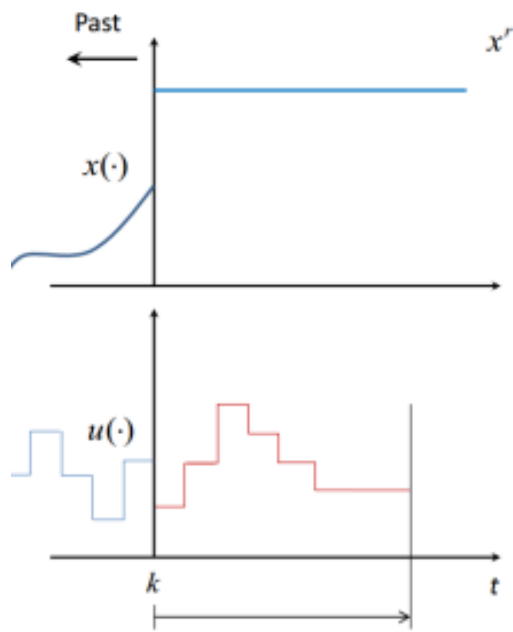


Figure 4.4: Predicted optimum Control action

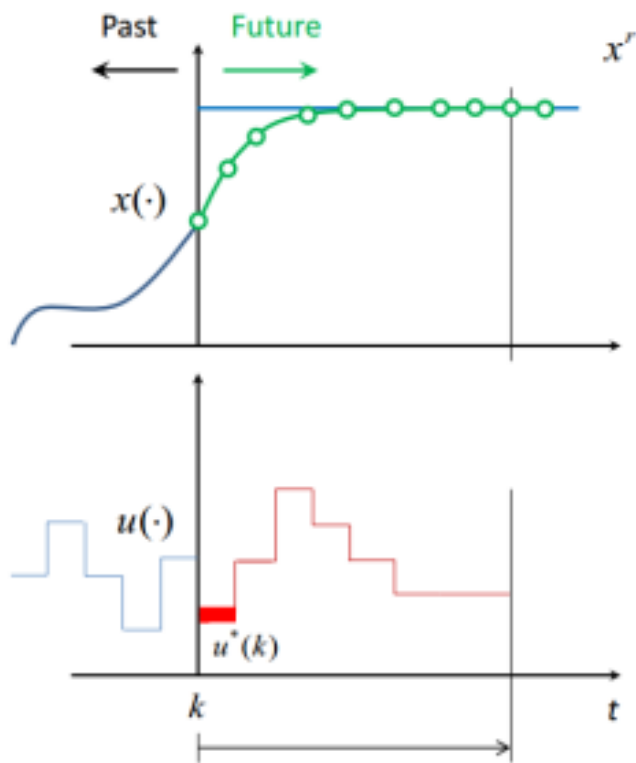


Figure 4.5: Predicted State

Figure 4.6 and figure 4.7 illustrate MPC next step prediction.

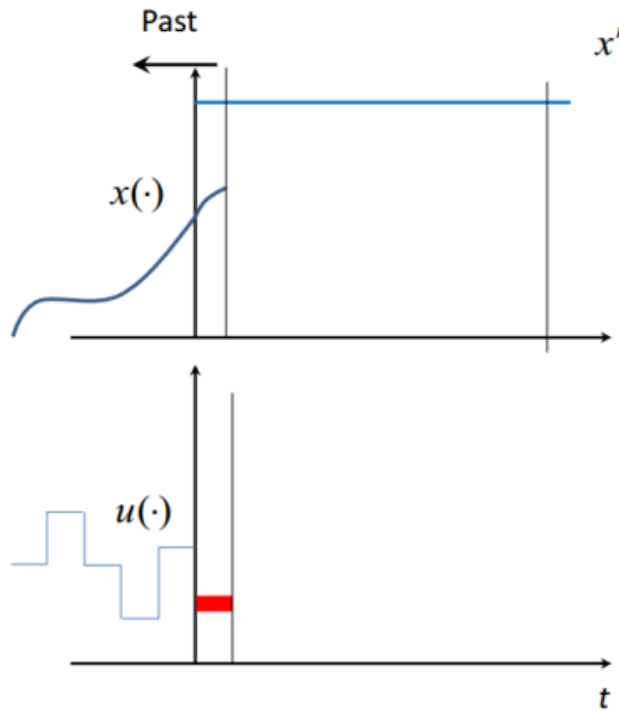


Figure 4.6: Actual State

4.2.2 Design parameters of MPC

Choosing appropriate MPC parameters is crucial for both controller performance and algorithm complexity, as they address an online optimization issue at each time step. MPC can be expressed mathematically as follows:

$$\min_{\mathbf{U}, \mathbf{X}} J(\mathbf{X}, \mathbf{U}; N, M) = \sum_{k=0}^N (X_{\text{pred}} - X_{\text{ref}})^T * Q * (X_{\text{pred}} - X_{\text{ref}}) + (U(k)^T * R * U(k))$$

(4.1)

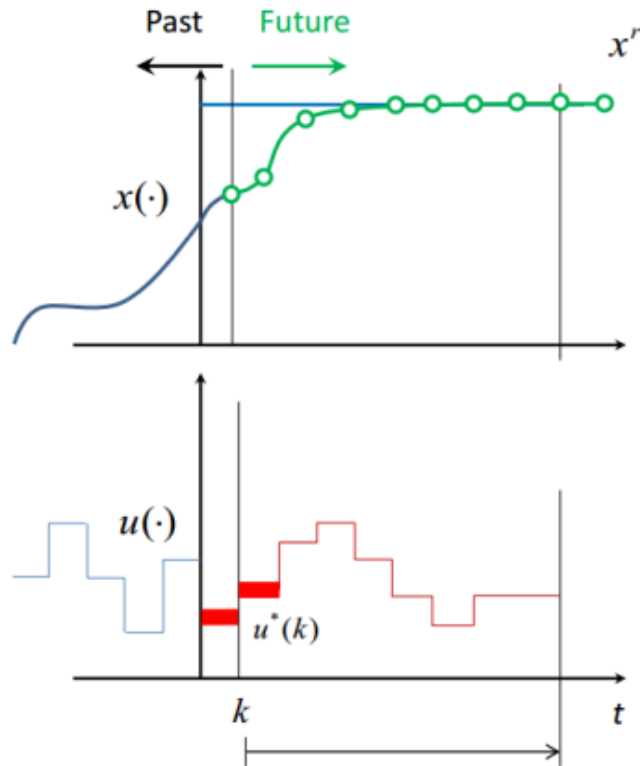


Figure 4.7: Next Step Prediction

Where N and M are parameters.

$$\begin{aligned} \text{s.t. } & X_U(k+1) = f(X_U(k), U(k)) \\ & X_U(k) \in X, \forall k \in [0, N] \\ & U(k) \in U, \forall k \in [0, M] \end{aligned}$$

Sample time(T_s) The controller executes the control algorithm at a rate determined by T_s and time t . If the disturbance is too large, the controller may struggle to respond quickly. Smaller controllers can respond quickly to disturbances, but they may have a higher processing load. The objective is to find the right balance between performance and computing effort.

Prediction horizon(N) The MPC's prediction horizon reveals how far into the future it looks. It is commonly expressed as the number of future time steps or the length of time in the future. MPC, also known as Receding or Moving horizon control, is named after the forward-moving character of the prediction horizon. Increasing N yields less forceful control action. If the forecast horizon is too tiny, necessary futures may be missed. Disturbances could go undetected if the predicted horizon is too

large. Choose a prediction horizon that encompasses the system's major dynamics.

Control horizon(M) The Control horizon refers to the number of control motions per time step M , while the remainder of the input remains constant (see fig 4.8). The optimizer must compute each free variable in the control horizon (fig 4.9). Smaller control horizons lead to fewer computations. Selecting a control horizon of 1 may not provide optimal maneuvering results. Increasing M increases the controller's aggressiveness and computational work, but also improves prediction accuracy.

figure 4.8 and 4.9 illustrate Control Horizon

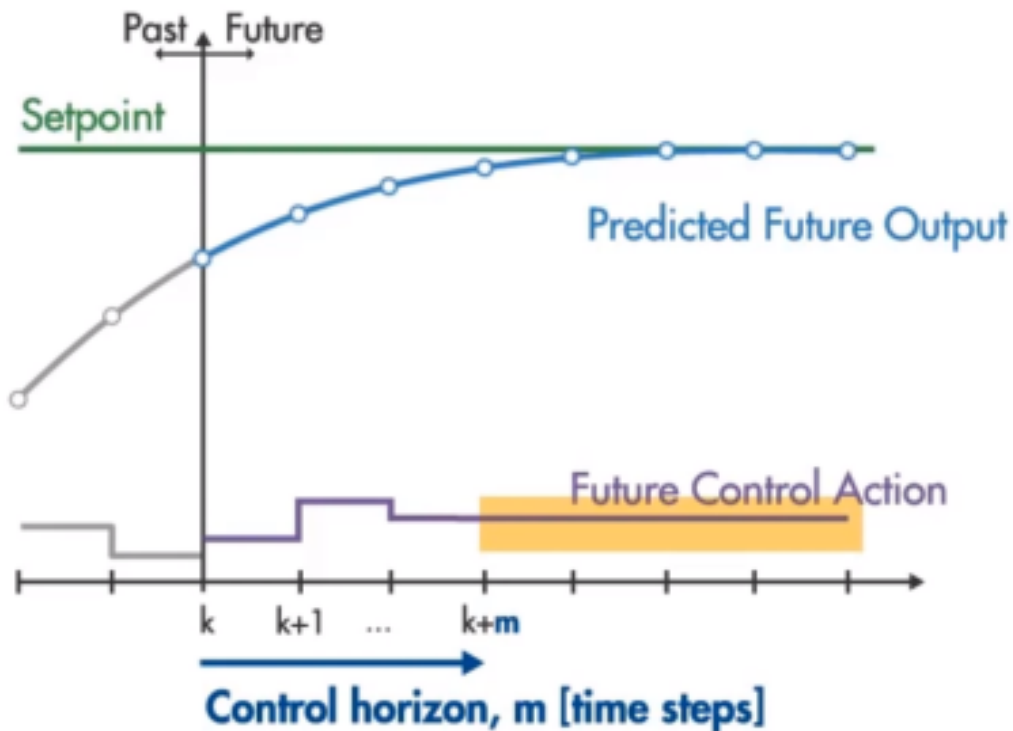


Figure 4.8: Control Horizon with constant value after M steps

Weight(Q and R) Equation 4.2.2 suggests that the output should be as close to the specified points as possible while also maintaining smooth control moves. Q : This term measures the convergence rate (rise and settling time). R : This phrase penalizes aggressive input use. If $Q \gg R$, reducing the discrepancy between desired and predicted values is more important than punishing the input. Conversely, if $R \gg Q$, minimizing control effort is recommended.

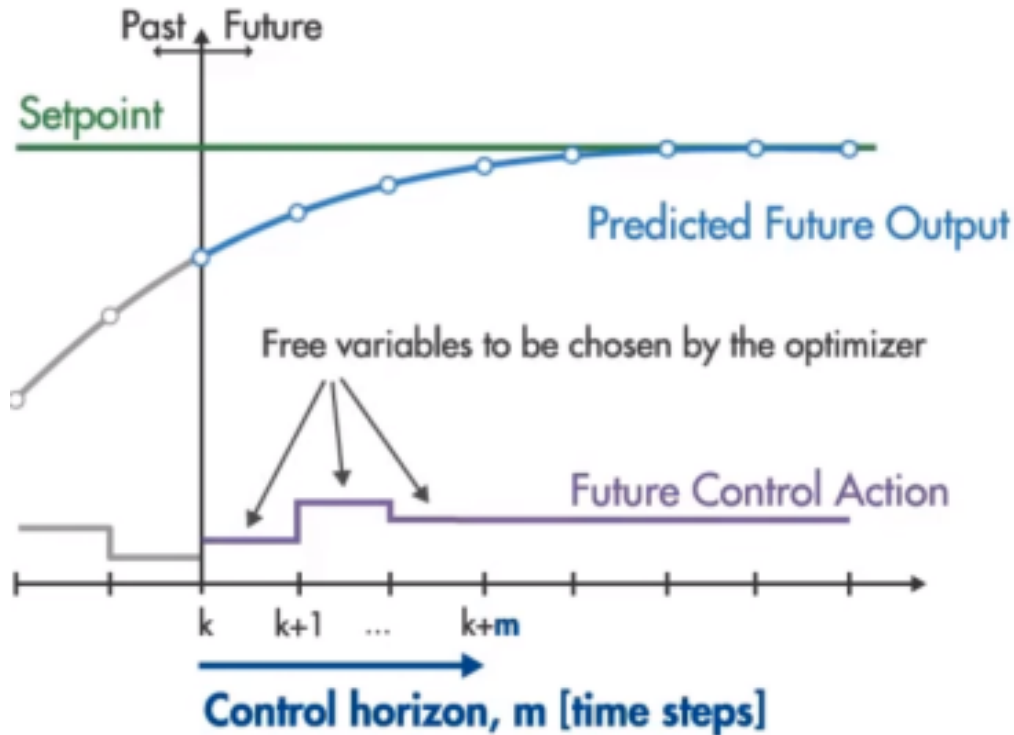


Figure 4.9: Control moves to be computed by the optimizer

4.2.3 Mathematical formulation of NMPC

The process for formulating MPC mathematically is as follows.

I. The Running(Stage) Cost will be specified, defining the control aim,

$$l(X; U) = (X_{pred} - X_{ref})^T * Q * (X_{pred} - X_{ref}) + (U(k)^T * R * U(k)).$$

It penalizes the discrepancy between expected and reference states, and does the same for control actions.

II. The Cost function: The total running costs throughout the course of the forecast horizon is this.

$$J_N(X, U; N, M) = \sum_{k=0}^N l(X_U(k), U(k)), \text{ Where } N \text{ and } M \text{ are parameters.}$$

III. The objective of the MPC problem, which is to minimize the cost function using optimization variables, may be expressed as an optimum control problem (OCP). The link between the control action U and the X prediction is taken into account while minimizing the cost function.

$$(X_U(k + 1) = f(X_U(k), U(k)))$$

$$X_U(t_0) = X_0 \text{--Initial state value}$$

$$(U(k) \in U; \forall k \in [0 : M]) \text{--control action constraint And}$$

$$(X_U(k) \in X; \forall k \in [0 : N]) \text{-- state constraint}$$

$$\min_{U, X: N, M} J_N(X, U) = \sum_{k=0}^N l(X_U(k), U(k))$$

(4.2)

s.t

$$X_U(k + 1) = f(X_U(k), U(k)) \quad X_U(t_0) = X_0 \quad U(k) \in U; \forall k \in [0 : M] \quad X_U(k) \in X; \forall k \in [0 : N]$$

(4.3)

IV. To solve the optimal control problem (OCP) numerically, it must be turned into a non linear programming (NLP). NLP is a standard problem formulation.

numerical optimization having the general form:

$$\min_w$$

$$\phi(w); \text{ Objective function}$$

$$\text{s.t : } g_1(w) \leq 0; \text{ Inequality constraint}$$

$$g_2(w) = 0; \text{ Equality constraint}$$

Therefore, NLP comprises of the following three ingredients:

- An objective function, $\phi(w)$, to reduce or maximize.

- A decision variable, w , to choose from.
- Respectable constraints, such as $g_1(w)=0$ (equality constraints) or $g_2(w) \geq 0$ (inequality constraints).

Special cases of NLP include the following:

- **Linear programming (LP)** occurs when $\phi(w)$, $g_1(w)$, and $g_2(w)$ are affine functions that may be represented as a linear combination of w 's elements.
- **Quadratic programming (QP)** occurs when $g_1(w)$ and $g_2(w)$ are affine but the objective function $\phi(w)$ is linear quadratic.

V. Methods for expressing an OCP as an NLP. There are various numerical methods for solving continuous time optimal control problem(OCP). All approaches need discretization of the infinite-dimensional problem.

- **Indirect methods** Discretization happens at the end in this technique, which uses algebraic operations to find optimality criteria in continuous time. Indirect approaches are sometimes described as "first optimizing, then discretizing". It can resolve minor issues.

- **Direct Methods:** discretize the continuous time OCP to create a finite-dimensional optimization problem. Numerical optimization strategies can be modified to solve the finite-dimensional issue. Direct approaches are frequently described as "first discretize, then optimize". These approaches are mostly employed in MPC applications. Here are some popular direct methods:

a. Direct Single-Shooting. The problem decision variable is simply the input: $w = [U_0, U_1, \dots, U_N]$. The single-shooting approach is a completely sequential strategy that considers all intermediate state values created during the numerical integration process to be hidden variables and solves the optimization issue with just control parameters and starting values. The primary drawback of Direct Single Shooting is nonlinearity propagation: over long prediction horizons (N), the integrator function becomes extremely nonlinear. This approach is not appropriate for optimizing nonlinear or unstable systems with long prediction horizons.

b. Direct multiple shootings. Direct Multiple Shooting is another technique to represent the optimal control issue as an NLP. In multiple shooting, the optimization issue considers both states (X) and input control (U) as decision variables. Break down system integration into short-term intervals and use the system model as a state constraint in each optimization step. Multiple shooting involves applying the equality constraint (difference between predicted state and model output) at each prediction or shooting step, hence the name.

VI. To solve the NLP, utilize CasADi as a facilitator.

CasADi: is a free and open source program with a broad scope of numerical optimization. This flexible approach to optimal control enables the implementation of efficient algorithms, including direct multiple shooting and direct single shooting. CasADi offers comparable performance across MATLAB, Python, and C++ [51]. CasADi can tackle four standard problems:

- Quadratic programming.
- Nonlinear programs.
- Root finding problems.
- Initial-value problems in ODE (ordinary differential equations).

Several NLP solutions are integrated with CasADi. CasADi installations often contain and make use of IPOPT (Interior Point Optimizer), an open-source method for primal-dual interior points.

4.2.4 MPC mathematical formulation for three wheeler HEV

MPC optimizes a problem's objective function while considering constraints. The cost function compares prediction model outputs to intended set values and assigns a weight to deviations to minimize them. Inputs receive a separate weighting. Control inputs are manipulated variables [52]. The math-

emtical representation of a nonlinear system is as follows.

I. Dynamics of Three wheeler HEV

$$\dot{x} = f(x, u) \quad (4.4)$$

$$X(k+1) = X(k) + T * F(X(k), U(K)) \quad (4.5)$$

$$f(x, u) = \begin{bmatrix} c_f (P_{req} - P_b) \\ -\frac{V_{oc} - \sqrt{V_{oc}^2 - 4R_b P_b}}{2R_b Q_b} \\ A_1 T_e + A_2 T_m + \left(A_1 \frac{S+R}{S} - A_2 \frac{R}{S} \right) T_g - \frac{A_2}{g_f} T_d \end{bmatrix} \quad (4.6)$$

The initial value for the battery is 0.8% its range is between 0.65 and 0.75

$$F(X(k), U(k)) = \begin{bmatrix} c_f (P_{req}(k) - P_b(K)) \\ -\frac{V_{oc} - \sqrt{V_{oc}^2 - 4R_b P_b(K)}}{2R_b Q_b} \\ A_1 T_e(K) + A_2 T_m(K) + \left(A_1 \frac{S+R}{S} - A_2 \frac{R}{S} \right) T_g(K) - \frac{A_2}{g_f} T_d(K) \end{bmatrix} \quad (4.7)$$

Where

$$x \in R^n$$

$$u \in R^m$$

$$X(K) \in R^n$$

$$U(K) \in R^m$$

i.e

$$x = [m_f, soc, \omega_e]^T \quad (4.8)$$

$$X(K) = [m_f(K), soc(K), \omega_e(K)]^T \quad (4.9)$$

$$u = [T_e, T_g, T_m, \omega_g]^T \quad (4.10)$$

$$U(K) = [T_e(K), T_g(K), T_m(K), \omega_g]^T \quad (4.11)$$

There are n states, and n = 3.

The number of inputs (m) is equal to four.

II. Control Objective

The goal of control is to minimize a cost function that is given by:

$$J_{\min u} = \sum_{k=0}^N (X(k) - X_{\text{ref}})^T * Q * (X(k) - X_{\text{ref}}) + (U(k)^T * R * U(k)) \quad (4.12)$$

III. Weight(Q and R)

As there are 3 states and 4 input, the sizes of weight matrices of Q and R are 3 by 3 and 4 by 4 respectively. Their value are:

$$Q = \begin{bmatrix} 2 & 0 & 0 \\ 0 & 5 & 0 \\ 0 & 0 & 2 \end{bmatrix}$$

$$R = \begin{bmatrix} 1 & 0 & 0 & 0 \\ 0 & 0.5 & 0 & 0 \\ 1 & 0 & 0.1 & 0 \\ 1 & 0 & 0 & 0.1 \end{bmatrix}$$

The weight value of the states(Q) have given higher values to maintain the states values around the reference values.

IV. Running Cost

The running cost is referred to as:

$$(x_e, u_e) = (x_e^T Q x_e + u_e^T R u_e) = (X(k) - X_{\text{ref}})^T * Q * (X(k) - X_{\text{ref}}) + (U(k)^T * R * U(k)) \quad (4.13)$$

where x_e and u_e are the errors of outputs and inputs from respective reference trajectory and weight matrices are denoted by Q and R . Hence,

V. Cost function

$$J_{\min u} = \sum_{k=0}^N \left((X(k) - X_{\text{ref}})^T Q (X(k) - X_{\text{ref}}) + (U(k)^T R U(k)) \right) \quad (4.14)$$

VI. The optimisation problem for nonlinear MPC is summarised as below:

$$\min_u J(x_e, u_e) = \sum_{k=0}^N \left((X(k) - X_{\text{ref}})^T Q (X(k) - X_{\text{ref}}) + (U(k)^T R U(k)) \right) \quad (4.15)$$

subject to:

$$X(k+1) = X(k) + T * F(X(k), U(k))$$

$$X_U(N) = X_0$$

$$U(k) \in U; \forall k \in [0, N]$$

$$X(k) \in X; \forall k \in [0, N]$$

$$\begin{aligned}
\dot{m}_{f \min} &\leq \dot{m}_f \leq \dot{m}_{f \max} \\
soc_{\min} &\leq SOc \leq soc_{\max} \\
\omega_{e \min} &\leq \omega_e \leq \omega_{e \max} \\
T_{e \min} &\leq T_e \leq T_{e \max} \\
T_{g \min} &\leq T_g \leq T_{g \max} \\
T_{m \min} &\leq T_m \leq T_{m \max} \\
\omega_{g \min} &\leq \omega_g \leq \omega_{g \max}
\end{aligned} \tag{4.16}$$

The equation $X_U(N)=X_0$ suggests that the initial state for the subsequent time step is determined by taking the N^{th} value of the current time state value step.

The terminal output equality restrictions $X_U(N) = X_0$ ensure the algorithm's stability[53]. The aforementioned optimum control problems are solved across the chosen prediction horizon (N) at each time step T to determine the best decision variable. The shift function is used by the code to apply just the first element of the optimum control sequence. The method is repeated for the subsequent time step as the prediction horizon advances.

VII. Multiple Shooting: used to transform the OCP to NLP.

$\min_w \phi(w)$, Objective function

subject to $g_1(w) \leq 0$, Inequality constraint

$g_2(w) = 0$, Equality constraint

- The decision variables(w) are the combination of :

The 3 States $[m_f, Soc, We]$ and 4 inputs $[T_e, T_m, T_g, W_g]$

i.e is $w = [U0, \dots, UM; X0, \dots, XN]$

- Multiple shooting involves adding path constraints at each optimization phase (shooting step).

The difference between $X(k + 1)$ and $f(X(k); U(k)) = 0$ defines the model.

- Inequality Constraint (Control Inputs, map margins):

This inequality requirement must be respected throughout all prediction phases.

- Equality Constraint (System dynamics)

$$\begin{bmatrix} \bar{X}_0 - X_0 \\ f(X_0, U_0) - X_1 \\ \vdots \\ f(X_{N-1}, U_{N-1}) - X_N \end{bmatrix}$$

Where ,

\bar{X}_0 is the optimization variable and

X_0 is the predicted state

VIII. Utilize CasADi's IPOPT solver to solve the NLP: CasADi assists, but does not solve, NLPs. The open-source software tool IPOPT was used to handle large-scale non-linear optimization problems. It can address general natural language processing problems. To create NLP solvers, utilize the "nlsol" function from CasADi. Plugins are used to implement different solutions and interfaces.

- To solve NLP with Ipopt, the decision variables (states and input) must be in a column matrix.

The states are $3 * N$ for prediction horizons and $4 * M$ for control horizons.

OPT-variables-euler = [reshape(X pre-euler ; $3 * N$; 1); reshape(U-euler ; $4 * M$; 1)]

- Create a structure that includes an objective function, decision variables, constraints, and parameters.

NLP_prob_euler = struct('f', obj_euler,'x', OPT_variables_euler,'g', g_euler,'p', P_euler).

- Optional settings include maximum iteration, acceptable tolerance, and other parameters.

- Now the solver can be called:

Solver_euler = nlsol('solver' , 'ipopt', NLP_prob_euler , opts).

4.3 Algorithm for the proposed MPC strategy

The suggested MPC algorithm's flow chart is displayed in Figure 4.10. As mentioned in Chapter 3, simulations employ a simplified mathematical model of power-split HEVs. Based on the algorithm developed as shown in Figure 4.10, the suggested MPC strategy may be simulated. Beginning with the initial data point of the driving cycle, all output states and control inputs have starting values of zero, with the exception of the battery's state of charge, which is equal to 0.8. In order to initialize the following data point in the cycle from the second to the last, the preceding control input values are utilized.

A control and prediction horizon of 15 future time steps (3.5 seconds) and 0.3 seconds sampling time is employed to simulate a single data point in the driving cycle. The sample time is set at 0.3 seconds. The anticipated output state trajectory is used to plan future control input moves. However, just the initial moves are performed, ignoring the remaining moves. The method is repeated with a different prediction horizon. The freeware CasADi is used to build the code for the suggested MPC approach, and it can be imported into MATLAB. CasADi offers unique capabilities such as handling symbolic expressions, integrating with other solvers like "Ipopt," and allowing for computer-readable inputs.

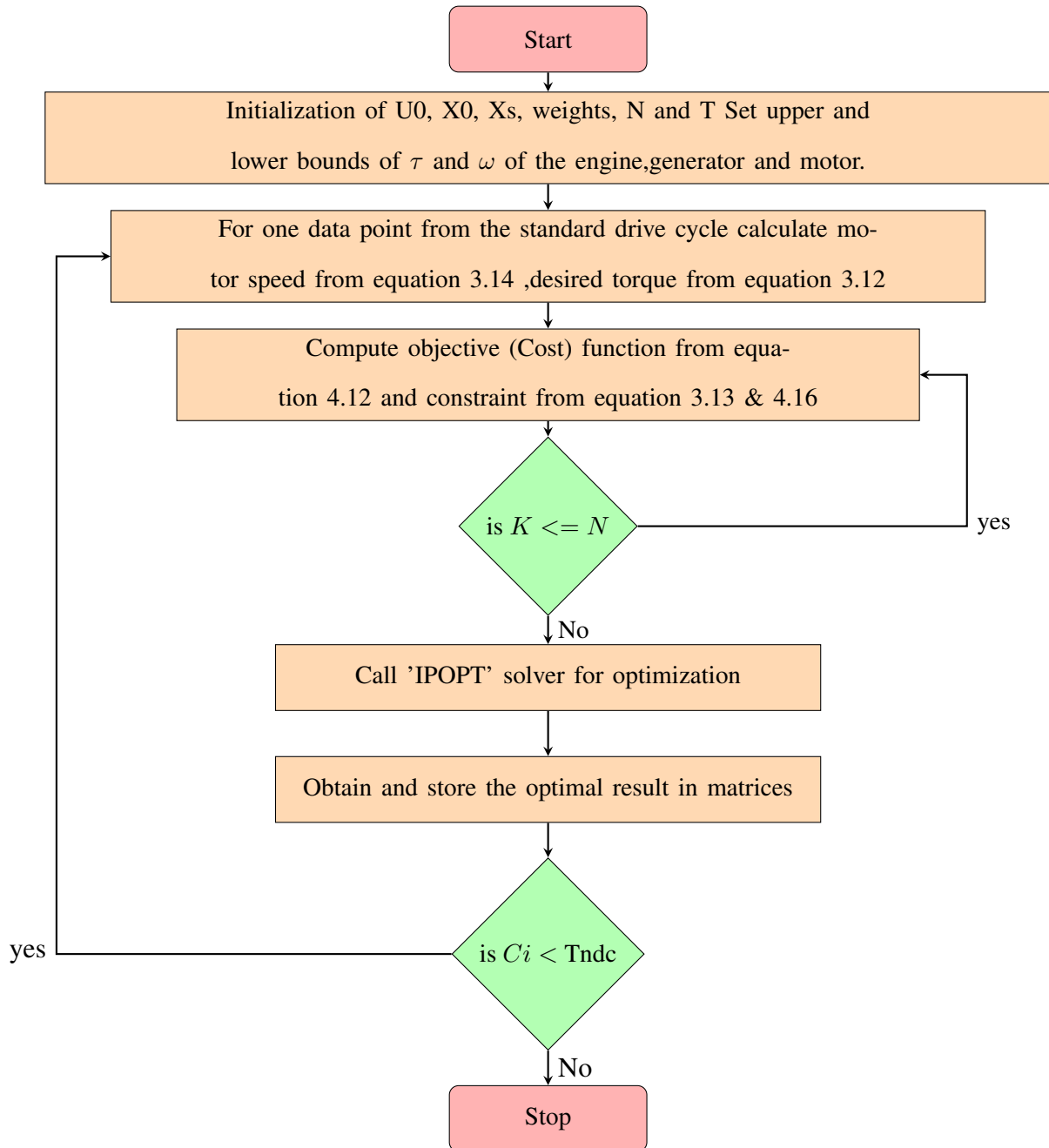


Figure 4.10: Algorithm of the proposed MPC strategy

5 Simulation Result

5.1 The simulation procedure

Simulations are run using CasADi and ADVISOR 2003 software.

5.1.1 CasADi

CasADi is an open-source software that run MATLAB that enables linear or nonlinear optimization. It doesn't address model predictive control problems, but rather facilitate to solve nonlinear difficulties.

Mehrez developed nonlinear MPC in CasADi to track a robot's fixed position within a restricted region. This work requires the numerical implementation of MPC in CasADi. Optimal control issues are turned into linear or nonlinear problems for numerical implementation of MPC.

There are various approaches for this goal, such as single shooting, multiple shooting, and collocation. Compared to the single shot system, the multiple shooting technique is far faster. States and control inputs are treated as decision variables in multiple shooting approaches. Applying equality constraints with zero higher and lower limits is necessary for this [53]. The rule-based approach in ADVISOR 2003 is contrasted with the suggested MPC technique in the CasADi software.

5.1.2 ADVISOR

ADVISOR 2003 is open-source software for analyzing various cars. It runs in the MATLAB® environment. The National Renewable Energy Laboratory(NREL) established this initiative to support research on hybrid propulsion systems for the US Department of Energy. ADVISOR 2003 aimed to improve understanding of multidimensional parametric studies and optimisation, enable flexible analysis of powertrain systems, and be user-friendly for those without extensive vehicle modeling knowledge.

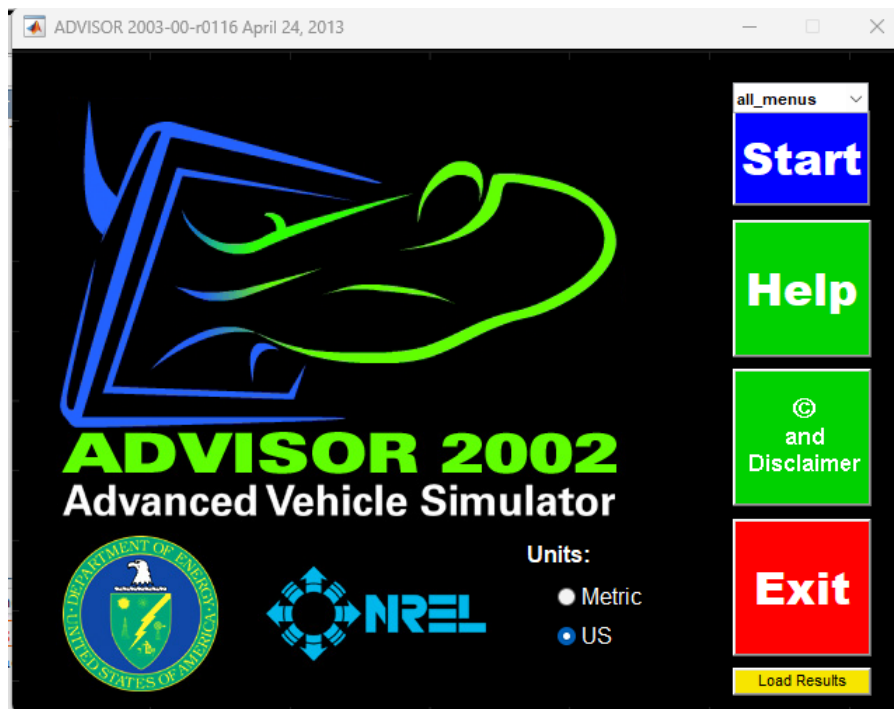


Figure 5.1: ADVISOR first page

Users can get driving cycles, motor, generator, and engine efficiency maps from the software's database [54]. This program supports block diagrams, script files, and graphic user interfaces (GUIs) and operates in MATLAB. This approachable initiative is to expedite research in the field of hybrid electric vehicle technology and assist academics and industry in understanding the diverse linkages of these vehicles.

ADVISOR 2003 can use a backward-facing method, assuming the vehicle is traveling at the intended speed, which eliminates the requirement for modeling driver behavior. The speed is computed using a backwards-facing driving cycle. The graphic user interfaces(GUIs) provides for easy customization of vehicles, hybrid electric combinations, components, driving cycles, and vehicle mass. There are three graphic user interfaces (GUIs): vehicle input, simulation setup, and results. Figures 23, 24, and 25 depict vehicle input, simulation setup, and outcome pages, respectively. The software's result page provides charts for driving cycle, state of charge (SOC), emissions, and other information. The fuel efficiency is also shown on the results page.

Simulation on Advanced Vehicle Simulator(ADVISOR) 2003 is simple, allowing users to analyze the impact of altering motors and generators on fuel efficiency. There are various vehicle configura-

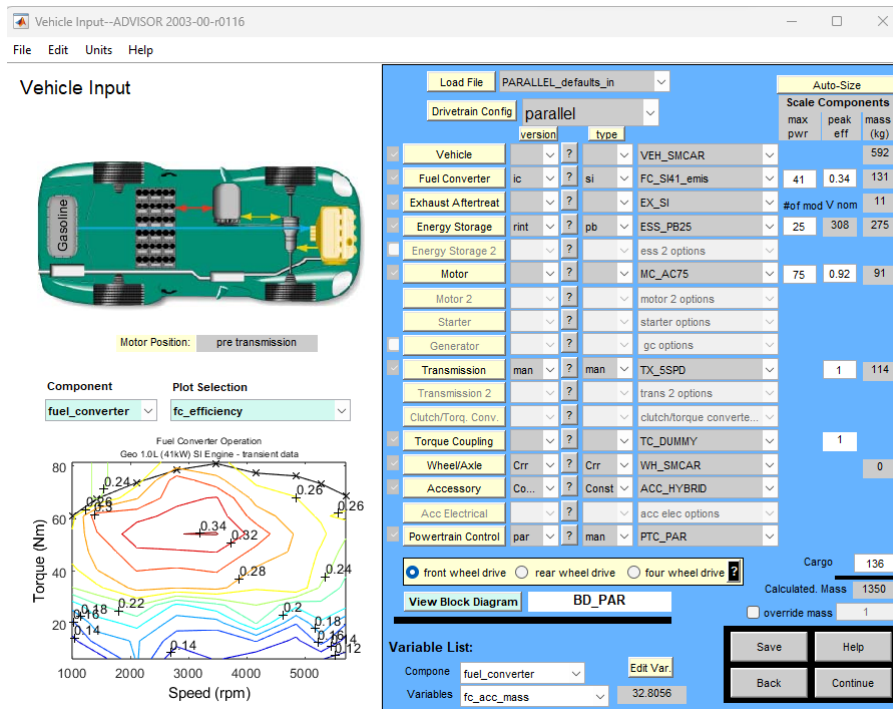


Figure 5.2: ADVISOR second page

tions and types available for study. Advanced Vehicle Simulator (ADVISOR) 2003 allows users to pick a component type from a drop-down menu on the input screen, such as vehicle, fuel converter, exhaust after treatment, motor, and generator. Choosing a hybrid electric vehicle architecture, driving cycles, and cycle counts is easy. The second page displays the simulation setup window. The third page is the result window, which displays a summary of results. The result page displays the overall distance traveled based on the driving cycle and fuel usage in liters per hundred kilometers [54, 55].

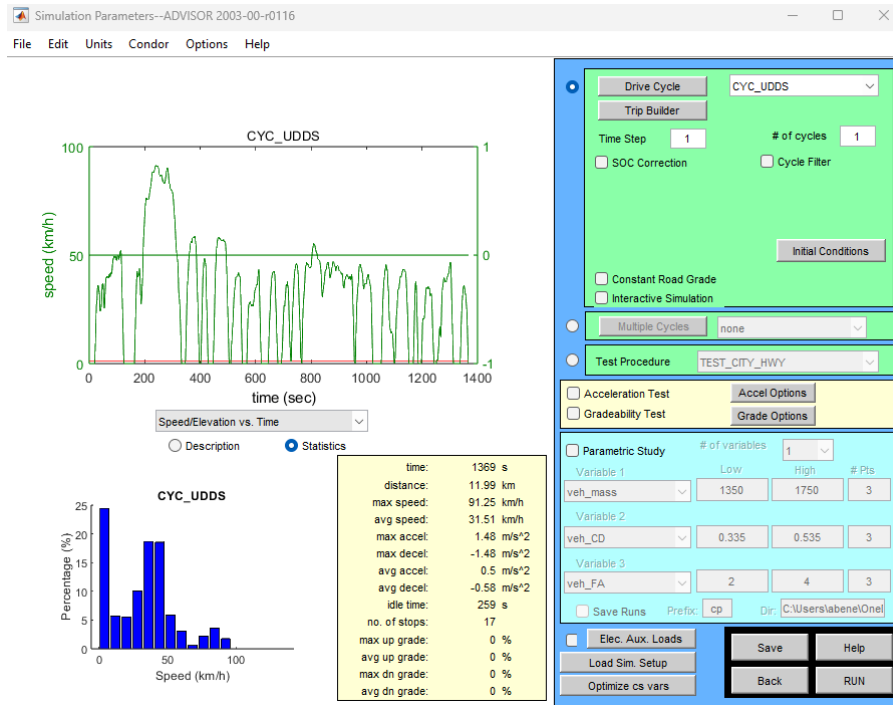


Figure 5.3: ADVISOR third page

5.2 Simulation Result

This study uses the Ipopt solver (interior-point optimiser solver). Andreas Wächter developed Ipopt, an open-source nonlinear optimization solver distributed under the Eclipse Public License(EPL). This C++-based solution is more efficient than MATLAB’s built-in 'fmincon' solver. This solver uses 'g' to represent nonlinear constraints with lower and upper bounds. Equality restrictions can be enforced by setting upper and lower limits to zero. Table 5.1 shows the parameters utilized in the simulations, which were taken from the ADVISOR 2003 database.

Figures 5.5 and 5.6 demonstrate the driving cycles used in both simulations: The modified Highway Fuel Economy Test Cycle (HWFET) and Extra Urban Driving Cycle (EUDC). Table 5.2 compares the two driving cycles.

The results of the proposed MPC methodology and ADVISOR 2003 for battery state of charge for the EUDC(modified) cycle are displayed in Figures 5.7 and 5.9, and for the HWFET(modified) cycle, in Figures 5.8 and 5.10. The supported MPC approach, as opposed to the rule-based ADVISOR strategy, keeps the battery’s state of charge (SOC) closer to the reference value of 0.7, according to re-

Symbols	Value	Symbols	Value
m	610kg	V_{oc}	174V
A_f	$1.86m^2$	R_b	1.12
C_d	0.44	Q_b	6Ah
ρ	$1.2kg/m^3$	SOC_{max}	0.75
μ	0.015	SOC_r	0.7
r_w	0.2m	SOC_{min}	0.65
g	$9.81m/s^2$	C_f	0.0874
I_E	$0.18kgm^2$	R	78
I_m	$0.0226kgm^2$	S	30
I_g	$0.0226kgm^2$	T_{gmax}	55Nm
I_w	$3.3807kgm^2$	T_{gmin}	-55Nm
W_{gmax}	575.9587rad/s	T_{mmax}	305Nm
W_{gmin}	-575.9587rad/s	T_{min}	-305Nm
W_{mmax}	628.3185rad/s	T_{emax}	101.9712Nm
W_{min}	-628.318rad/s	g_f	4.24
W_{emax}	418.8790rad/s	\dot{m}_{fmin}	0g/s
\dot{m}_{fr}	0g/s	\dot{m}_{fmax}	0.4g/s

Table 5.1: Different parameters utilized in the modeling process for the three-wheeler HEV.

Symbols	HWFET(modified)	EUDC(modified)
Time	765s	400s
Distance	7.38 km	2.18 km
Maximum speed	$43.09km/h$	$37.55km/h$
Average speed	$34.68km/h$	$19.54km/h$
Maximum acceleration	$0.64m/s^2$	$0.22m/s^2$
Maximum deceleration	$-0.66m/s^2$	$-0.43m/s^2$
Average acceleration	$0.09m/s^2$	$0.11m/s^2$
Average deceleration	$-0.1m/s^2$	$-0.29m/s^2$
Idle time	6s	42s
Number of stops	1	1

Table 5.2: Drive cycle characteristics

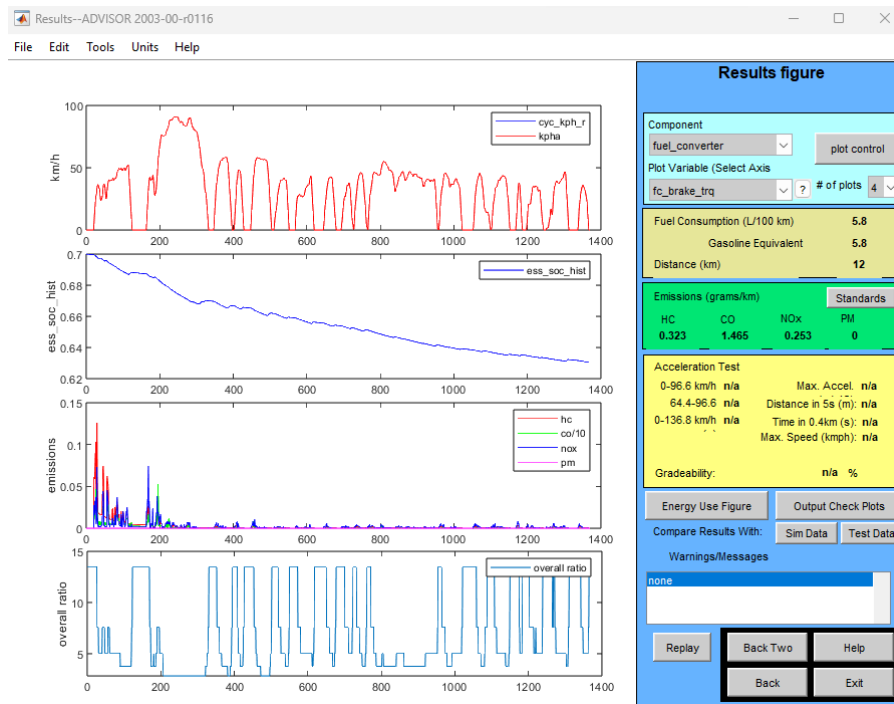


Figure 5.4: ADVISOR 4th page

sults from the EUDC(modified) and HWFET(modified) cycles (see Table 5.3). Imposing appropriate boundaries ensures that the state of charge remains close to the reference value. This approach fulfills all input and output criteria. The code for the proposed MPC strategy is successful as the torques and rotational speeds of three components (motor, generator, and engine) are within allowable limits for both cycles, as shown in Figures from 5.11 to 5.22.

The fuel efficiency of the predictive control approach is based on a simplified model of a gasoline-powered internal combustion engine's mass flow rate. An upper bound is given to the fuel mass flow rate while developing a model-predictive control problem. The modified HWFET cycle uses less power than the Extra-Urban Driving Cycle (EUDC) due to fewer stops, peak speed, and average acceleration. This tendency may also be seen in torques. The Extra-Urban Driving Cycle(EUDC)(modified) cycle requires higher peak speeds than the HWFET(modified) cycle, The proposed MPC model allows for less optimisation in the Extra-Urban Driving Cycle(EUDC)(modified) cycle. Furthermore, the rule-based technique follows predefined rules. The rule-based technique consumes more energy than the proposed MPC strategy across the HWFET cycle.

Figure 5.11, 5.12 and 5.13 show Speed of engine, Motor and Generator in HWFET(modified) drive cycle.

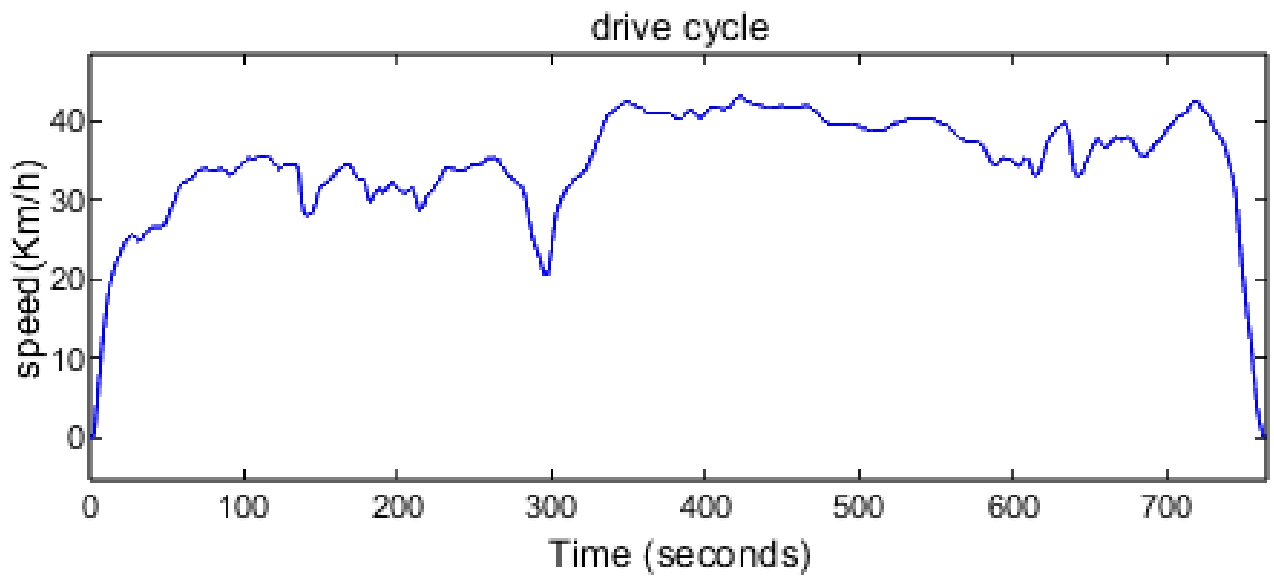


Figure 5.5: HWFET(modified) drive cycle

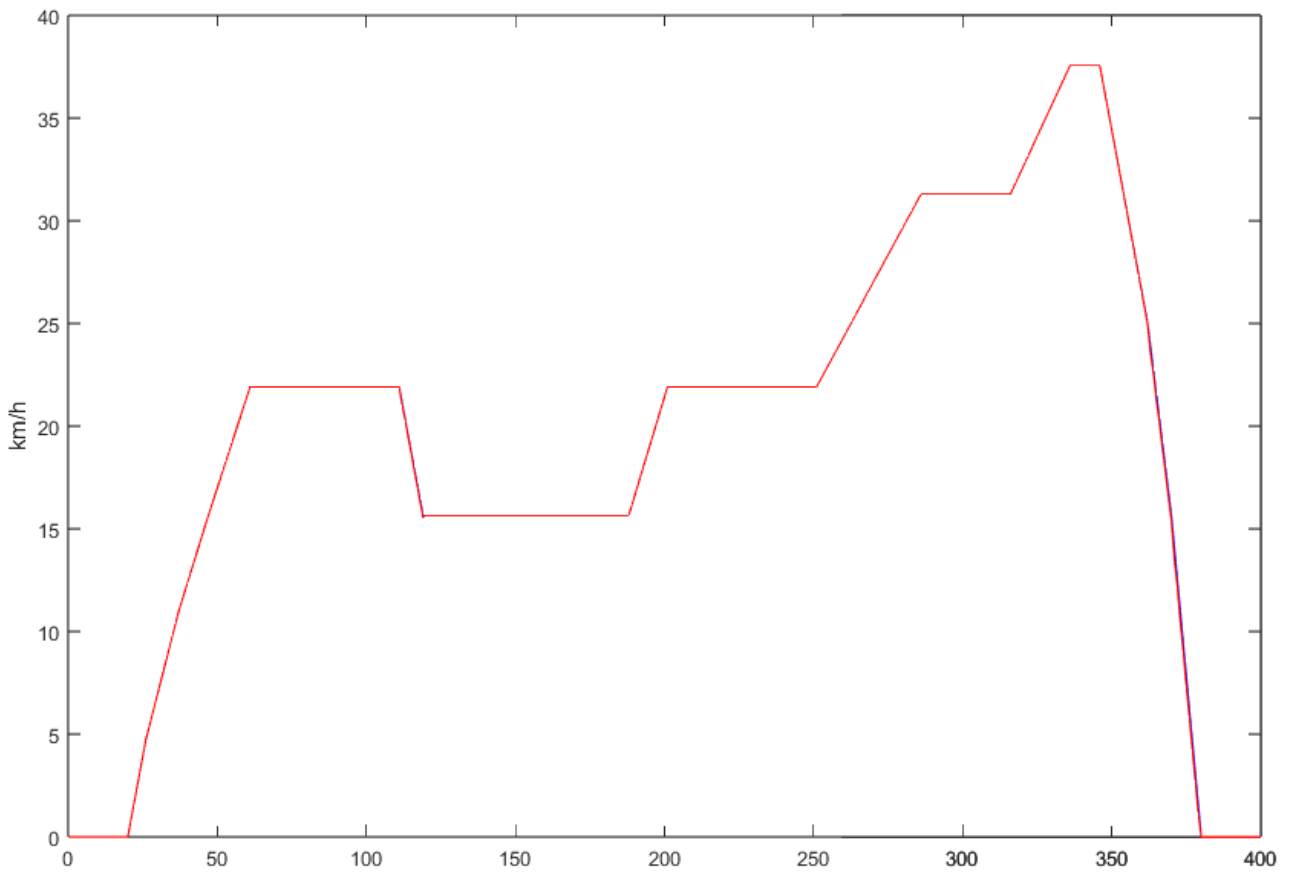


Figure 5.6: EUDC(modified) drive cycle

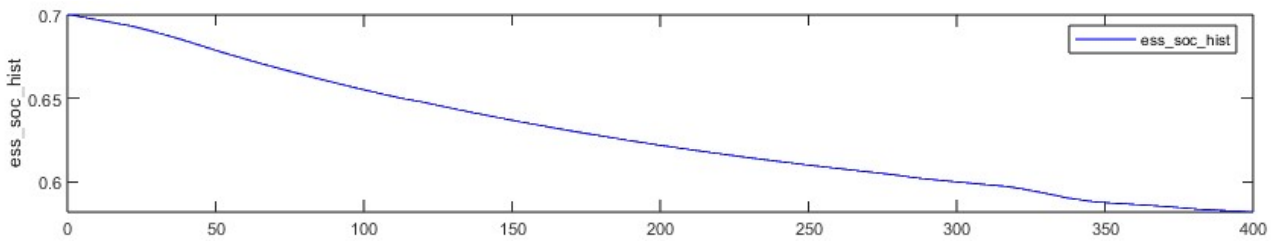


Figure 5.7: Battery SoC using ADVISOR2003 in EUDC(modified) drive cycle

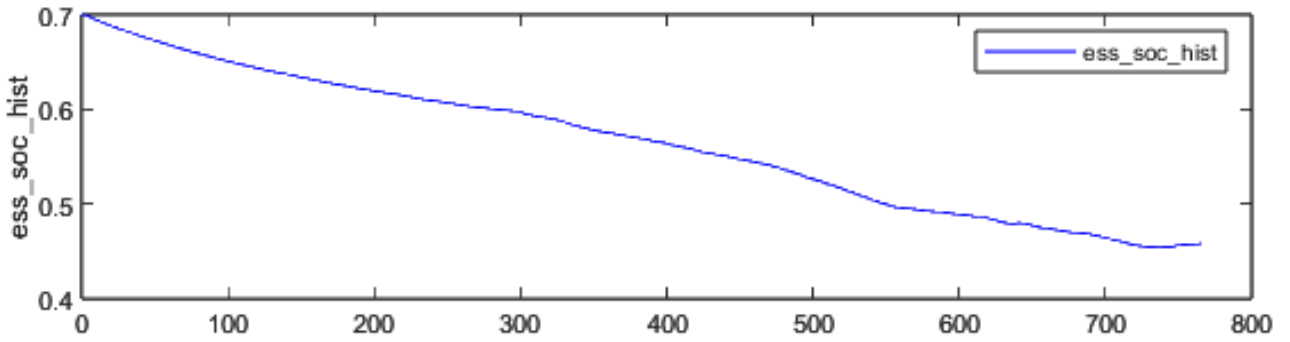


Figure 5.8: Battery SoC using ADVISOR2003 in HWFET(modified) drive cycle

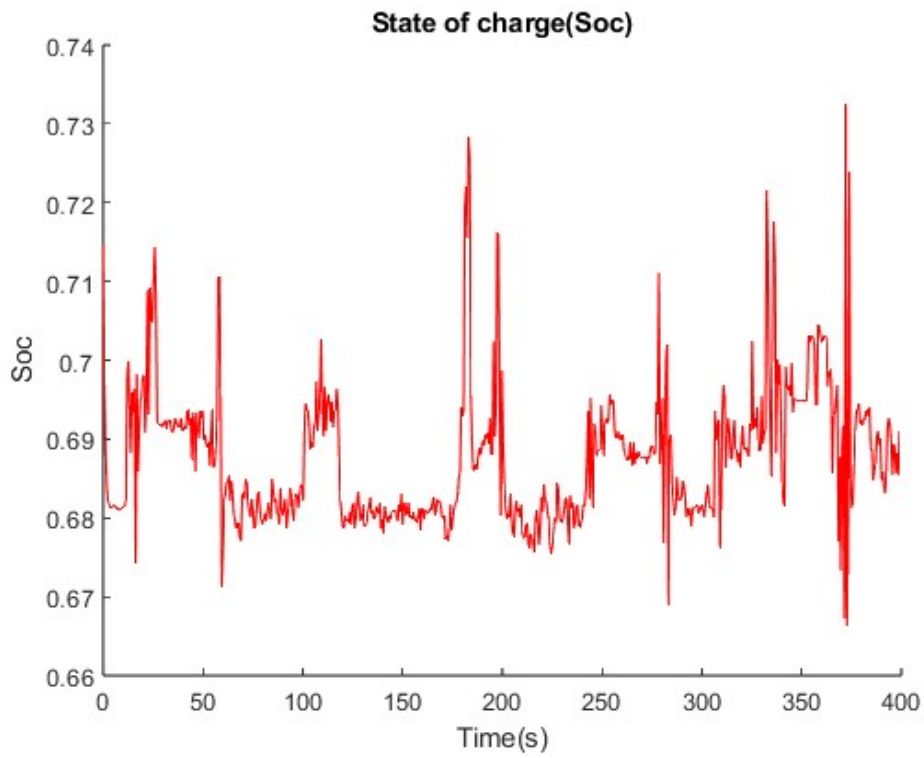


Figure 5.9: Battery SoC using the proposed MPC over EUDC(modified)

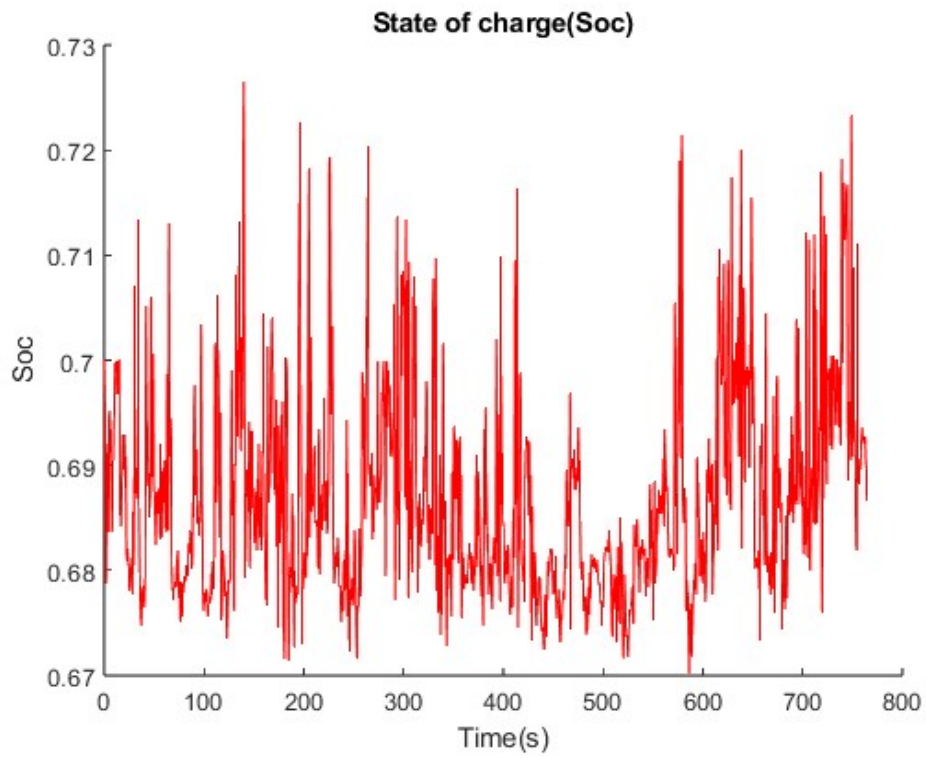


Figure 5.10: Battery SoC using the proposed MPC over HWFET(modified)

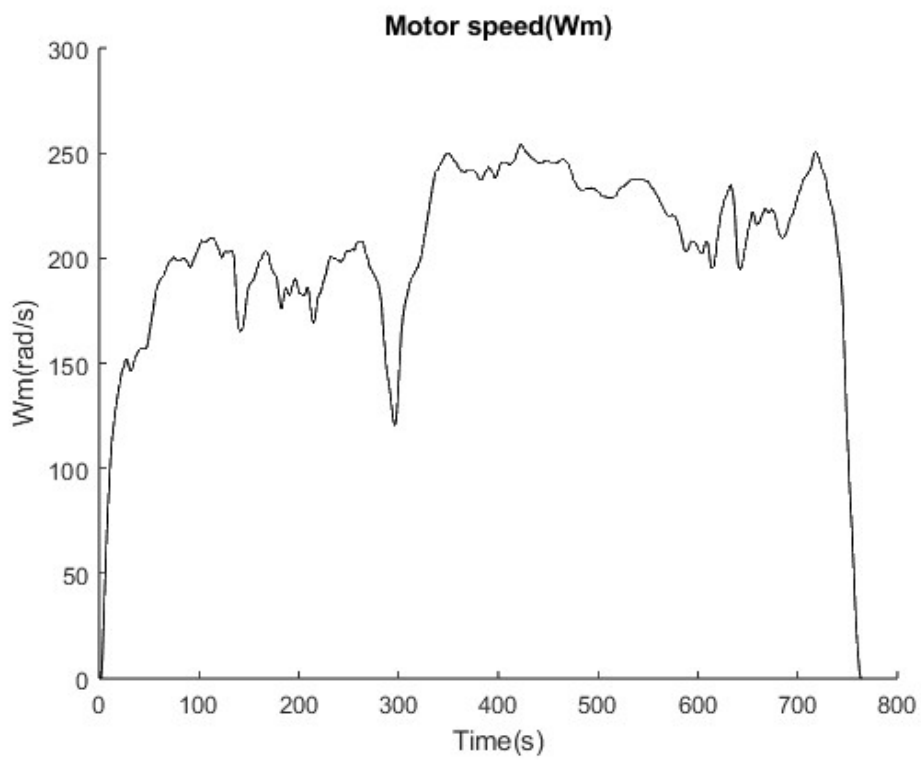


Figure 5.11: Motor speed in HWFET(modified) cycle

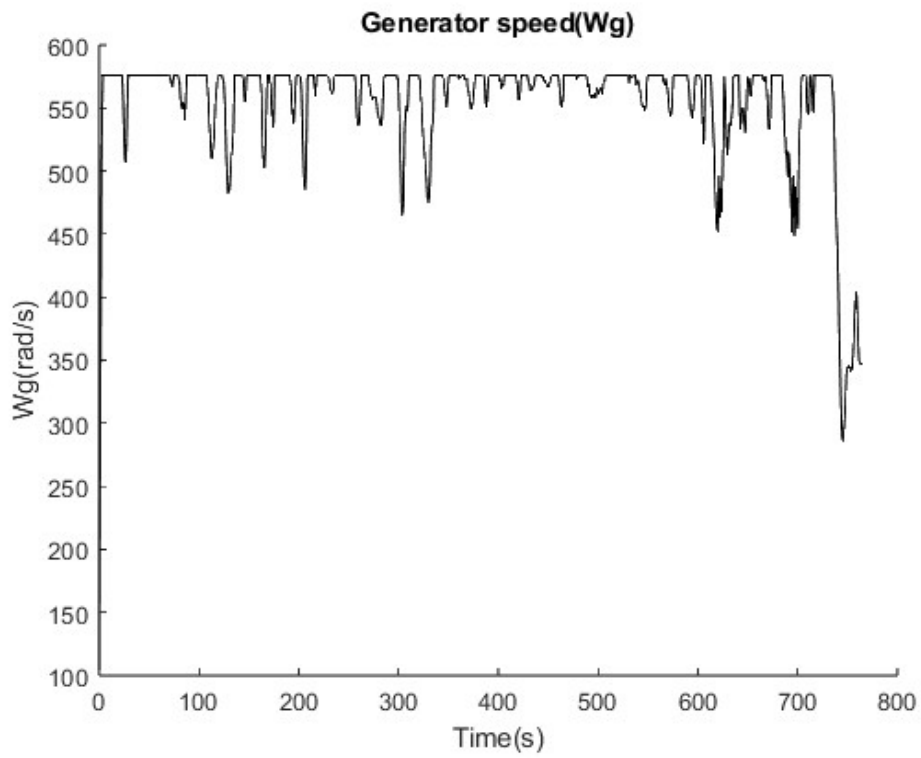


Figure 5.12: Generator speed in HWFET(modified) cycle

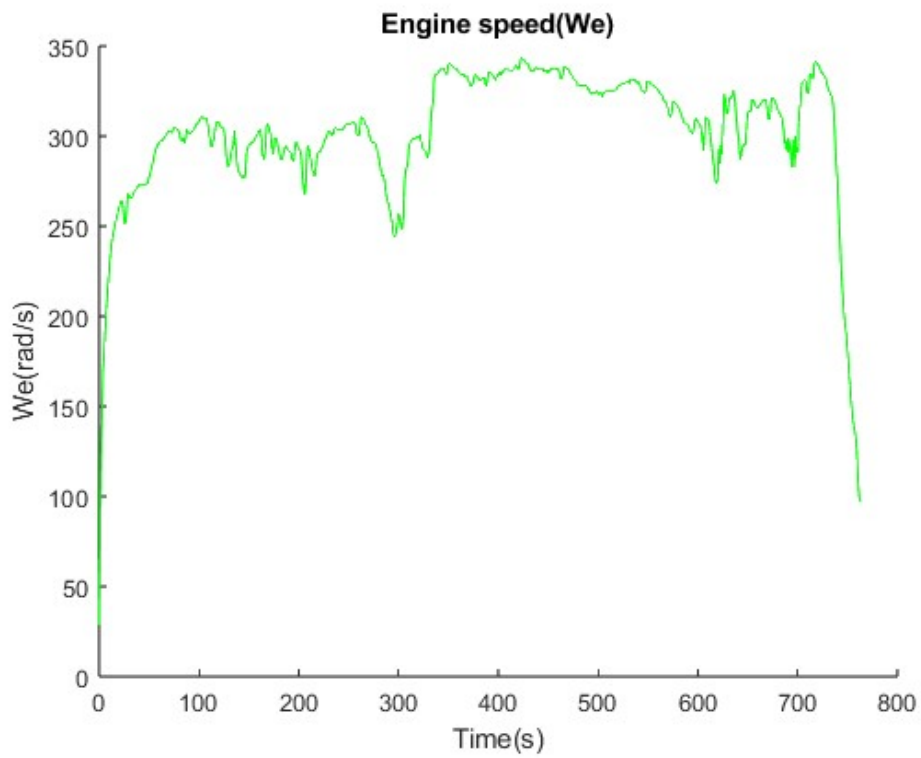


Figure 5.13: Engine speed in HWFET(modified) cycle

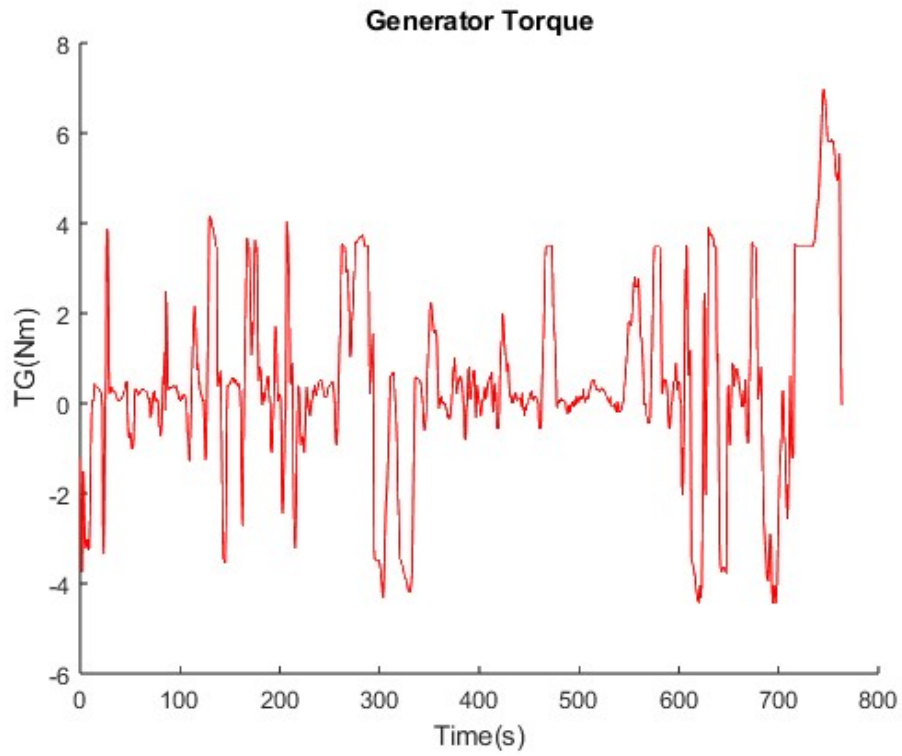


Figure 5.14: Generator torque in HWFET(modified) cycle

Figure 5.14, 5.15 and 5.16 show torque of Motor, Generator and engine in HWFET(modified) drive cycle.

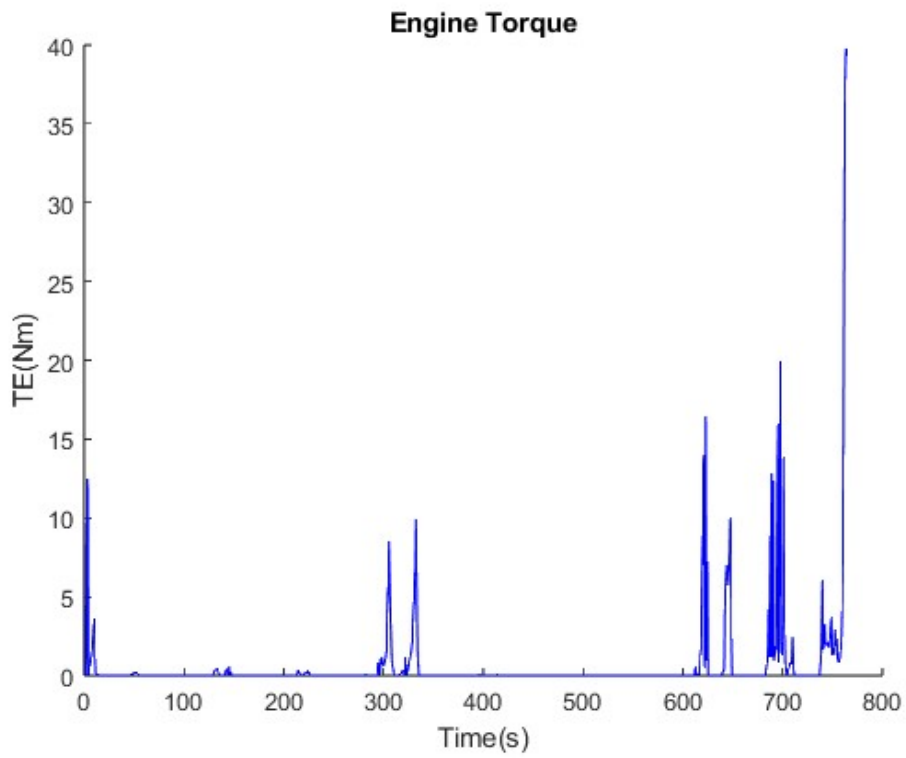


Figure 5.15: Engine torque in HWFET(modified) cycle

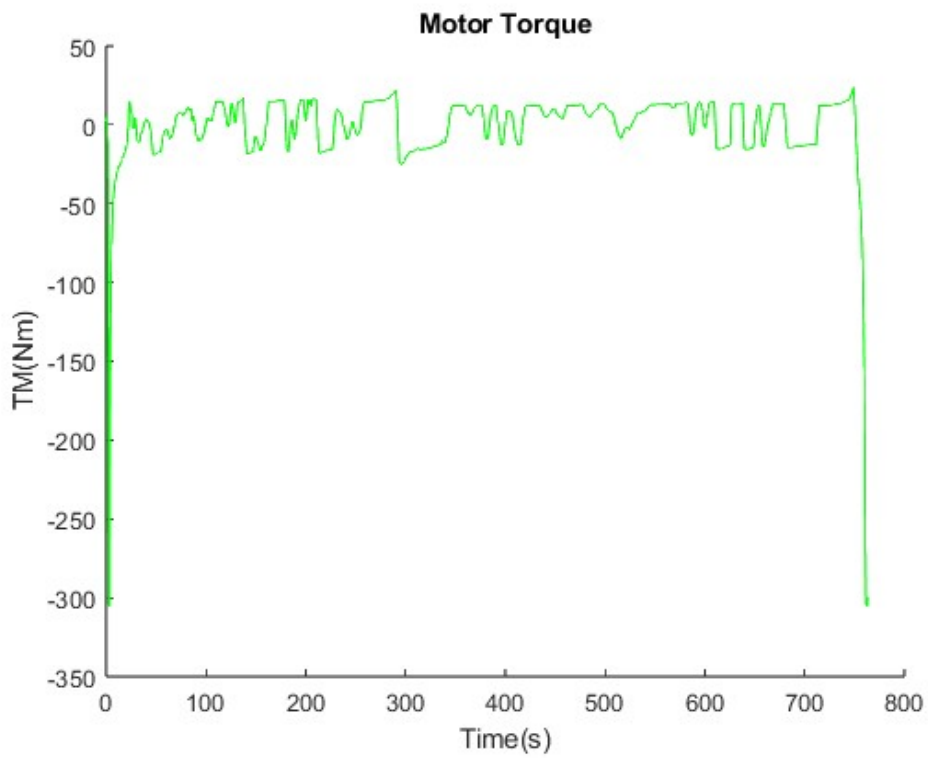


Figure 5.16: Motor torque in HWFET(modified) cycle

Driving Cycle	Method	Initial Soc	Final Soc	Fuel Economy
HWFET(modified)	ADVISOR	0.8	0.47	1L/100km
HWFET(modified)	MPC	0.8	0.662	0.5161/100km(+48.39%)
EUDC(modified)	ADVISOR	0.8	0.53	1.1L/100km
EUDC(modified)	MPC	0.8	0.665	0.5817L/100km(+47.12%)

Table 5.3: Fuel economy comparison.

Table 5.3 presents a comparison of fuel economy. Simulations on ADVISOR 2003 indicate that a rule-based strategy results in a fuel economy of 1 liters per hundred kilometers over HWFET(modified) and 1.1 liters per hundred kilometers over the EUDC(modified) cycle, as shown in the result windows. The suggested Model predictive control(MPC)simulations indicate that the Highway Fuel Economy Test Cycle(HWFET)(modified) cycle consumes 0.5161 liters per 100 kilometers, while the Extra-Urban Driving Cycle(EUDC)(modified) cycle consumes 0.5817 liters per 100 kilometers. The proposed MPC method improves fuel efficiency by 47.12% and 48.39% compared to Extra-Urban Driving Cycle(EUDC)(modified) and Highway Fuel Economy Test Cycle(HWFET)(modified) cycles, respectively. The results align with the discussion above. It can be concluded that the proposed technique has the potential for real-time deployment.

Figure 5.17, 5.18 and 5.19 show Speed of Motor, Generator and Engine in Extra-Urban Driving Cycle(EUDC)(modified) drive cycle.

Figure 5.20, 5.21 and 5.22 show torque of Motor, Generator and engine in Extra-Urban Driving Cycle(EUDC)(modified) drive cycle.

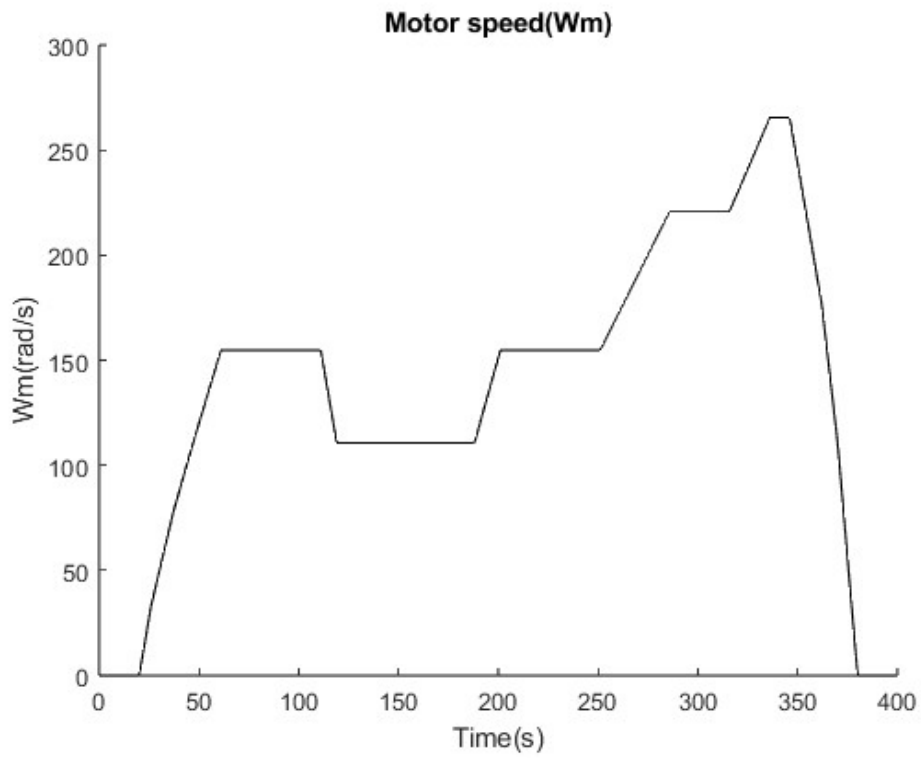


Figure 5.17: Motor Speed in EUDC(modified) cycle

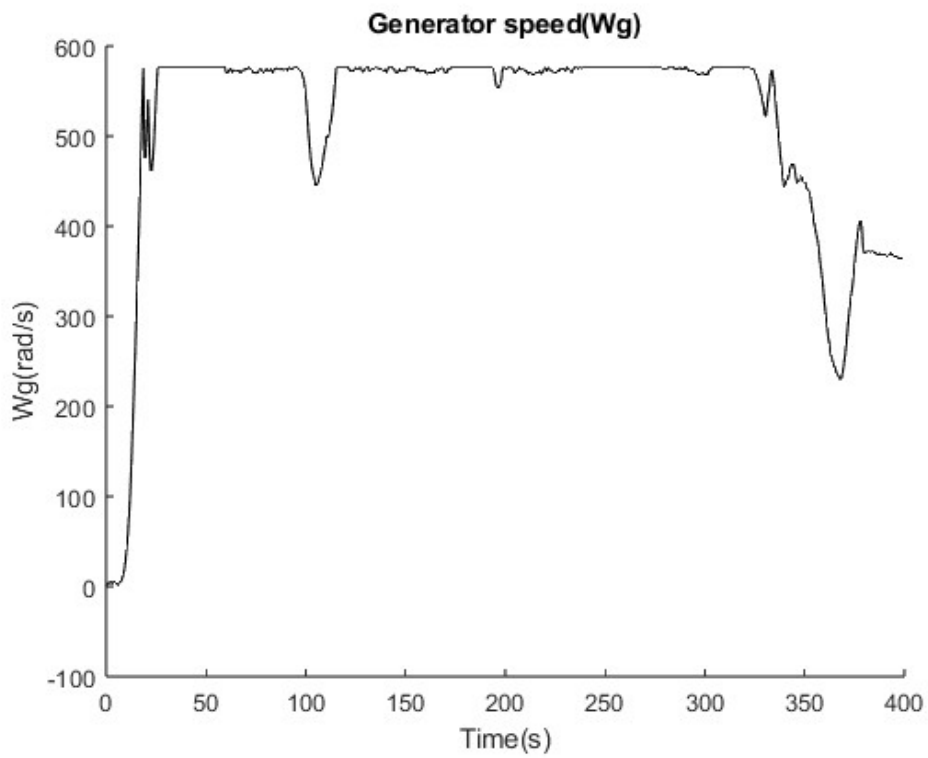


Figure 5.18: Generator Speed in EUDC(modified) cycle

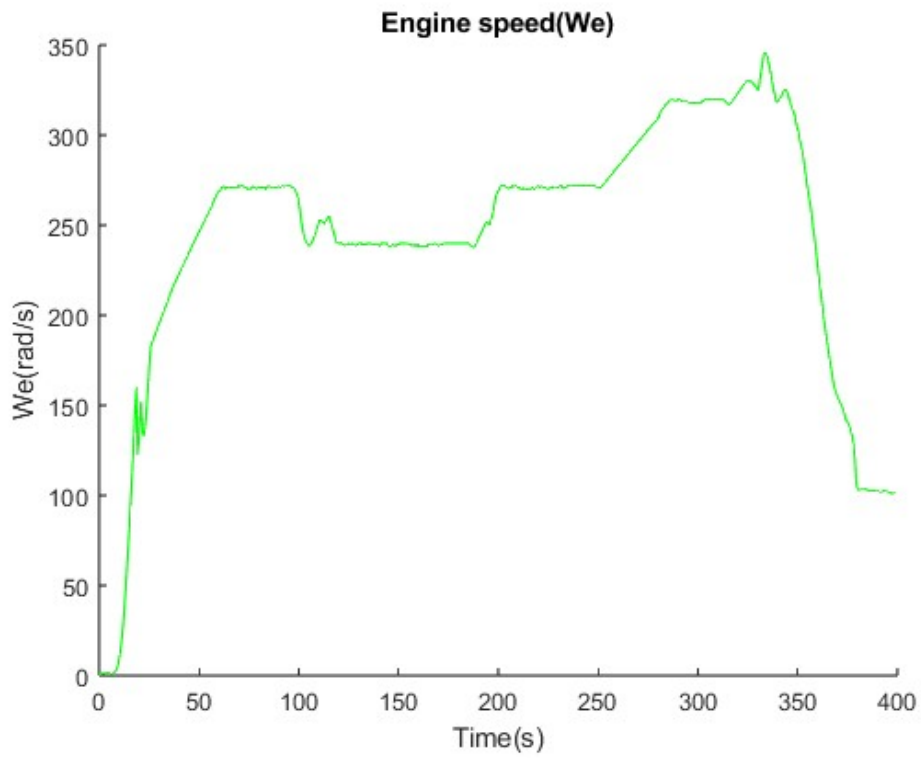


Figure 5.19: Engine Speed in EUDC(modified) cycle

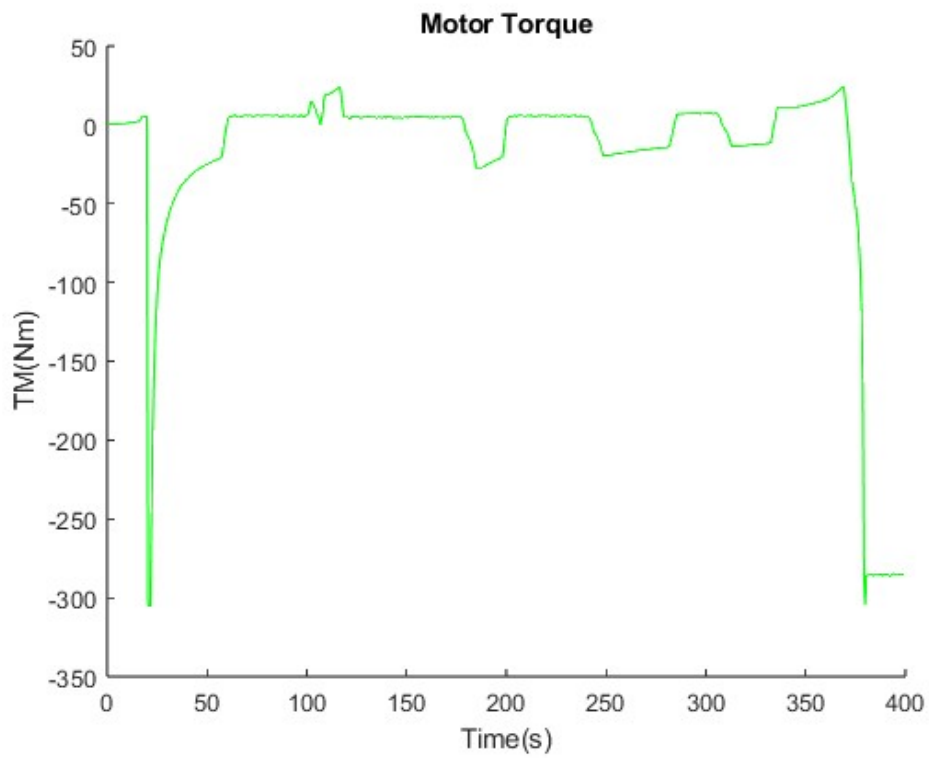


Figure 5.20: Motor torque in EUDC(modified) cycle

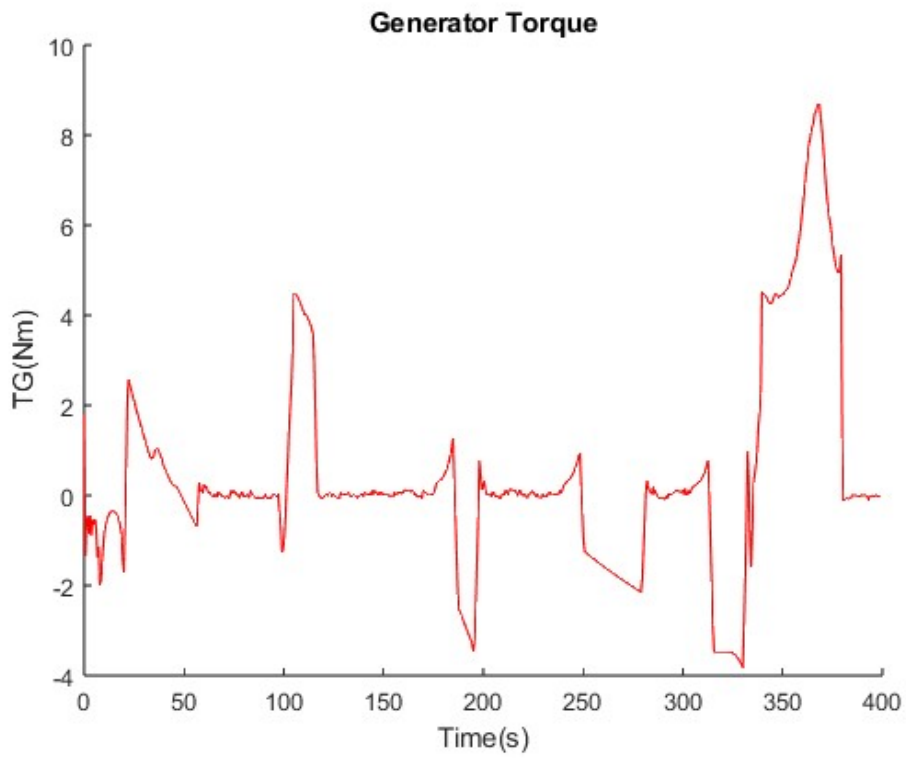


Figure 5.21: Generator torque in EUDC(modified) cycle

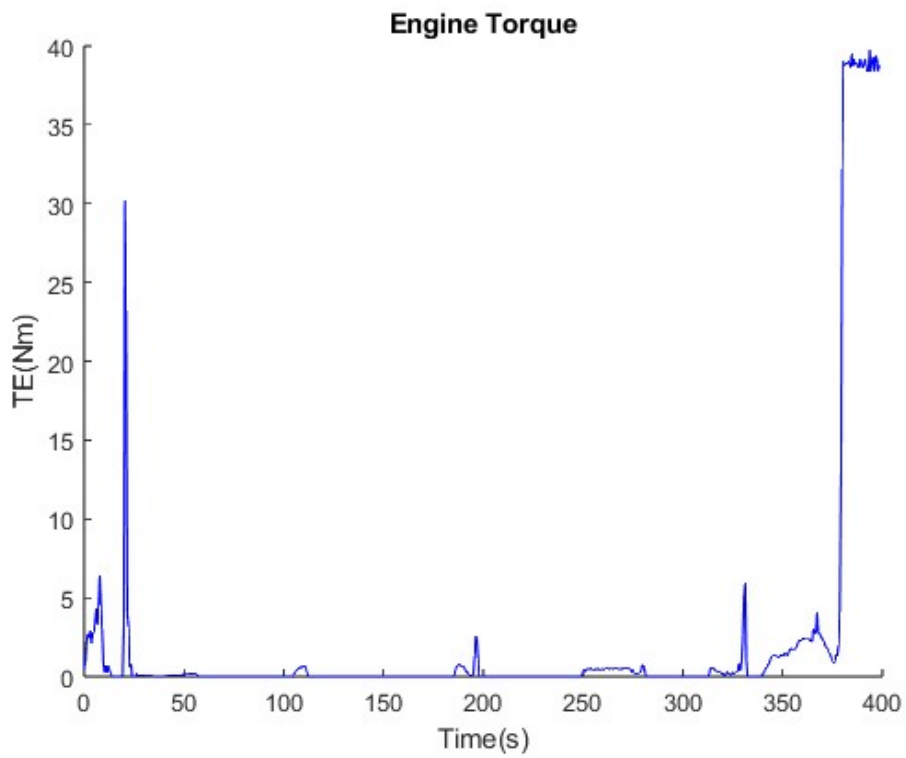


Figure 5.22: Engine torque in EUDC(modified) cycle

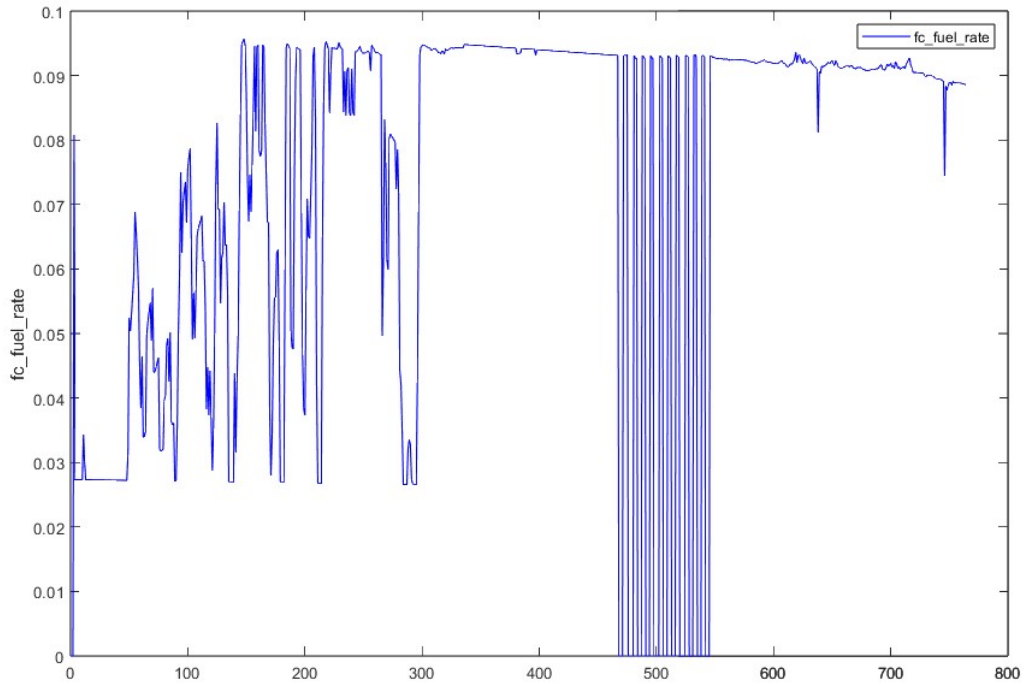


Figure 5.23: Fuel flow rate under HWFET(modified) drive cycle in ADVISOR

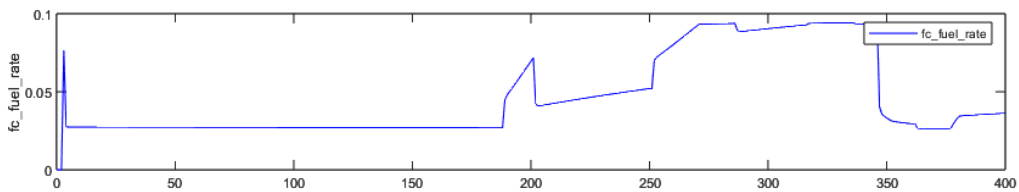


Figure 5.24: Fuel flow rate under EUDC(modified) drive cycle in ADVISOR

Figures 5.23 to 5.25 compare the fuel consumption of the Advanced Vehicle Simulator(ADVISOR) and the proposed MPC in Highway Fuel Economy Test Cycle(HWFET)(modified) and Extra-Urban Driving Cycle(EUDC)(modified) drive cycle. Fuel consumption for internal combustion engines of HWFET(modified) drive cycle ranges from 0 to nearly 0.09 g/s in ADVISOR and 0 to 0.05 g/s in the proposed MPC in Highway Fuel Economy Test Cycle(HWFET)(modified) for most of the time as shown in figure 5.23 and 5.25 respectively. For EUDC (modified) it varies from 0 to nearly 0.1 g/s in (Advanced Vehicle Simulator(ADVISOR)) and 0 to nearly 0.03 g/s in the proposed MPC in Extra-Urban Driving Cycle(EUDC)(modified) drive cycle as shown in figure 5.24 and 5.26 respectively.

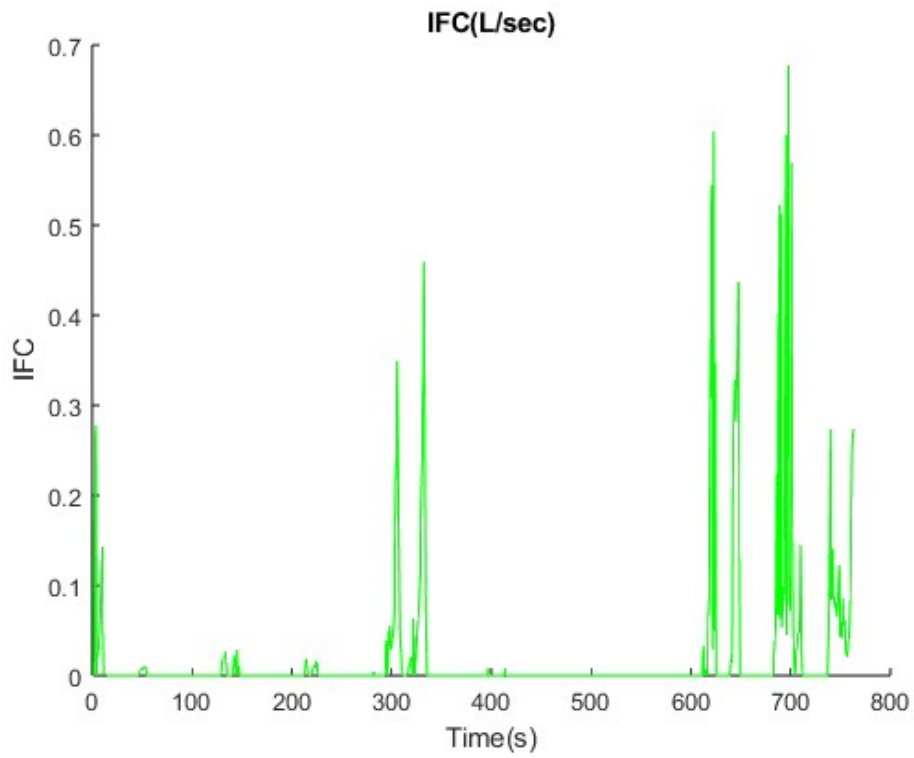


Figure 5.25: Fuel flow rate by MPC under HWFET(modified) drive cycle

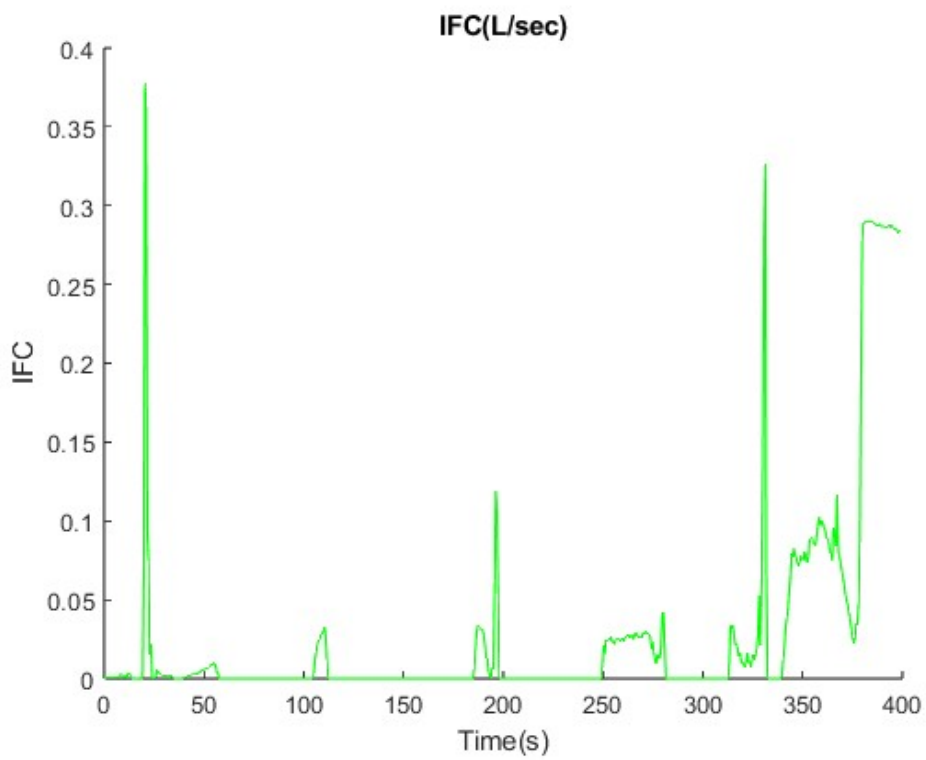


Figure 5.26: Fuel flow rate by MPC under EUDC(modified) drive cycle

6 Conclusion and Future Work

Electric vehicles play a crucial role in addressing pollution, fossil fuel depletion, and future energy demands. However, they can take several hours to charge and have few charging outlets. As a result, a power split hybrid electric vehicle is an excellent option from both internal combustion engine(ICE) vehicles and full electric vehicle(EV), offering all of the advantages of series and parallel systems. This study aimed to reduce fuel consumption in power-split hybrid electric vehicles by regulating power from two sources: internal combustion engine(ICE) and batteries, using an interior point optimiser-based nonlinear model predictive control strategy. The model predictive control approach has the advantage of considering input and output restrictions, making it a superior strategy. Furthermore, it can make better use of the engine and batteries. Nonlinear model predictive control is applied to a simplified control model of a power split hybrid electric car.

MPC findings are compared to ADVISOR 2003's rule-based technique for fuel economy throughout typical Extra-Urban Driving Cycle(EUDC)(modified) and Modified HWFET cycles. The study found that a nonlinear model predictive control method improved fuel economy by 48.39% and 47.12% in HWFET(modified) and EUDC(modified). Throughout the driving cycle, the battery charge state (state of charge(SOC)) maintains within its limit and eventually approaches the reference value of 0.7. The results show that the proposed non-linear model predictive control(NMPC) technique can be implemented in real-time.

The study focuses on optimizing the energy of power-split three wheeler HEVs using a fast algorithm based on interior-point optimisation. However, in the future additional research could be included;

- i. Considering road slope as a function of driving cycle data points
- ii. Environmental factors like temperature, wind, and terrain.
- iii. While MPC has the potential for real-time implementation, it is assumed that the driving cycle is known ahead of time. This is because driving habits are difficult to characterize and the relationship

between the driver's demand and traffic environment is unpredictable.

iv. Dynamic losses of the motor and generator can be included in the analysis by modifying the simulation code.

And three wheeler hybrid electric vehicles with power split configurations will use a combination of rule-based and model predictive control strategies to adapt to various driving cycles and road conditions.

References

- [1] W. Enang and C. Bannister, “Modelling and control of hybrid electric vehicles (a comprehensive review),” *Renewable and Sustainable Energy Reviews*, vol. 74, pp. 1210–1239, 2017.
- [2] S. Gonsrang and R. Kasper, “Optimisation-based power management system for an electric vehicle with a hybrid energy storage system,” *International Journal of Automotive and Mechanical Engineering*, vol. 15, no. 4, pp. 5729–5747, 2018.
- [3] F. Zhang, L. Wang, S. Coskun, H. Pang, Y. Cui, and J. Xi, “Energy management strategies for hybrid electric vehicles: Review, classification, comparison, and outlook,” *Energies*, vol. 13, no. 13, p. 3352, 2020.
- [4] M. Asghar, A. I. Bhatti, and T. Izhar, “Benchmark fuel economy for a parallel hybrid electric three-wheeler vehicle (rickshaw),” *Advances in Mechanical Engineering*, vol. 10, no. 12, p. 1687814018808657, 2018.
- [5] “The first hybrid vehicle,available link:F.porche link link,last access:[06-03-2024].”
- [6] A. Vezzini, H. Sharan, and L. Umanand, “Low-pollution three-wheeler autorickshaw with power-assist series hybrid and novel variable dc-link voltage system,” *Journal of the Indian Institute of Science*, vol. 85, no. 2, p. 105, 2005.
- [7] S. Amjad, R. Rudramoorthy, S. Neelakrishnan, S. Gurusubramanian, J. Dheepan Raja, R. Mathew, and M. Sundaravel, “Plug-in hybrid conversion of three wheeler using a novel drive strategy,” *International Journal of Alternative Propulsion*, vol. 2, no. 2, pp. 148–164, 2012.
- [8] T. Hofman, S. Van Der Tas, W. Ooms, E. Van Meijl, and B. Laugeman, “Development of a micro-hybrid system for a three-wheeled motor taxi,” *World Electric Vehicle Journal*, vol. 3, no. 3, pp. 572–580, 2009.
- [9] R. V. Jijith and S. Indulal, “Hybrid electric three-wheeler with ann controller,” in *2018 International Conference on Circuits and Systems in Digital Enterprise Technology (ICCSDET)*. IEEE, 2018, pp. 1–5.
- [10] V. Padmanaban, A. Ramasubramanian, and T. Subramaniam, “Investigation on use of plug-in hybrid electric vehicle (phev) technology using renewable energy for an autorickshaw,” *Journal of KONES*, vol. 19, no. 2, pp. 383–394, 2012.

- [11] W. Maddumage, K. Abeyasighe, M. Perera, R. Attalage, and P. Kelly, “Comparing fuel consumption and emission levels of hybrid powertrain configurations and a conventional powertrain in varied drive cycles and degree of hybridization,” , no. 1, pp. 20–33, 2020.
- [12] X. Zhou, D. Qin, and J. Hu, “Multi-objective optimization design and performance evaluation for plug-in hybrid electric vehicle powertrains,” *Applied Energy*, vol. 208, pp. 1608–1625, 2017.
- [13] M. Josevski and D. Abel, “Energy management of parallel hybrid electric vehicles based on stochastic model predictive control,” *IFAC Proceedings Volumes*, vol. 47, no. 3, pp. 2132–2137, 2014.
- [14] J. Tang, L. Guo, B. Gao, Q. Liu, S. Yu, and H. Chen, “Energy management of a parallel hybrid electric vehicle with cvt using model predictive control,” in *2016 35th Chinese Control Conference (CCC)*. IEEE, 2016, pp. 4396–4401.
- [15] L. Li, S. You, C. Yang, B. Yan, J. Song, and Z. Chen, “Driving-behavior-aware stochastic model predictive control for plug-in hybrid electric buses,” *Applied Energy*, vol. 162, pp. 868–879, 2016.
- [16] H. Wang, Y. Huang, A. Khajepour, and Q. Song, “Model predictive control-based energy management strategy for a series hybrid electric tracked vehicle,” *Applied Energy*, vol. 182, pp. 105–114, 2016.
- [17] S. Zhang, R. Xiong, and F. Sun, “Model predictive control for power management in a plug-in hybrid electric vehicle with a hybrid energy storage system,” *Applied energy*, vol. 185, pp. 1654–1662, 2017.
- [18] S. East and M. Cannon, “Energy management in plug-in hybrid electric vehicles: Convex optimization algorithms for model predictive control,” *IEEE Transactions on Control Systems Technology*, vol. 28, no. 6, pp. 2191–2203, 2019.
- [19] R. Wang and S. M. Lukic, “Dynamic programming technique in hybrid electric vehicle optimization,” in *2012 IEEE international electric vehicle conference*. IEEE, 2012, pp. 1–8.
- [20] C.-C. Lin, Z. Filipi, L. Louca, H. Peng, D. Assanis, and J. Stein, “Modelling and control of a medium-duty hybrid electric truck,” *International Journal of Heavy Vehicle Systems*, vol. 11, no. 3-4, pp. 349–371, 2004.

- [21] C.-C. Lin, H. Peng, J. W. Grizzle, and J.-M. Kang, "Power management strategy for a parallel hybrid electric truck," *IEEE transactions on control systems technology*, vol. 11, no. 6, pp. 839–849, 2003.
- [22] S. Hadj-Said, G. Colin, A. Ketfi-Cherif, and Y. Chamailard, "Energy management of a parallel hybrid electric vehicle equipped with a voltage booster," *IFAC-PapersOnLine*, vol. 51, no. 31, pp. 606–611, 2018.
- [23] A. Brahma, Y. Guezennec, and G. Rizzoni, "Optimal energy management in series hybrid electric vehicles," in *Proceedings of the 2000 American Control Conference. ACC (IEEE Cat. No. 00CH36334)*, vol. 1, no. 6. IEEE, 2000, pp. 60–64.
- [24] M. Salman, N. J. Schouten, and N. A. Kheir, "Control strategies for parallel hybrid vehicles," in *Proceedings of the 2000 American Control Conference. ACC (IEEE Cat. No. 00CH36334)*, vol. 1, no. 6. IEEE, 2000, pp. 524–528.
- [25] M. Montazeri-Gh and M. Mahmoodi-k, "Development a new power management strategy for power split hybrid electric vehicles," *Transportation Research Part D: Transport and Environment*, vol. 37, pp. 79–96, 2015.
- [26] H.-D. Lee and S.-K. Sul, "Fuzzy-logic-based torque control strategy for parallel-type hybrid electric vehicle," *IEEE Transactions on Industrial Electronics*, vol. 45, no. 4, pp. 625–632, 1998.
- [27] H.-D. Lee, E.-S. Koo, S.-K. Sul, J.-S. Kim, M. Kamiya, H. Ikeda, S. Shinohara, and H. Yoshida, "Torque control strategy for a parallel-hybrid vehicle using fuzzy logic," *IEEE Industry Applications Magazine*, vol. 6, no. 6, pp. 33–38, 2000.
- [28] B. M. Baumann, G. Washington, B. C. Glenn, and G. Rizzoni, "Mechatronic design and control of hybrid electric vehicles," *IEEE/ASME Transactions On Mechatronics*, vol. 5, no. 1, pp. 58–72, 2000.
- [29] H. Tian, X. Wang, Z. Lu, Y. Huang, and G. Tian, "Adaptive fuzzy logic energy management strategy based on reasonable soc reference curve for online control of plug-in hybrid electric city bus," *IEEE Transactions on Intelligent Transportation Systems*, vol. 19, no. 5, pp. 1607–1617, 2017.

- [30] Y. Wang, Z. Wu, Y. Chen, A. Xia, C. Guo, and Z. Tang, "Research on energy optimization control strategy of the hybrid electric vehicle based on pontryagin's minimum principle," *Computers & Electrical Engineering*, vol. 72, pp. 203–213, 2018.
- [31] S. Wang, S. Zhang, D. Shi, X. Sun, and J. He, "Research on instantaneous optimal control of the hybrid electric vehicle with planetary gear sets," *Journal of the Brazilian Society of Mechanical Sciences and Engineering*, vol. 41, pp. 1–12, 2019.
- [32] E. Taherzadeh, S. Javadi, and M. Dabbaghjamanesh, "New optimal power management strategy for series plug-in hybrid electric vehicles," *International Journal of Automotive Technology*, vol. 19, pp. 1061–1069, 2018.
- [33] S.-Y. Chen, C.-H. Wu, Y.-H. Hung, and C.-T. Chung, "Optimal strategies of energy management integrated with transmission control for a hybrid electric vehicle using dynamic particle swarm optimization," *Energy*, vol. 160, pp. 154–170, 2018.
- [34] F. U. Syed, M. L. Kuang, J. Czuby, and H. Ying, "Derivation and experimental validation of a power-split hybrid electric vehicle model," *IEEE Transactions on Vehicular Technology*, vol. 55, no. 6, pp. 1731–1747, 2006.
- [35] J. Liu and H. Peng, "Modeling and control of a power-split hybrid vehicle," *IEEE transactions on control systems technology*, vol. 16, no. 6, pp. 1242–1251, 2008.
- [36] H. A. Borhan, A. Vahidi, A. M. Phillips, M. L. Kuang, and I. V. Kolmanovsky, "Predictive energy management of a power-split hybrid electric vehicle," in *2009 American control conference*. IEEE, 2009, pp. 3970–3976.
- [37] K. Yu, M. Mukai, and T. Kawabe, "Model predictive control of a power-split hybrid electric vehicle system," *Artificial Life and Robotics*, vol. 17, pp. 221–226, 2012.
- [38] K. Yu, Q. Liang, Z. Hu, J. Yang, and H. Zhang, "Performance of an eco-driving model predictive control system for hevs during car following," *Asian Journal of Control*, vol. 18, no. 1, pp. 16–28, 2016.
- [39] A. Hawary and M. Ramdan, "Hybrid hydraulic vehicle parameter optimization using multi-objective genetic algorithm," *International Journal of Automotive and Mechanical Engineering*, vol. 16, no. 3, pp. 7007–7018, 2019.

- [40] A. Sciarretta and L. Guzzella, “Control of hybrid electric vehicles,” *IEEE control systems magazine*, vol. 27, no. 2, pp. 60–70, 2007.
- [41] F. Zhang, X. Hu, R. Langari, and D. Cao, “Energy management strategies of connected hevs and phevs: Recent progress and outlook,” *Progress in Energy and Combustion Science*, vol. 73, pp. 235–256, 2019.
- [42] S. Onori, L. Serrao, and G. Rizzoni, “Hybrid electric vehicles: Energy management strategies,” 2016.
- [43] M. Ehsani, Y. Gao, S. E. Gay, and A. Emadi, “Modern electric, hybrid electric, and fuel cell vehicles,” (*No Title*), 2004.
- [44] W. Liu, *Introduction to hybrid vehicle system modeling and control*. John Wiley & Sons, 2013.
- [45] E. H. Mamdani, “Application of fuzzy algorithms for control of simple dynamic plant,” in *Proceedings of the institution of electrical engineers*, vol. 121, no. 12. IET, 1974, pp. 1585–1588.
- [46] T. Takagi and M. Sugeno, “Fuzzy identification of systems and its applications to modeling and control,” *IEEE transactions on systems, man, and cybernetics*, no. 1, pp. 116–132, 1985.
- [47] H. Yu, D. Tarsitano, X. Hu, and F. Cheli, “Real time energy management strategy for a fast charging electric urban bus powered by hybrid energy storage system,” *Energy*, vol. 112, pp. 322–331, 2016.
- [48] B. Kouvaritakis and M. Cannon, “Model predictive control,” *Switzerland: Springer International Publishing*, vol. 38, 2016.
- [49] E. F. Camacho, C. Bordons, E. Camacho, and C. Bordons, “Nonlinear model predictive control,” *Model predictive control*, pp. 249–288, 2007.
- [50] J. B. Rawlings, D. Q. Mayne, and M. Diehl, *Model predictive control: theory, computation, and design*. Nob Hill Publishing Madison, WI, 2017, vol. 2.
- [51] “Casadi,available link:CasADi link,last access:[06-03-2024].”
- [52] L. Wang, *Model predictive control system design and implementation using MATLAB®*. Springer Science & Business Media, 2009.

- [53] M. W. Mehrez, G. K. Mann, and R. G. Gosine, “Stabilizing nm-pc of wheeled mobile robots using open-source real-time software,” in *2013 16th International Conference on Advanced Robotics (ICAR)*. IEEE, 2013, pp. 1–6.
- [54] K. B. Wipke, M. R. Cuddy, and S. D. Burch, “Advisor 2.1: A user-friendly advanced power-train simulation using a combined backward/forward approach,” *IEEE transactions on vehicular technology*, vol. 48, no. 6, pp. 1751–1761, 1999.
- [55] T. Markel, A. Brooker, T. Hendricks, V. Johnson, K. Kelly, B. Kramer, M. O’Keefe, S. Sprik, and K. Wipke, “Advisor: a systems analysis tool for advanced vehicle modeling,” *Journal of power sources*, vol. 110, no. 2, pp. 255–266, 2002.
- [56] J. B. Heywood, “Internal combustion engine fundamentals,” (*No Title*), 1988.

7 Appendices

7.1 Fuel consumption

The equation is used to model fuel consumption (mf).

$$BSFC = \frac{\dot{m}_f}{P_e} \quad (7.1)$$

$$BSFC(T_e, N_e) = b_0 + b_1 * N_e + b_2 * T_e + b_3 * N_e^2 + b_4 * N_e * T_e + b_5 * T_e^2$$

$$+ b_6 * N_e^3 + b_7 * N_e * T_e + b_8 * N_e * T_e^2 + b_9 * T_e^3$$

The equation above links fuel flow, power, and BSFC (Brake Specific Fuel Consumption) [56]. GT-Suite provides a map of the BSFC measured from the engine. The following function can be discovered by estimating the map as a function of engine torque and engine rotational speed represented as [rpm].

$$b_0 = 6.9933 * 10^2, b_1 = 6.5760 * 10^3, b_2 = 1.8639 * 10^1$$

$$b_3 = 3.1841 * 10^6, b_4 = 9.7399 * 10^5, b_5 = 2.27 * 10^1$$

$$b_6 = 2.6412 * 10^{10}, b_7 = 2.1534 * 10^8, b_8 = 8.4366 * 10^7$$

$$b_9 = 8.5085 * 10^4.$$

The unit for BSFC is $[\frac{g}{kWh}]$. Since $P = T \cdot \omega$, Fuel consumption per second can be computed using the equation

Figure 7.1 shows a plot of the BSFC as a function of T_e and N_e . According to the GT-Suite map, the BSFC values range from 201 to 720 $[\frac{g}{kWh}]$.

$$\dot{m}_f = \frac{T_e * W_e * BSFC(T_e, N_e)}{3.6 * 10^6}, \left[\frac{g}{s} \right] \quad (7.2)$$

$$IFC = \dot{m}_f / \text{fuel} - \text{density}, \left[\frac{L}{sec} \right] \quad (7.3)$$

The equation above links Instant fuel consumption (IFC) in terms of $\frac{L}{s}$, Fuel flow rate (\dot{m}_f), and fuel-density (749 g/l)

$$\text{Total} - \text{fuel} - \text{consumption} = \sum_{n=1}^N IFC \quad (7.4)$$

where; N-total number of data cycle

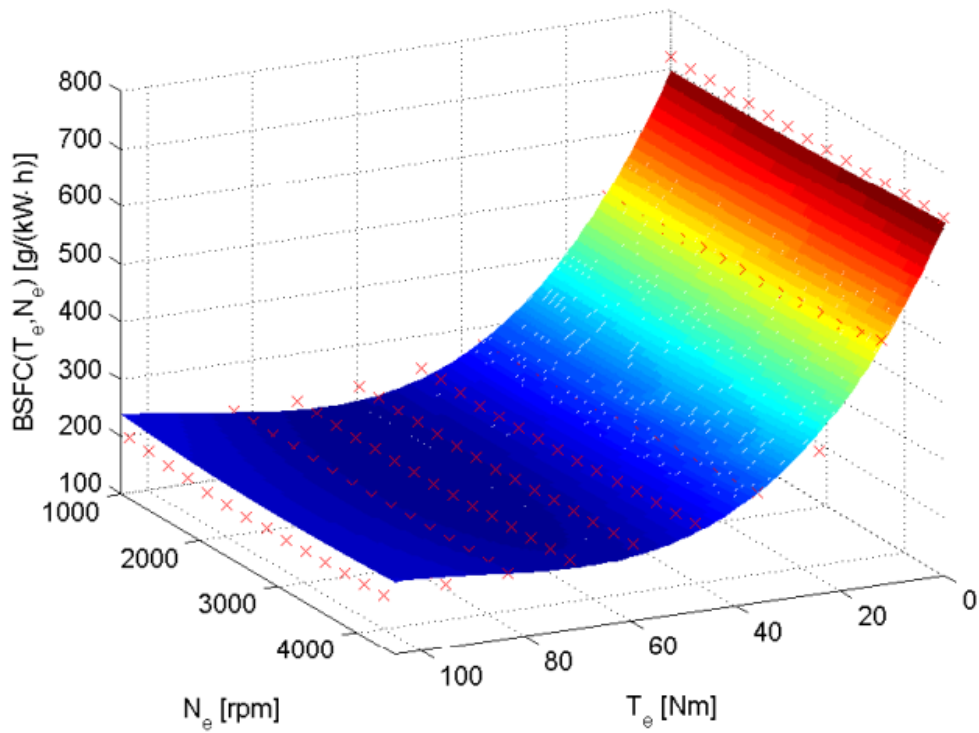


Figure 7.1: Approximation of BSFC as a function of T_e and N_e , together with map data from GT-Suite